

No. 302
April 1986

TIME-DOMAIN ANALYSIS OF SHIP MOTIONS

Stergios John Liapis



No. 302
April 1986

TIME-DOMAIN ANALYSIS
OF SHIP MOTIONS

by

Stergios John Liapis

A dissertation submitted in partial fulfillment
of the requirements for the degree of
Doctor of Philosophy
(Naval Architecture and Marine Engineering)
in The University of Michigan
1986

Doctoral Committee:

Professor Robert Beck, Chairman
Associate Professor Armin Troesch
Professor William Vorus
Professor Chia-Shun Yih



Department of Naval Architecture
and Marine Engineering
College of Engineering
The University of Michigan
Ann Arbor, Michigan 48109

ACKNOWLEDGMENTS

There are many people that have invariably contributed to this work whom I would like to thank individually. My foremost appreciation and thanks go to my advisor Professor Beck for his guidance and encouragement. The discussions with him were inspiring and played an invaluable role in the development of this work. Many thanks and appreciation are extended to Professor Troesch who provided numerous suggestions and comments. I am also indebted to Professor Vorus for his prompt attention and suggestions. Professor Yih has been very helpful with his advice for which I am grateful. Furthermore, his introductory courses on Fluid Mechanics and Water Waves initiated my interest in this area.

Special thanks are extended to Professor Doctors for his friendly display of skepticism. The discussions with him have been particularly helpful for this work. In addition, I would like to thank Stuart Cohen for conducting the experiments and Luella Miller for the typing of this manuscript.

This work was in part supported by the Naval Sea System Command General Hydromechanics Research Program, administered by the David Taylor Naval Ship Research and

Development Center, Contract No. N00014-78-C-0109 and the ONR Special Focus Research Program, Contract No. N00014-85-K-0118. This support has made this work possible.

Finally, I would like to express my appreciation to my wife Gina for her understanding and support throughout my student career. Her standing at my side, has made this thesis a very enjoyable thing to remember.

TABLE OF CONTENTS

ACKNOWLEDGMENT	ii
LIST OF FIGURES	vi
LIST OF APPENDICES	vii
 CHAPTER	
I. INTRODUCTION	1
II. MATHEMATICAL FORMULATION	6
II.1. The Boundary Value Problem	6
II.2. Derivation of the Integral Equation	9
II.3. Decomposition of the Problem by Introducing the Impulse Response Function	15
II.4. Pressure and Force Calculation	25
II.5. The Integral Equation for a Source Distribution	29
III. NUMERICAL METHODS	33
III.1. Approximate Representation of the Body Surface by Plane Quadrilaterals	33
III.2. Numerical Solution of the Integral Equations for ψ_{1k} , ψ_{2k}	34
III.3. Numerical Solution of the Integral Equations for χ_k	36
III.3.a. Zero Forward Speed Case .	36
III.3.b. Case of Non-zero Forward Speed	40

III.4.	Numerical Evaluation of the Influence Coefficients	45
IV.	NUMERICAL RESULTS	60
IV.1.	Numerical Evaluation of the Force Coefficients in the Time and Frequency Domain for a Sphere, a Cylinder and a Series 60 Ship .	60
IV.1.a.	Case of Zero Forward Speed	60
IV.1.b.	Case of Non-zero Forward Speed	77
IV.2.	Motion of a Freely Floating Sphere	82
V.	CONCLUSIONS	87
APPENDICES	89
REFERENCES	121

LIST OF FIGURES

Figure

1. Coordinate System and Control Volume	6
2. Computational Domain for \tilde{G}	50
3. Nondimensional Memory Function for Heave Force on a Hemisphere versus Nondimensional Time ...	66
4. Nondimensional Memory versus Nondimensional Time	67
5. Nondimensional Added Mass Coefficient for a Sphere in Heave versus Nondimensional Frequency	68
6. Nondimensional Damping Coefficient for a Sphere in Heave versus Nondimensional Frequency	69
7. Nondimensional Memory Function for a Right Circular Cylinder in Heave versus Nondimensional Time	70
8. Nondimensional Memory Function for Sway Force on a Hemisphere versus Nondimensional Time	71
9. Memory Function for Heave Force on a Series 60 ($C_B = .70$) Model at $F_n = 0$	72
10. Panel Distribution	72
11. Heave Added Mass and Damping Coefficients for a Series 60 ($C_B = .70$) Model at $F_n = 0$	73
12. Heave Pitch Cross Coupling Coefficients for a Series 60 ($C_B = .70$) Model at $F_n = 0$	74
13. Pitch Added Mass and Damping Coefficients for a Series 60 ($C_B = .70$) Model at $F_n = 0$	75
14. Heave Added Mass and Damping Coefficients for a Series 60 ($C_B = .70$) Model at $F_n = 0.2$	80
15. Pitch Added Mass and Damping Coefficients for a Series 60 ($C_B = .70$) Model at $F_n = 0.2$	81

16.	Nondimensional Heave Displacement versus Nondimensional Time for a Hemisphere Released from a Height h	86
A-1	Coordinate System for a Maneuvering Ship	91
D-1	Coordinate Mapping of Arbitrary Quadrilateral into a Square	110

LIST OF APPENDICES

Appendix

A.	Extension of the Theory to Ship Maneuvering	90
B.	Derivation of the Integral Equation for the Components of the Potential ψ_{1k} , x_k	99
C.	Derivation of Equation (31) Relating the Present Formulation to that of Ogilvie (1964)	105
D.	Integration over an Element	109
E.	Asymptotic Analysis of the Integral Term in Equation (64)	112

CHAPTER I
INTRODUCTION

During the last twenty years there has been growing interest in numerical methods for calculating the wave loads on fixed structures and the oscillatory motions of vessels. The first analyses were limited to bodies of special geometry such as submerged circles, spheres and ellipsoids. Another special case of body shape that has been studied extensively is that of a slender ship using various techniques from perturbation theory. Despite its utility, this analysis gives very poor results near the bow and the stern of a typical ship where the slenderness assumptions are no longer valid. Furthermore it cannot be used for typical offshore structures. The advent of large, high-speed computers led to the development of numerical methods that removed the geometrical restrictions of the earlier methods.

In all these models the problem is formulated in the frequency domain leading to equations that have meaning only if the body motions are strictly sinusoidal in time. In more general situations, such as a ship performing a maneuver with varying speed, the frequency-domain approach is meaningless. An alternative to the frequency-domain

approach is to formulate the problem directly in the time domain. The solutions in the frequency domain and time domain can be related through the use of Fourier transforms. For any particular problem involving only zero forward speed, one formulation or the other may be more convenient. However, for problems involving forward speed it appears that the time-domain approach requires much less computational effort and can be easily extended to more general cases.

Cummins (1962) and Ogilvie (1964) first discussed the use of time-domain analysis to solve unsteady body motion problems in the presence of a free surface. The zero forward speed problem is examined in detail by Wehausen (1967, 1971). The method of analysis is based on the work of Finkelstein (1957), which is expanded on in both Stoker (1957) or Wehausen and Laitone (1960).

Few results using time-domain analysis are available and they are all for zero forward speed. Direct solutions in two-dimensions are presented by Adachi and Ohmatsu (1980), Ikebuchi (1981) and Yeung (1982). Two-dimensional time-domain analysis was also used by Daoud (1975) and Yeung and Kim (1984) as part of the development for slender-body theories of ships with constant forward speed. Ursell (1964) and Maskell and Ursell (1970) developed solutions in the time domain for a floating semi-circle using the Fourier transform of the frequency-domain solution.

The same technique was used by Kotik and Lurye (1968) for a floating hemisphere. Lin (1966) developed a mathematical formulation of the time-domain problem with forward speed. His formulation leads to equations that are very complicated and are not amenable to numerical computation.

Recently, Newman (1985) has used time-domain analysis to determine the impulse response function for a right circular cylinder. Because of the axial symmetry of the problem he was able to use "ring sources" and reduce the problem to solving a one-dimensional integral equation at each time step.

The work presented here is the next step in the continuing development of the time-domain analysis method. A mathematical model has been developed to analyze hydrodynamic problems involving three-dimensional bodies of arbitrary shape moving at a constant forward speed. The basic assumptions are that the fluid is inviscid and incompressible and that the flow is irrotational so that potential theory is applicable. In this work consideration is only given to the radiation problem where a body moving at a constant forward speed is forced to oscillate around a mean position in otherwise calm water. The extension of the theory to include nonconstant forward speed and curved trajectories is in principle straightforward and is described in Appendix A.

The mathematical formulation of the problem is

presented in Chapter II. The flow created by the body motions is represented by a singularity distribution on the body surface. Green's theorem is used to derive integral equations for the singularity strength at each point of the body. In order to decouple the hydrodynamic problem from the unknown body motion an impulse response function is defined similar to what Cummins (1962) and Ogilvie (1964) initially proposed. In Chapter III, numerical techniques based on panel methods are used to solve the integral equations and find the hydrodynamic forces acting on the body. The body surface is approximated by an ensemble of plane quadrilateral elements of constant singularity strength. The integral equations are satisfied at collocation points giving a system of algebraic equations which are solved for the singularity strengths.

Computed results for the cases of a sphere, a right circular cylinder and a Series 60 ship are presented in Chapter IV. The numerical results using a source distribution or solving for the velocity potential directly are compared with analytic results in both the time and the frequency domain. The influence of the so called irregular frequencies on the results is also discussed. After computing the impulse response function, the dynamic equations of motion may be solved for any initial conditions. As an example, the heave displacement of a sphere which has been released from an initial displacement at time $t=0$ is com-

puted and compared with experimental results. Finally, Chapter V summarizes the contributions of this dissertation and offers suggestions for further work.

CHAPTER II
 MATHEMATICAL FORMULATION

II.1 The Boundary Value Problem

The axis system shown in Figure 1 is used to formulate the linearized problem in the time domain. The axis system is fixed to the mean position of the ship and travels in the positive x-direction with constant velocity U_0 . The z-axis points upward and positive x is toward the bow. The x-y plane is coincident with the calm water level and the origin is at midship. The ship is undergoing small unsteady motions around its mean position in otherwise calm water.

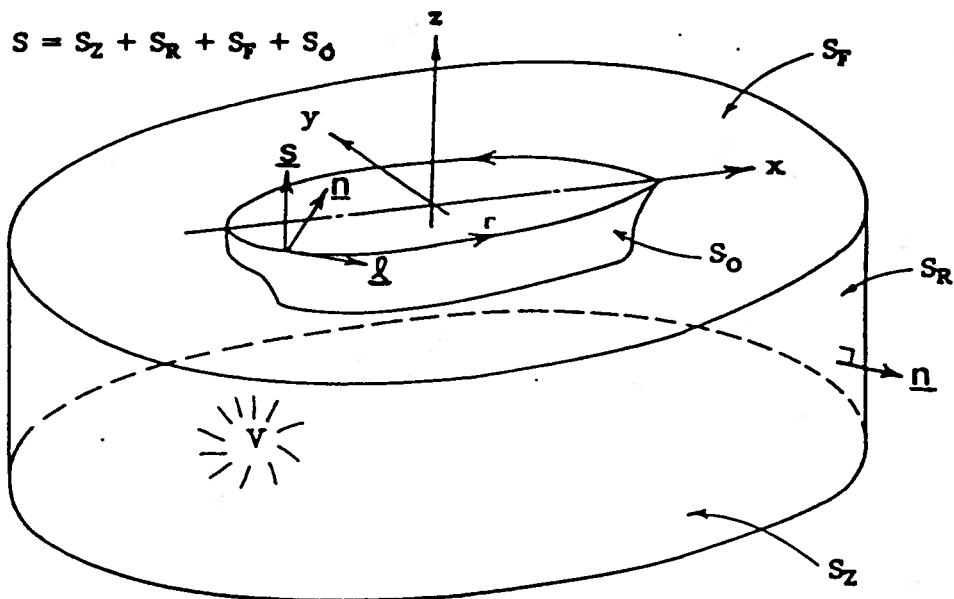


Figure 1. Coordinate System and Control Volume

It is assumed that the fluid is incompressible and inviscid and that the flow is irrotational. To set up a linearized problem it is assumed that the fluid disturbances due to the steady forward motion and the unsteady oscillations are small and can be separated. In this case the total velocity potential can be written as

$$\phi_T = -U_0 x + \phi_0(x, y, z) + \phi(x, y, z, t) \quad (1)$$

where the term $(-U_0 x + \phi_0(x, y, z))$ is the potential due to the steady translation of the vessel and the potential $\phi(x, y, z, t)$ contains all the unsteady effects. In the fluid domain, each of the potentials must satisfy the Laplace equation subject to boundary conditions on the free surface, the body, at infinity and appropriate initial conditions.

The free surface condition is linearized on the assumption of small elevation. Furthermore the effect of the steady wave is neglected so that the boundary condition on the radiation potential reduces to

$$\left(\frac{\partial}{\partial t} - U_0 \frac{\partial}{\partial x}\right)^2 \phi + g \frac{\partial \phi}{\partial z} = 0 \quad \text{on } z = 0 \quad (2)$$

where g = acceleration on gravity. The kinematic boundary condition on the hull can be linearized to give

$$\frac{\partial \phi}{\partial n} = \sum_{k=1}^6 (n_k \dot{\zeta}_k + m_k \zeta_k) \quad \text{on } S_0 \quad (3)$$

where

S_0 = mean underwater hull surface

n_k = components of generalized unit normal

out of fluid domain

$(n_1, n_2, n_3) = \underline{n}$

$(n_4, n_5, n_6) = \underline{r} \times \underline{n}$

$\underline{r} = (x, y, z)$

ζ_k = amplitude of unsteady motion in six degrees of freedom

$(\zeta_1, \zeta_2, \zeta_3)$ = linear translation along the x, y, z axes respectively

$(\zeta_4, \zeta_5, \zeta_6)$ = rotational motions about the x, y, z axes respectively

m_k = gradients of the steady velocities in the normal direction

$(m_1, m_2, m_3) = -(\underline{n} \cdot \nabla) \underline{W}$

$(m_4, m_5, m_6) = -(\underline{n} \cdot \nabla) (\underline{r} \times \underline{W})$

\underline{W} = velocity vector due to steady translation
 $= \nabla(-U_0 x + \phi_0)$

and the overdot represents differentiation with respect to time.

The unsteady problem is coupled to the steady problem because of the presence of the steady velocity vector \underline{W} in the body boundary condition. By assuming that the bodies of interest are slender, the perturbation of the steady flow field due to the ship is neglected giving

$\underline{W} = -U_0 \mathbf{i}$. In this work, this simplification will be made. This assumption reduces \underline{m} to:

$$\underline{m} = (0, 0, 0, 0, U_0 n_3, -U_0 n_2)$$

Since an initial value problem is being solved the gradient of the radiation potential must vanish at infinity. In addition the initial conditions of

$$\phi = 0, \quad \frac{\partial \phi}{\partial t} = 0 \quad \text{for } t < 0 \quad (4)$$

must be imposed.

II.2 Derivation of the Integral Equation

At this point we must note a very important peculiarity of the problem. Since the ultimate goal is finding the hydrodynamic forces on the hull, we only need the values of the potential ϕ and its derivatives on the hull. The values of ϕ inside the fluid domain are of no interest. This feature combined with the fact that the fluid domain extends to infinity explains why finite difference or finite element techniques are rarely used in this type of problem. What is considered more efficient is replacing the body by a suitable distribution of source singularities. The source potential is also known as a Green function and will be denoted here as G . The source strength at each point may be determined by solving a Fredholm integral equation of the second kind over the body surface. For this problem the appropriate Green function represents an impulsive source below a free surface and is given as:

$$\begin{aligned}
G(P,Q,t-\tau) &= \left(\frac{1}{r} - \frac{1}{r'}\right)\delta(t - \tau) + H(t - \tau) \\
&\times 2\int_0^{\infty} dk \sqrt{kg} \sin(\sqrt{kg}(t - \tau)) e^{k(z+\zeta)} J_0(kR) \\
&= \left(\frac{1}{r} - \frac{1}{r'}\right)\delta(t - \tau) + H(t - \tau)\tilde{G}(P,Q,t-\tau) \quad (5)
\end{aligned}$$

where $P = (x, y, z)$ is the field point
 $Q = (\xi, \eta, \zeta)$ is the source point
 $r^2 = (x - \xi)^2 + (y - \eta)^2 + (z - \zeta)^2$
 $r'^2 = (x - \xi)^2 + (y - \eta)^2 + (z + \zeta)^2$
 $R^2 = (x - \xi + U_0(t - \tau))^2 + (y - \eta)^2$
 $\delta(t - \tau)$ = delta function
 $H(t - \tau)$ = unit step function
 $= 0 \quad t - \tau < 0$
 $= 1 \quad t - \tau > 0$

The Green function represents the potential at the field point P and at time t due to an impulsive source at the point Q suddenly created and annihilated at time τ . This source acts like an underwater disturbance which generates a Cauchy-Poisson type wave system as represented by the $\tilde{G}(P,Q,t-\tau)$ term. The integrated form of (5) is given by Wehausen and Laitone (1960) as the potential for a source of arbitrary strength moving below a free surface. It is easily shown that the Green function solves the following differential system:

$$\nabla^2 G = -4\pi \delta(P - Q) \delta(t - \tau)$$

$$\left(\frac{\partial}{\partial t} - U\frac{\partial}{\partial x}\right)^2 G + g\frac{\partial}{\partial z}G = 0 \quad \text{on } z = 0$$

$$G, \frac{\partial G}{\partial t} = 0 \quad \text{for } t < 0 \quad (6)$$

Applying Green's theorem to the fluid volume shown in Figure 1 and enclosed by $S_Z \cup S_r \cup S_f \cup S_0$ yields

$$\iiint_V [\phi \nabla^2 G - G \nabla^2 \phi] dV = \iint_S \left(\phi \frac{\partial G}{\partial n} - G \frac{\partial \phi}{\partial n} \right) dS \quad (7)$$

Integrating both sides of (7) with respect to τ from 0^- to t^+ and using the properties of $G(P, Q, t-\tau)$ and the fact that ϕ satisfies the Laplace equation everywhere in the fluid domain gives:

$$\begin{aligned} \phi(P, t) = & -\frac{1}{4\pi} \int_0^t d\tau \iint_S dS \left(\phi(Q, \tau) \frac{\partial G(P, Q, t-\tau)}{\partial n_Q} \right. \\ & \left. - G(P, Q, t-\tau) \frac{\partial \phi(Q, \tau)}{\partial n_Q} \right) \end{aligned} \quad (8)$$

There is no contribution to the right hand side from the surfaces at infinity because both G and ϕ vanish at infinity.

The contribution to (8) from the surface integral over the free surface can be reduced to a line integral about the waterline of the vessel. From equation (2) it is found that the free surface boundary condition gives

$$\frac{\partial}{\partial n} \equiv \frac{\partial}{\partial \zeta} = -\frac{1}{g} \left(\frac{\partial}{\partial \tau} - U_0 \frac{\partial}{\partial \xi} \right)^2 \quad \text{on } z = 0$$

Hence the contribution to (8) from the free surface may be written:

$$\begin{aligned} \phi_F = & \frac{1}{4\pi g} \int_0^t d\tau \iint_{S_F} dS \left[\phi(Q, \tau) \left(\frac{\partial}{\partial \tau} - U_0 \frac{\partial}{\partial \xi} \right)^2 G(P, Q, t-\tau) \right. \\ & \left. - G(P, Q, t-\tau) \left(\frac{\partial}{\partial \tau} - U_0 \frac{\partial}{\partial \xi} \right)^2 \phi(Q, \tau) \right] \end{aligned} \quad (9)$$

ϕ_F may be separated into two parts which can be reduced independently as follows:

$$\phi_F = \phi_{F1} + \phi_{F2} \quad (10)$$

$$\begin{aligned} \phi_{F1} = & \frac{1}{4\pi g} \int_0^t d\tau \iint_{S_F} dS \left[\phi(Q, \tau) G_{\tau\tau}(P, Q, t-\tau) \right. \\ & \left. - G(P, Q, t-\tau) \phi_{\tau\tau}(Q, \tau) \right] \\ = & \frac{1}{4\pi g} \iint_{S_F} dS \int_0^t d\tau \frac{\partial}{\partial \tau} \left[\phi(Q, \tau) G_{\tau}(P, Q, t-\tau) \right. \\ & \left. - G(P, Q, t-\tau) \phi_{\tau}(Q, \tau) \right] \\ = & \frac{1}{4\pi g} \iint_{S_F} dS \left[\phi(Q, \tau) G_{\tau}(P, Q, t-\tau) \right. \\ & \left. - G(P, Q, t-\tau) \phi_{\tau}(Q, \tau) \right] \Big|_0^t \end{aligned} \quad (11)$$

where the subscript denotes differentiation with respect to the given variable. Because of the initial conditions on ϕ and G the last expression equals zero. The ϕ_{F2} term is

$$\begin{aligned} \phi_{F2} = & \frac{1}{4\pi g} \int_0^t d\tau \iint_{S_F} dS [U_0^2 (\phi G_{\xi\xi} - G\phi_{\xi\xi}) \\ & - 2U_0 (\phi G_{\xi\tau} - G\phi_{\xi\tau})] \end{aligned}$$

Integrating one half of the last term by parts with respect to τ gives:

$$\begin{aligned} \phi_{F2} = & \frac{1}{4\pi g} \int_0^t d\tau \iint_{S_F} dS [U_0^2 (\phi G_{\xi\xi} - G\phi_{\xi\xi}) \\ & - U_0 (\phi_{\xi} G_{\tau} - G_{\xi} \phi_{\tau} + \phi G_{\xi\tau} - G\phi_{\xi\tau})] \\ = & \frac{1}{4\pi g} \int_0^t d\tau \iint_{S_F} dS \frac{\partial}{\partial \xi} [U_0^2 (\phi G_{\xi} - \phi_{\xi} G) \\ & - U_0 (\phi G_{\tau} - \phi_{\tau} G)] \end{aligned} \quad (12)$$

Applying Stokes' theorem to the last form of (12) yields

$$\begin{aligned} \phi_{F2} = & - \frac{1}{4\pi g} \int_0^t d\tau \int_{\Gamma} d\eta [U_0^2 (\phi G_{\xi} - \phi_{\xi} G) \\ & - U_0 (\phi G_{\tau} - \phi_{\tau} G)] \end{aligned} \quad (13)$$

where Γ = intersection of the mean hull surface and the plane $z = 0$. The positive sense of the line integral is in the counter-clockwise direction.

The final result for ϕ at a point in the fluid is

$$\begin{aligned} \phi(P,t) = & - \frac{1}{4\pi} \int_0^t d\tau \iint_{S_0} dS \left[\phi \frac{\partial G}{\partial n} - G \frac{\partial \phi}{\partial n} \right] \\ + & \frac{1}{4\pi g} \int_0^t d\tau \int_{\Gamma} d\eta \left(U_0^2 \left(G \frac{\partial \phi}{\partial \xi} - \phi \frac{\partial G}{\partial \xi} \right) - U_0 \left(\frac{\partial \phi}{\partial \tau} G - \phi \frac{\partial G}{\partial \tau} \right) \right) \end{aligned} \quad (14)$$

Although equation (14) is derived for constant forward speed along a straight trajectory, it may easily be generalized for arbitrary speed and trajectory (see Appendix A).

In the usual manner of potential theory equation (14) can be reduced to a pure source distribution of density $\sigma(Q, \tau)$ by considering the interior flow and subtracting it from equation (14). The final result is:

$$\begin{aligned} \phi(P, t) = & - \frac{1}{4\pi} \int_0^t d\tau \iint_{S_0} dS G(P, Q, t-\tau) \sigma(Q, \tau) \\ & - \frac{U_0^2}{4\pi g} \int_0^t d\tau \int_{\Gamma} d\eta \sigma(Q, \tau) n_1 G(P, Q, t-\tau) \end{aligned} \quad (15)$$

where n_1 is the x component of the normal vector.

For the case of steady state oscillation of frequency ω at constant forward speed, equation (15) can be reduced by setting $\sigma(Q, \tau) = \sigma(Q) e^{i\omega\tau}$. Making the substitutions and interchanging the orders of integration it can be found:

$$\begin{aligned} \phi(P) = & - \frac{1}{4\pi} \iint_{S_0} dS \sigma(Q) \int_0^t d\tau e^{i\omega\tau} G(P, Q, t-\tau) \\ & - \frac{U_0^2}{4\pi g} \int_{\Gamma} d\eta \sigma(Q) n_1 \int_0^t d\tau e^{i\omega\tau} G(P, Q, t-\tau) \end{aligned} \quad (16)$$

As $t \rightarrow \infty$ Wehausen and Laitone (1960) show that the time integration of the Green function reduces to the usual Green function for a source translating with constant forward speed and sinusoidal strength. In this case equation (16) is identical to the form of the potential used by Chang (1977).

An integral equation for the source strength may be found by differentiating (15) with respect to the normal on the body and setting it equal to the body boundary condition. Thus, we may write:

$$\begin{aligned} \frac{\partial \phi}{\partial n_p} = & - \frac{\sigma(P, t)}{2} - \frac{1}{4\pi} \int_0^t d\tau \iint_{S_0} dS \sigma \frac{\partial G}{\partial n_p} \\ & - \frac{U_0^2}{4\pi g} \int_0^t d\tau \int_{\Gamma} d\eta \sigma n_1 \frac{\partial G}{\partial n_p} \end{aligned} \quad (17)$$

II.3 Decomposition of the Problem by Introducing the Impulse Response Function

Since the body boundary condition is represented by the sum of six individual components, it is useful to divide the potential into six individual problems each of which satisfies:

$$\frac{\partial \phi_k}{\partial n} = n_k \zeta_k + m_k \zeta_k \quad (18)$$

The coefficients m_k as defined in (3) contain the influence of the steady velocity field on the body boundary condition.

One feature of the problem which complicates its

solution is that the right hand side in equation (18) involves the unknown body motion. That is, the hydrodynamic problem is coupled with the dynamics equation of the body.

A method of decomposition is to model the ship as a linear system, the input being the ship motion in each of its six modes and the output the generalized hydrodynamic force. Contrary to the infinite fluid case, where the fluid motion stops when the body stops, in our case the presence of the free surface causes the linear system to have memory. As is widely used in many similar cases, it is possible to define an impulse response function for each mode of motion. This impulse response function completely characterizes the linear system model since the hydrodynamic force due to an arbitrary motion may be found by linear superposition.

In order to define the impulse response function, consider the fictitious case where at $t = 0$ the ship jumps instantaneously from 0 to 1 in the k th mode. This jump is impulsive, so that the velocity is $\dot{\zeta}_k = \delta(t)$. The force exerted on the body by the surrounding fluid for this special case of motion is the impulse response function. Due to the waves generated by the body motion this force persists indefinitely in time.

We now proceed to formulate the hydrodynamic problem which results from this impulsive motion. The velocity

potential, which we denote by ϕ_k , must satisfy the body boundary condition:

$$\frac{\partial \phi_k}{\partial n} = n_k \delta(t) + m_k H(t) \quad (19)$$

The body boundary condition (19) suggests that the potential ϕ_k can be decomposed into an impulsive and a memory part such that:

$$\phi_k(P,t) = \psi_{1k}(P)\delta(t) + \chi_k(P,t) \quad (20)$$

If we set

$$\frac{\partial \psi_{1k}}{\partial n} = n_k \quad \text{on } S_0 \quad (21)$$

$$\frac{\partial \chi_k}{\partial n} = m_k \quad \text{on } S_0$$

then the body boundary condition (19) is satisfied for all time.

The integral equations which must be solved to determine ψ_{1k} and χ_k are found by applying integral equation (14) on the body surface and substituting equations (20) and (21). Gathering terms proportional to $\delta(t)$ gives an integral equation for ψ_{1k} and the remaining terms yield an equation for χ_k . The details of the derivation may be found in Appendix B; the final results are:

$$\begin{aligned} \psi_{1k}(P) + \frac{1}{2\pi} \iint_{S_0} dS \psi_{1k} \frac{\partial}{\partial n_Q} \left(\frac{1}{r} - \frac{1}{r'} \right) \\ = \frac{1}{2\pi} \iint_{S_0} dS \left(\frac{1}{r} - \frac{1}{r'} \right) n_k \end{aligned} \quad (22)$$

$$\begin{aligned}
x_k(P, t) &+ \frac{1}{2\pi} \iint_{S_0} dS x_k \frac{\partial}{\partial n_Q} \left(\frac{1}{r} - \frac{1}{r'} \right) \\
&+ \frac{1}{2\pi} \int_0^t d\tau \iint_{S_0} dS x_k \frac{\partial \tilde{G}(P, Q, t-\tau)}{\partial n_Q} \\
&+ \frac{U_0^2}{2\pi g} \int_0^t d\tau \int_{\Gamma} d\eta \left(x_k \frac{\partial \tilde{G}}{\partial \xi} - \tilde{G} \frac{\partial x_k}{\partial \xi} \right) \\
&- \frac{U_0}{\pi g} \int_0^t d\tau \int_{\Gamma} d\eta x_k \frac{\partial \tilde{G}}{\partial \tau} \\
&= \frac{1}{2\pi} \iint_{S_0} dS m_k \left(\frac{1}{r} - \frac{1}{r'} \right) \\
&+ \frac{1}{2\pi} \int_0^t d\tau \iint_{S_0} dS m_k \tilde{G}(P, Q, t-\tau) \\
&+ \frac{1}{2\pi} \iint_{S_0} dS n_k \tilde{G}(P, Q, t) \\
&- \frac{1}{2\pi} \iint_{S_0} dS \psi_{1k} \frac{\partial \tilde{G}(P, Q, t)}{\partial n_Q} \tag{23}
\end{aligned}$$

The ψ_{1k} problem describes the fluid motion during the impulsive stage and may be interpreted as an infinite fluid problem satisfying

$$\psi_{1k} = 0 \quad \text{on} \quad z = 0$$

$$\frac{\partial \psi_{1k}}{\partial n} = n_k \quad \text{on} \quad S_0$$

$$\nabla \psi_{1k} \rightarrow 0 \quad \text{at} \quad \infty$$

The χ_k potential represents the motion of the fluid subsequent to the initial impulse and can be considered as composed of two components. The first results because of a change in body orientation due to the impulse in velocity. After the impulse in velocity the body will have a unit displacement in the k^{th} mode, which, in the presence of the steady velocity flow field, results in a change of fluid velocity on the body surface. In order for the body boundary condition to remain satisfied this change must be cancelled out. Therefore, $\partial\chi_k/\partial n$ must have the value m_k on the body surface for all $t > 0$.

The second component is the result of the impulsive velocity (the ψ_{1k} problem) inducing a disturbance into the flow field which in subsequent times will propagate as a wave motion away from the body. Consequently, χ_k will satisfy the complete free surface condition for $t > 0$. At $t = 0$ χ_k will meet the following initial conditions

$$\chi_k = 0 \quad \text{on } z = 0$$

$$\frac{\partial\chi_k}{\partial t} = -g \frac{\partial\psi_{1k}}{\partial z} \quad \text{on } z = 0$$

To aid in computational efficiency it is convenient to explicitly identify the two components of χ_k as

$$\chi_k(P, t) = \psi_{2k}(P) H(t) + \bar{\chi}_k(P, t) \quad (24)$$

In equation (24) the $\psi_{2k}(P)$ function represents the value of χ_k during the impulsive phase of the motion. It satisfies the following boundary conditions:

$$\begin{aligned} \frac{\partial \psi_{2k}}{\partial n} &= m_k \quad \text{on } S_0 \\ \psi_{2k} &= 0 \quad \text{on } z = 0 \\ \nabla \psi_{2k} &\rightarrow 0 \quad \text{at } \infty \end{aligned} \quad (25)$$

In order for χ_k to meet the proper boundary conditions it is not difficult to show that $\bar{\chi}_k(P, t)$ satisfies the following conditions:

$$\begin{aligned} \bar{\chi}_k &= 0 \quad \text{at } t = 0 \\ \frac{\partial \bar{\chi}_k}{\partial t} &= -g \frac{\partial \psi_{1k}}{\partial z} \quad \text{on } z = 0 \text{ at } t = 0 \\ \frac{\partial \bar{\chi}_k}{\partial n} &= 0 \quad \text{on } S_0 \text{ for } t > 0 \\ \left(\left(\frac{\partial}{\partial t} - U_0 \frac{\partial}{\partial x} \right)^2 + g \frac{\partial}{\partial z} \right) (\bar{\chi}_k + \psi_{2k}) &= 0 \quad \text{on } z = 0 \\ &\quad \text{for } t > 0 \end{aligned} \quad (26)$$

From the boundary conditions on the free surface and the integral equation for $\bar{\chi}_k$ it can be shown that

$$\frac{\partial^2 \bar{\chi}_k}{\partial t^2} = -g \frac{\partial \psi_{2k}}{\partial z} \quad \text{on } z = 0 \quad t = 0 \quad (27)$$

The integral equation for $\psi_{2k}(P)$ is found by taking the limit of the integral equation for χ_k (equation (23)) at $t = 0$. This gives

$$\begin{aligned}
\psi_{2k}(P) + \frac{1}{2\pi} \iint_{S_0} dS \psi_{2k}(Q) \frac{\partial}{\partial n_Q} \left(\frac{1}{r} - \frac{1}{r'} \right) \\
= \frac{1}{2\pi} \iint_{S_0} dS m_k \left(\frac{1}{r} - \frac{1}{r'} \right)
\end{aligned} \tag{28}$$

Subtracting (28) from (23) gives the following integral equation for $\bar{X}_k(P, t)$:

$$\begin{aligned}
\bar{X}_k(P, t) + \frac{1}{2\pi} \iint_{S_0} dS \bar{X}_k \frac{\partial}{\partial n_Q} \left(\frac{1}{r} - \frac{1}{r'} \right) \\
+ \frac{1}{2\pi} \int_0^t d\tau \iint_{S_0} dS \bar{X}_k \frac{\partial \tilde{G}(P, Q, t-\tau)}{\partial n_Q} \\
+ \frac{U_0^2}{2\pi g} \int_0^t d\tau \int_{\Gamma} d\eta \left(\bar{X}_k \frac{\partial \tilde{G}}{\partial \xi} - \tilde{G} \frac{\partial \bar{X}_k}{\partial \xi} \right) \\
- \frac{U_0}{\pi g} \int_0^t d\tau \int_{\Gamma} d\eta \bar{X}_k \frac{\partial \tilde{G}(P, Q, t-\tau)}{\partial \tau} \\
= \frac{1}{2\pi} \int_0^t d\tau \iint_{S_0} dS m_k \tilde{G}(P, Q, t-\tau) \\
+ \frac{1}{2\pi} \iint_{S_0} dS n_k \tilde{G}(P, Q, t) \\
- \frac{1}{2\pi} \iint_{S_0} dS \psi_{1k} \frac{\partial \tilde{G}(P, Q, t)}{\partial n_Q} \\
- \frac{1}{2\pi} \int_0^t d\tau \iint_{S_0} dS \psi_{2k} \frac{\partial \tilde{G}(P, Q, t-\tau)}{\partial n_Q}
\end{aligned} \tag{29}$$

The potential for an arbitrary forced motion in the k^{th} direction is found as the convolution of $\phi_k(P, t)$ with the velocity of the motion. Using equations (19) and (24),

the expression for the velocity potential due to arbitrary motion becomes:

$$\begin{aligned}
 \phi_k(P, t) &= \int_0^t d\tau \phi_k(P, t-\tau) \dot{\zeta}_k(\tau) \\
 &= \psi_{1k}(P) \dot{\zeta}_k(t) + \psi_{2k}(P) \zeta_k(t) \\
 &\quad + \int_0^t d\tau \bar{\chi}_k(P, t-\tau) \dot{\zeta}_k(\tau)
 \end{aligned} \tag{30}$$

where the integral equations which must be solved to find $\psi_{1k}(P)$, $\psi_{2k}(P)$ and $\bar{\chi}_k(P, t)$ are given by (22), (28) and (29) respectively. We must show that $\phi_k(P, t)$ satisfies the body boundary condition, the free surface condition, and the conditions at infinity for all t .

Taking the normal derivative of ϕ_k on the body we find:

$$\begin{aligned}
 \frac{\partial \phi_k}{\partial n} &= \frac{\partial \psi_{1k}(P)}{\partial n} \dot{\zeta}_k(t) + \frac{\partial \psi_{2k}(P)}{\partial n} \zeta_k(t) \\
 &\quad + \int_0^t d\tau \dot{\zeta}_k(t-\tau) \frac{\partial \bar{\chi}_k(P, t)}{\partial n} \\
 &= n_k \dot{\zeta}_k(t) + m_k \zeta_k(t)
 \end{aligned}$$

where the last equality follows by substituting the normal

derivatives $\frac{\partial \psi_{1k}}{\partial n}$, $\frac{\partial \psi_{2k}}{\partial n}$, $\frac{\partial \bar{\chi}_k}{\partial n}$ with their values. This

proves that the potential ϕ_k satisfies the body boundary condition. It also satisfies the condition at infinity since ψ_{1k} , ψ_{2k} , $\bar{\chi}_k$ satisfy it.

On the free surface $z=0$ we compute the terms in the

boundary conditions:

$$\begin{aligned}
 & \frac{\partial^2 \phi_k}{\partial t^2} + U^2 \frac{\partial^2 \phi_k}{\partial x^2} - 2 U \frac{\partial^2 \phi_k}{\partial x \partial t} + g \frac{\partial \phi_k}{\partial z} = \\
 & = \psi_{1k}(P) \zeta_k(t) + \psi_{2k}(P) \ddot{\zeta}_k(t) + \left. \frac{\partial \bar{X}_k}{\partial t} \right|_{t=0} \dot{\zeta}_k(t) \\
 & \quad + \bar{X}_k(0) \ddot{\zeta}_k(t) + \int_0^t d\tau \frac{\partial^2 \bar{X}_k(t-\tau)}{\partial t^2} \dot{\zeta}_k(\tau) \\
 & + U^2 \frac{\partial^2 \psi_{1k}}{\partial x^2} \dot{\zeta}_k(t) + U^2 \frac{\partial^2 \psi_{2k}}{\partial x^2} \zeta_k(t) \\
 & \quad + U^2 \int_0^t d\tau \frac{\partial^2 \bar{X}_k(t-\tau)}{\partial x^2} \dot{\zeta}_k(\tau) - \\
 & - 2 U \frac{\partial \psi_{1k}}{\partial x} \ddot{\zeta}_k(t) - 2 U \frac{\partial \psi_{2k}}{\partial x^2} \dot{\zeta}_k(t) - 2 U \frac{\partial \bar{X}_k(0)}{\partial x} \zeta_k(t) - \\
 & - 2 U \int_0^t d\tau \frac{\partial^2 \bar{X}_k(t-\tau)}{\partial x \partial t} \dot{\zeta}_k(\tau) + g \frac{\partial \psi_{1k}}{\partial z} \zeta_k(t) \\
 & \quad + g \frac{\partial \psi_{2k}}{\partial z} \dot{\zeta}_k(t) + g \int_0^t d\tau \frac{\partial \bar{X}_k(t-\tau)}{\partial z} \dot{\zeta}_k(\tau)
 \end{aligned}$$

Rearranging terms we write:

$$\begin{aligned}
 & \frac{\partial^2 \phi_k}{\partial t^2} + U^2 \frac{\partial^2 \phi_k}{\partial x^2} - 2 U \frac{\partial^2 \phi_k}{\partial x \partial t} + g \frac{\partial \phi_k}{\partial z} = \\
 & = \psi_{1k}(P) \zeta_k(t) + \psi_{2k}(P) \ddot{\zeta}_k(t) + \bar{X}_k(0) \ddot{\zeta}_k(t) \\
 & \quad + U^2 \frac{\partial^2 \psi_{1k}}{\partial x^2} \dot{\zeta}_k(t) +
 \end{aligned}$$

$$\begin{aligned}
& + U^2 \frac{\partial^2 \psi_{2k}}{\partial x^2} \zeta_k(t) - 2 U \frac{\partial \psi_{1k}}{\partial x} \dot{\zeta}_k(t) + \frac{\partial \psi_{2k}}{\partial x} \dot{\zeta}_k(t) \\
& - 2 U \frac{\partial \bar{X}_k(0)}{\partial x} \zeta_k(t) + \left\{ \frac{\partial \bar{X}_k}{\partial t} \right|_{t=0} \dot{\zeta}_k(t) + g \frac{\partial \psi_{1k}}{\partial z} \zeta_k(t) \} + \\
& + \int_0^t d\tau \left\{ \frac{\partial^2 \bar{X}_k(t-\tau)}{\partial t^2} + U^2 \frac{\partial^2 \bar{X}_k(t-\tau)}{\partial x^2} - 2 U \frac{\partial^2 \bar{X}_k(t-\tau)}{\partial x \partial t} + \right. \\
& \left. + g \left(\frac{\partial \bar{X}_k(t-\tau)}{\partial z} + \frac{\partial \psi_{2k}}{\partial z} \right) \right\} \dot{\zeta}_k(\tau)
\end{aligned}$$

The first eight terms each equal zero from conditions (25) and (26). The sum of the two terms in braces is zero from condition (26). Finally the integral term equals zero from condition (26). Consequently the right hand side is zero and the potential ϕ_k satisfies the free surface condition (2).

The form of the general potential (30) can be directly compared to the formulation developed by Ogilvie (1964, equation (11)). Ogilvie has four potentials ψ_{1k} , χ_{1k} , ψ_{2k} , and χ_{2k} . His ψ_{1k} and ψ_{2k} are identical to the presently defined ψ_{1k} and ψ_{2k} . Ogilvie's memory potentials, χ_{1k} and χ_{2k} , have been combined into the present \bar{X}_k . In fact, as we show in Appendix C

$$\bar{X}_k = \chi_{1k} + \int_0^t d\tau \chi_{2k} \quad (31)$$

After determining the hydrodynamic forces acting on the body, Ogilvie uses an integration by parts to combine the effects of χ_{1k} and χ_{2k} into a single memory function K_{jk} . In the present work, χ_{1k} and χ_{2k} have just been combined at an earlier stage of the development. Integral equation (29) for $\bar{\chi}_k$ can be obtained by combining the integral equations which would have to be solved to determine Ogilvie's χ_{1k} and χ_{2k} . The advantage of the present formulation is that it saves computational effort, since only one integral equation needs to be solved.

II.4 Pressure and Force Calculation

The unsteady pressure in the fluid is given by the linearized Bernoulli equation:

$$p = -\rho \frac{\partial \phi_k}{\partial t} - \rho \underline{W} \cdot \nabla \phi_k \quad (32)$$

The forces acting on the body are found by integrating the pressure over the instantaneous underwater hull surface. However, it is much more convenient to be able to integrate the pressure over the mean position of the hull. To do this, the pressure is expanded in a Taylor series about the undisturbed hull position and integrated. Furthermore, because of the waves on the free surface and the motion of the hull, an additional contribution is obtained from a line integral around the waterline of the undisturbed hull. The details of this derivation may be found in Ogilvie (1964). The resulting expressions for the

forces involve the usual pressure integral terms over the undisturbed hull surface given in equation (33) and extra terms involving products of the steady perturbation velocities and gradients of the unsteady potential. These extra terms are generally assumed small and neglected. Apparently, there are no numerical results to verify this assumption. Since the extra terms increase the complexity of the expressions for the hydrodynamic forces acting on the body, and because they will all equal zero under the simplifying assumption made for the numerical calculations presented in this paper, the extra term will be left off in the subsequent derivation. The reduced expression for the linearized forces acting on the body is

$$\begin{aligned}
 F_{jk}(t) &\approx -\rho \iint_{S_0} dS p n_j \\
 &= -\rho \iint_{S_0} dS \frac{\partial \phi_k}{\partial t} n_j - \rho \iint_{S_0} dS (\underline{W} \cdot \nabla \phi_k) n_j \quad (33)
 \end{aligned}$$

The second term of (33) involves derivatives of the ϕ_k potential, a quantity which is difficult to evaluate. This gradient of the potential may be eliminated using the following theorem developed by Tuck and presented in Ogilvie and Tuck (1969) (or see Ogilvie (1977)):

$$\iint_{S_0} dS [m_j \phi_k + n_j (\underline{W} \cdot \nabla \phi_k)] = - \int_{\Gamma} d\ell n_j \phi_k (\underline{\ell} \times \underline{n}) \cdot \underline{W} \quad (34)$$

where $\underline{\ell}$ = unit vector tangential to the waterline curve Γ . For wall-sided vessels $(\underline{\ell} \times \underline{n}) = \underline{k}$, the unit vector in

the z-direction. Applying (34) to the second term in (33), the expression for the unsteady forces acting on the hull is:

$$\begin{aligned}
 F_{jk}(t) = & -\rho \iint_{S_0} dS \frac{\partial \phi_k}{\partial t} n_j + \rho \iint_{S_0} dS \phi_k m_j \\
 & + \rho \int_{\Gamma} d\ell n_j \phi_k (\underline{\ell} \times \underline{n}) \cdot \underline{W}
 \end{aligned} \tag{35}$$

Equation (35) can be reduced further by using the form of ϕ_k given in (30). The final expression for the unsteady force acting on the body in the j^{th} direction due to arbitrary motion in the k^{th} direction is

$$\begin{aligned}
 F_{jk}(t) = & -\mu_{jk} \ddot{\zeta}_k(t) - b_{jk} \dot{\zeta}_k(t) - c_{jk} \zeta_k(t) \\
 & - \int_0^t d\tau K_{jk}(t - \tau) \dot{\zeta}_k(\tau)
 \end{aligned} \tag{36}$$

where

$$\begin{aligned}
 \mu_{jk} &= \rho \iint_{S_0} dS \psi_{1k} n_j \\
 b_{jk} &= \rho \left[\iint_{S_0} dS \psi_{2k} n_j - \iint_{S_0} dS \psi_{1k} m_j \right. \\
 &\quad \left. - \int_{\Gamma} d\ell \psi_{1k} n_j (\underline{\ell} \times \underline{n}) \cdot \underline{W} \right] \\
 c_{jk} &= \rho \left[-\iint_{S_0} dS \psi_{2k} m_j \right. \\
 &\quad \left. - \int_{\Gamma} d\ell \psi_{2k} n_j (\underline{\ell} \times \underline{n}) \cdot \underline{W} \right] \\
 K_{jk}(t) &= \rho \left[+ \iint_{S_0} dS \frac{\partial \bar{x}_k(Q, t)}{\partial t} n_j \right. \\
 &\quad - \iint_{S_0} dS \bar{x}_k(Q, t) m_j \\
 &\quad \left. - \int_{\Gamma} d\ell n_j \bar{x}_k(Q, t) (\underline{\ell} \times \underline{n}) \cdot \underline{W} \right]
 \end{aligned}$$

Equation (36) is in a form useful for the calculation of ship motions because all of the coefficients are independent of the past history of the unsteady motion. The coefficient μ_{jk} is a constant depending only on ship geometry, b_{jk} and c_{jk} are constants which depend on ship geometry and forward speed. In the equations of motion for the vessel the c_{jk} term adds to the hydrostatic restoring force coefficient. The μ_{jk} and b_{jk} are part of the added mass and damping terms respectively. All the memory of the fluid response is contained in the function $K_{jk}(t)$, which is dependent on ship geometry, speed, and time.

The coefficients μ_{jk} , b_{jk} , c_{jk} and K_{jk} can be directly related to the more usual frequency-domain coefficients. Consider a motion amplitude of the form

$$\begin{aligned} \zeta_k(t) &= 0 & t < 0 \\ &= e^{i\omega t} & t > 0 \end{aligned} \quad (37)$$

Substituting the motion (37) into the force equation (36) and taking the limit as time goes to infinity yields

$$\begin{aligned} F_{jk}(t) &= [\omega^2 \mu_{jk} - i\omega b_{jk} - c_{jk} \\ &\quad - \int_0^{\infty} d\tau i\omega e^{-i\omega\tau} K_{jk}(\tau)] e^{i\omega t} \end{aligned} \quad (38)$$

In the frequency domain, the hydrodynamic force on the body for sinusoidal motion is given by

$$F_{jk} = [\omega^2 A_{jk}(\omega) - i\omega B_{jk}(\omega) - C_{jk}] e^{i\omega t} \quad (39)$$

where

$A_{jk}(\omega)$ = added mass coefficient in the frequency domain

$B_{jk}(\omega)$ = damping coefficient in the frequency domain

C_{jk} = restoring force coefficient

Equating the real and imaginary parts of (38) and (39) gives the following expressions for A_{jk} , B_{jk} , and C_{jk} in terms of the time-domain coefficients:

$$A_{jk}(\omega) = \mu_{jk} - \frac{1}{\omega} \int_0^{\infty} d\tau K_{jk}(\tau) \sin \omega \tau$$

$$B_{jk}(\omega) = b_{jk} + \int_0^{\infty} d\tau K_{jk}(\tau) \cos \omega \tau$$

$$C_{jk} = c_{jk} \tag{40}$$

As can be seen from equation (40), μ_{jk} and b_{jk} are the frequency independent parts of the added mass and damping respectively. All frequency dependence of the added mass and damping are contained in the memory function K_{jk} . The coefficient C_{jk} is a frequency independent modification to the hydrostatic restoring force coefficient.

II.5 The Integral Equation for a Source Distribution

The same type of decomposition, which has just been developed for the potential method, can also be used for the source distribution technique. The development exactly parallels the potential method. Therefore, only the final expressions will be given here. Similar to (20) and (24)

the source strength and potential are decomposed into

$$\sigma_k(P, t) = \alpha_k(P)\delta(t) + \beta_k(P)H(t) + \gamma_k(P, t) \quad (41)$$

and

$$\begin{aligned} \psi_{1k}(P) &= -\frac{1}{4\pi} \iint_{S_0} dS \alpha_k(Q) \left(\frac{1}{r} - \frac{1}{r'} \right) \\ \psi_{2k}(P) &= -\frac{1}{4\pi} \iint_{S_0} dS \beta_k(Q) \left(\frac{1}{r} - \frac{1}{r'} \right) \\ \bar{x}_k(P, t) &= -\frac{1}{4\pi} \int_0^t d\tau \iint_{S_0} dS \gamma_k(Q, \tau) G(P, Q, t-\tau) \\ &\quad - \frac{U_0^2}{4\pi g} \int_0^t d\tau \int_{\Gamma} d\eta n_l \gamma_k(q, \tau) \tilde{G}(P, Q, t-\tau) \\ &\quad - \frac{1}{4\pi} \iint_{S_0} dS \gamma_k(Q) \tilde{G}(P, Q, t) \\ &\quad - \frac{1}{4\pi} \int_0^t d\tau \iint_{S_0} dS \beta_k(Q) \tilde{G}(P, Q, t-\tau) \end{aligned} \quad (42)$$

where

$\alpha_k(P)$ = part of source strength due to impulsive velocity in k^{th} direction

$\beta_k(P)$ = part of source strength due to displacement in k^{th} direction

$\gamma_k(P, t)$ = time dependent part of source strength due to motion in the k^{th} direction

$\psi_{1k}, \psi_{2k}, \bar{x}_k$ = same meaning as in (20) and (24)

The integral equations for α_k , β_k and γ_k are found by gathering terms after substituting (41) into (17) and using (19). The final results are:

$$-\frac{\alpha_k(P)}{2} - \frac{1}{4\pi} \iint_{S_0} dS_Q \alpha_k(Q) \frac{\partial}{\partial n_P} \left(\frac{1}{r} - \frac{1}{r'} \right) = n_k \quad (43)$$

$$-\frac{\beta_k(P)}{2} - \frac{1}{4\pi} \iint_{S_0} dS_Q \beta_k(Q) \frac{\partial}{\partial n_P} \left(\frac{1}{r} - \frac{1}{r'} \right) = m_k \quad (44)$$

$$\begin{aligned} & -\frac{\gamma_k(P, t)}{2} - \frac{1}{4\pi} \iint_{S_0} dS_Q \gamma_k(Q, t) \frac{\partial}{\partial n_P} \left(\frac{1}{r} - \frac{1}{r'} \right) \\ & - \frac{1}{4\pi} \int_0^t d\tau \iint_{S_0} dS_Q \gamma_k(Q, \tau) \frac{\partial}{\partial n_P} \tilde{G}(P, Q, t-\tau) \\ & - \frac{U_0^2}{4\pi g} \int_0^t d\tau \int_{\Gamma} d\eta \, n_1 \gamma_k(Q, \tau) \frac{\partial}{\partial n_P} \tilde{G}(P, Q, t-\tau) \\ & = \frac{1}{4\pi} \iint_{S_0} dS_Q \alpha_k(Q) \frac{\partial}{\partial n_P} \tilde{G}(P, Q, t) \\ & + \frac{1}{4\pi} \int_0^t d\tau \iint_{S_0} dS_Q \beta_k(Q) \frac{\partial}{\partial n_P} \tilde{G}(P, Q, t-\tau) \end{aligned} \quad (45)$$

The source strength at any time for a prescribed motion is found by a convolution of σ_k and the motion velocity as follows.

$$\begin{aligned} \sum_k(P, t) &= \int_0^t d\tau \, \sigma_k(P, t-\tau) \dot{\zeta}(\tau) \\ &= \alpha_k(P) \dot{\zeta}(t) + \beta_k(P) \dot{\zeta}(t) \\ &+ \int_0^t d\tau \, \gamma_k(Q, t-\tau) \dot{\zeta}(\tau) \end{aligned} \quad (46)$$

The hydrodynamic forces acting on the body, the added mass, the damping and the hydrostatic restoring forces are found by substituting equations (42) into (36) and (40).

CHAPTER III
NUMERICAL METHODS

III.1 Approximate Representation of the Body
Surface by Plane Quadrilaterals

The integral equations for the potential method (eq. (22), (28) and (29)) or the source method (eq. (43), (44) and (45)) are solved numerically using a panel method. The body surface is described by a set of input points in the three-dimensional space. It is then replaced by an ensemble of plane quadrilateral elements each one defined by four input points. The first general routine for the technique was developed by Hess and Smith (1964). In their manner, the vertices of each panel are identified by the local numbering 1, 2, 3, 4 ordered in the clockwise direction. The two diagonal vectors are formed, the vector T_1 from point 1 to point 3 and the vector T_2 from point 2 to point 4. The normal vector on the panel is taken as the cross product of the diagonal vectors:

$$\underline{n} = \frac{\underline{T}_1 \times \underline{T}_2}{|\underline{T}_1 \times \underline{T}_2|}$$

In areas of compound curvature the four input points are not on the same plane. For those elements, the vertices of each panel are constructed by defining a plane

perpendicular to the normal vector and passing through the point whose coordinates are the averages of the coordinates of the four input points. The vertices are then obtained by projecting the input points on that plane. By this construction the resulting plane quadrilateral vertices are the closest to the input points in the least squares sense.

Most bodies of interest possess at least one symmetry plane. It is only necessary in that case to discretize the non-redundant fraction of the body. The remaining part is obtained by reflecting the panels.

III.2 Numerical Solution of the Integral

Equations for ψ_{1k} , ψ_{2k}

After approximating the arbitrary body surface by plane quadrilaterals, the unknown potential (or source) distribution is discretized by assuming a constant potential (or source) strength over each quadrilateral. This assumption reduces a continuous potential (or source) distribution over the body into a finite number of unknown potential (or source) strengths one for each quadrilateral. The integral equations are satisfied at collocation points giving a system of algebraic equations which are solved for the unknown potential (or source) strengths. It has been found (Hess and Smith (1964) or Doctors and Beck (1985)) that the location of the collocation point on each panel does not influence the results significantly. In this

work, the collocation points are chosen as the null point on each panel, that is the point, where the self-induced velocity on each panel is zero in its own plane in an infinite fluid.

In the presentation which follows only the numerical solution to the potential method will be discussed. The techniques used in the source method are very similar and therefore will be omitted.

The integral equations (22) and (28) for ψ_{1k} and ψ_{2k} contain no memory terms. Assuming constant values for ψ_{1k} and ψ_{2k} over each quadrilateral, equations (27) and (28) may be discretized as:

$$\sum_{m=1}^M A_{im} (\psi_{qk})_m = (B_q)_i \quad \begin{array}{l} i = 1, 2, \dots, M \\ q = 1, 2 \end{array} \quad (47)$$

where

M = number of quadrilateral elements

$(\psi_{qk})_m$ = strengths of ψ_{1k} , ψ_{2k} over the m^{th} element

$A_{im} = 1 \quad i = m$

$$= \frac{1}{2\pi} \iint_{S_m} dS \underline{n}_m \cdot \nabla \left(\frac{1}{r} - \frac{1}{r'} \right) \quad i \neq m$$

S_m = surface area of m^{th} quadrilateral

\underline{n}_m = unit normal vector to m^{th} quadrilateral

$$r^2 = (x_i - \xi)^2 + (y_i - \eta)^2 + (z_i - \zeta)^2$$

$$r'^2 = (x_i - \xi)^2 + (y_i - \eta)^2 + (z_i + \zeta)^2$$

x_i, y_i, z_i = coordinates of the i^{th} collocation point

$$(B_1)_i = \frac{1}{2\pi} \sum_{m=1}^M \iint_{S_m} dS \left(\frac{1}{r} - \frac{1}{r'} \right) (n_k)_m$$

$$(B_2)_i = \frac{1}{2\pi} \sum_{m=1}^M \iint_{S_m} dS \left(\frac{1}{r} - \frac{1}{r'} \right) (m_k)_m$$

$(n_k)_m$ $(m_k)_m$ are defined in eq. (3)

III.3 Numerical Solution of the Integral Equation for \bar{X}_k

The Integral Equation (29) for $\bar{X}_k(P,t)$ is a Volterra Integral Equation with respect to time. In order to solve it, a time stepping method must be used. This requires approximating the time integrals by a quadrature rule.

A different rule is used in the cases of zero and nonzero forward speed the reason being that in the case of zero forward speed the time integral of the Green function may be evaluated analytically.

The two different quadrature rules lead to different discretized forms of the integral equations. They are separately presented in the next two sections.

III.3a Case of Zero Forward Speed

For the special case of zero forward speed $m_{2k} \equiv 0$ from (3). Consequently ψ_{2k} is identically zero from eq. (25). Also the line integral terms vanish identically since they are multiplied by U_0 . As a result equation (29) simplifies to:

$$\bar{X}_k(P,t) + \frac{1}{2\pi} \iint_{S_0} dS \bar{X}_k \frac{\partial}{\partial n_Q} \left(\frac{1}{r} - \frac{1}{r'} \right)$$

$$\begin{aligned}
& + \frac{1}{2\pi} \int_0^t d\tau \iint_{S_0} dS \bar{X}_k \frac{\partial \tilde{G}(P, Q, t-\tau)}{\partial n_Q} \\
& = \frac{1}{2\pi} \iint_{S_0} dS n_k \tilde{G}(P, Q, t) - \frac{1}{2\pi} \iint_{S_0} dS \psi_{1k} \frac{\partial \tilde{G}(P, Q, t)}{\partial n_Q} \quad (48)
\end{aligned}$$

The integration over time can be done using a mid-point rule in which the value of the potential is approximated by the average value of the function over the interval. Thus, equation (48) is written

$$\begin{aligned}
& \bar{X}_k(P, t) + \frac{1}{2\pi} \iint_{S_0} dS \bar{X}_k(Q, t) \frac{\partial}{\partial n_Q} \left(\frac{1}{r} - \frac{1}{r'} \right) \\
& + \frac{1}{2\pi} \iint_{S_0} dS \left\{ \sum_{n=1}^N \frac{\bar{X}_k(Q, t_n) + \bar{X}_k(Q, t_{n-1})}{2} \cdot \int_{t_{n-1}}^{t_n} d\tau \frac{\partial}{\partial n_Q} \tilde{G}(P, Q, t-\tau) \right\} \\
& = - \frac{1}{2\pi} \iint_{S_0} dS \psi_k \frac{\partial}{\partial n_Q} \tilde{G}(P, Q, t) + \frac{1}{2\pi} \iint_{S_0} dS n_k \tilde{G}(P, Q, t) \quad (49)
\end{aligned}$$

The time integrals of the Green function memory part \tilde{G} can be performed exactly. As can be seen from equation (5) in the case where $U_0 = 0$, the argument R of the Bessel function J_0 is independent of time and only the factor $\sin(\sqrt{kg}(t-\tau))$ contains time. As a result in this case the time integral of the Green function may be found as:

$$\begin{aligned}
& \int_{t_1}^{t_2} \tilde{G}(P, Q, t-\tau) d\tau \\
& = \int_{t_1}^{t_2} d\tau \left[2 \int_0^{\infty} dk \sqrt{kg} \sin(\sqrt{kg}(t-\tau)) e^{k(z+\zeta)} J_0(kR) \right] \\
& = 2 \int_0^{\infty} dk \left[\cos \sqrt{kg}(t-t_2) - \cos \sqrt{kg}(t-t_1) \right] e^{k(z+\zeta)} J_0(kR)
\end{aligned}$$

The time stepping is started at $t_0 = 0$ where x_k equals zero. At each subsequent time step only $x_k(P, t_N)$ is unknown; all other values of $x_k(P, t)$ (i.e. $x_k(P, t_{N-1})$, $x_k(P, t_{N-2})$, ..., $x_k(P, 0)$) are known. By gathering terms, equation (33) may be rewritten to yield an equation for the unknown $x_k(P, t_N)$ at the latest (t_N) time step:

$$\begin{aligned}
 & \bar{x}_k(P, t_N) + \frac{1}{2\pi} \iint_{S_0} dS \bar{x}_k(Q, t_N) \frac{\partial}{\partial n_Q} \left(\frac{1}{r} - \frac{1}{r'} \right) \\
 & + \frac{1}{2\pi} \iint_{S_0} dS \frac{1}{2} \bar{x}_k(Q, t_N) \int_{t_{N-1}}^{t_N} d\tau \frac{\partial}{\partial n_Q} \bar{G}(P, Q, t-\tau) \\
 & = - \frac{1}{2\pi} \iint_{S_0} dS \psi_k \frac{\partial}{\partial n_Q} \bar{G}(P, Q, t_N) + \frac{1}{2\pi} \iint_{S_0} dS n_k \bar{G}(P, Q, t_N) \\
 & - \frac{1}{2\pi} \iint_{S_0} dS \frac{1}{2} \bar{x}_k(Q, t_{N-1}) \int_{t_{N-1}}^{t_N} d\tau \frac{\partial}{\partial n_Q} \bar{G}(P, Q, t - \tau) \\
 & - \frac{1}{2\pi} \iint_{S_0} dS \left\{ \sum_{n=1}^{N-1} \left[\frac{\bar{x}_k(Q, t_n) + \bar{x}_k(Q, t_{n-1})}{2} \right] \int_{t_{n-1}}^{t_n} d\tau \frac{\partial}{\partial n_Q} \bar{G}(P, Q, t-\tau) \right\}
 \end{aligned} \tag{50}$$

At each time step equation (50) may be solved using the same type of panel discretization used to solve for ψ_{1k} , ψ_{2k} . The linear simultaneous equations which must be solved are:

$$\sum_{m=1}^M A_{im} (\bar{x}_k(t_N))_m = B_i \quad i = 1, 2, \dots, M \tag{51}$$

where M = number of quadrilateral elements

N = number of time steps

$(\bar{\chi}_k(t_N))_m$ = value of $\bar{\chi}_k(P, t_N)$ over the m^{th} panel at the t_N time step

$$A_{im} = 1 + \frac{1}{4\pi} \iint_{S_m} dS \int_{t_{N-1}}^{t_N} d\tau \frac{\partial}{\partial n_Q} \bar{G}(P, Q, t - \tau) \quad i = m$$

$$= \frac{1}{2\pi} \iint_{S_m} dS \underline{n}_m \cdot \nabla \left(\frac{1}{r} - \frac{1}{r'} \right)$$

$$+ \frac{1}{4\pi} \iint_{S_m} dS \int_{t_{N-1}}^{t_N} d\tau \frac{\partial}{\partial n_Q} \bar{G}(P, Q, t - \tau) \quad i \neq m$$

$$B_i = - \frac{1}{2\pi} \sum_{m=1}^M \left[(\psi_k)_m \iint_{S_m} dS \underline{n}_m \cdot \nabla \bar{G} - (n_k)_m \iint_{S_m} dS \bar{G} \right]$$

$$+ \frac{1}{2} (\bar{\chi}_k(t_N))_m \iint_{S_m} dS \left\{ \int_{t_{N-1}}^{t_N} d\tau \underline{n}_m \cdot \nabla \bar{G}(P, Q, t_N - \tau) \right\}$$

$$+ \sum_{n=1}^{N-1} \left(\frac{(\bar{\chi}_k(t_N))_m + (\bar{\chi}_k(t_N))_m}{2} \right) \int_{t_{n-1}}^{t_n} d\tau \underline{n}_m \cdot \nabla \bar{G}(P, Q, t_N - \tau) \left. \right\}$$

A very useful property of (51) is that for constant time step size the kernel matrix, A_{im} , is independent of time; it need only be computed once at the beginning of the calculations. In fact, the first terms of A_{im} are identical to the kernel used to solve for ψ_{1k} and have been determined in that part of the computation. Since

A_{im} is independent of time, the kernel matrix and does not have to be inverted at each time step. For a sufficiently large number of panels this property results in a significant computational advantage over the frequency domain formulation where the kernel matrix has to be inverted for each frequency.

III. 3b Case of Non-zero Forward Speed

In this case the time integration of the Green function cannot be done exactly.

A trapezoidal rule is used to evaluate the convolution integrals with the result that:

$$\begin{aligned}
 \bar{X}_k(P,t) &+ \frac{1}{2\pi} \iint_{S_0} dS \bar{X}_k(Q,t) \frac{\partial}{\partial n_Q} \left(\frac{1}{r} - \frac{1}{r'} \right) \\
 &+ \frac{\Delta t}{2\pi} \sum_{n=1}^{N'} \iint_{S_0} dS \bar{X}_k(Q,t_n) \frac{\partial \tilde{G}(P,Q,t-t_n)}{\partial n_Q} \\
 &+ \sum_{n=1}^{N'} \Delta t \left[\frac{U_0^2}{2\pi g} \int_{\Gamma} dn \left(\bar{X}_k(Q,t_n) \frac{\partial \tilde{G}(P,Q,t-t_n)}{\partial \xi} \right. \right. \\
 &\quad \left. \left. - \tilde{G}(P,Q,t-t_n) \frac{\partial \bar{X}_k(Q,t_n)}{\partial \xi} \right) \right] \\
 &+ \frac{U_0}{\pi g} \int_{\Gamma} dn \bar{X}_k(Q,t_n) \frac{\partial \tilde{G}(P,Q,t-t_n)}{\partial t} \left. \right] \\
 &= \frac{1}{2\pi} \iint_{S_0} dS \left(n_k \tilde{G}(P,Q,t) - \psi_{1k} \frac{\partial \tilde{G}(P,Q,t)}{\partial n_Q} \right)
 \end{aligned}$$

$$+ \frac{\Delta t}{2\pi} \sum_{n=1}^N \iint_{S_0} (m_k \bar{G}(P, Q, t-t_n) - \psi_{2k} \frac{\partial \bar{G}(P, Q, t-t_n)}{\partial n_Q}) \quad (52)$$

where Δt = constant time step size and the prime on the summation symbol denotes that 1/2 weights are to be used for the end points of the trapezoidal integration rule.

The time stepping is started at $t_0 = 0$ where $\bar{\chi}_k$ equals zero. At each subsequent time step only $\bar{\chi}_k(P, t_N)$ is unknown; all other values of $\bar{\chi}_k(P, t)$ (i.e. $\bar{\chi}_k(P, t_{N-1})$, $\bar{\chi}_k(P, t_{N-2})$, ..., $\bar{\chi}_k(P, t_0)$) are known. Gathering terms, equation (48) may be rewritten to yield an equation for the unknown $\bar{\chi}_k(P, t_N)$ at the latest (t_N) time step:

$$\begin{aligned} \bar{\chi}_k(P, t_N) &+ \frac{1}{2\pi} \iint_{S_0} dS \bar{\chi}_k(Q, t_N) \frac{\partial}{\partial n_Q} \left(\frac{1}{r} - \frac{1}{r'} \right) \\ &+ \frac{\Delta t}{4\pi} \iint_{S_0} dS \bar{\chi}_k(Q, t_N) \frac{\partial \bar{G}(P, Q, 0)}{\partial n_Q} \\ &+ \frac{\Delta t}{2} \left[\frac{U_0^2}{2\pi g} \left(\int_{\Gamma} d\eta (\bar{\chi}_k(Q, t_N) \frac{\partial \bar{G}(P, Q, 0)}{\partial \xi} \right. \right. \\ &\quad \left. \left. - \bar{G}(P, Q, 0) \frac{\partial \bar{\chi}_k(Q, t_N)}{\partial \xi} \right) \right. \\ &\left. + \frac{U_0}{\pi g} \int_{\Gamma} d\eta \bar{\chi}_k(Q, t_N) \frac{\partial \bar{G}(P, Q, 0)}{\partial t} \right] \end{aligned}$$

$$\begin{aligned}
&= \frac{1}{2\pi} \iint_{S_0} dS \left(n_k \tilde{G}(P, Q, t_N) - \psi_{1k} \frac{\partial \tilde{G}(P, Q, t_N)}{\partial n_Q} \right) \\
&+ \frac{\Delta t}{2\pi} \sum_{n=1}^N \iint_{S_0} \left(m_k \tilde{G}(P, Q, t_N - t_n) \right. \\
&\quad \left. - \psi_{2k} \frac{\partial \tilde{G}(P, Q, t_N - t_n)}{\partial n_Q} \right) \tag{53} \\
&- \frac{\Delta t}{2\pi} \sum_{n=1}^{N-1} \iint_{S_0} dS \bar{\chi}_k(Q, t_n) \frac{\partial \tilde{G}(P, Q, t_N - t_n)}{\partial n_Q} \\
&- \Delta t \sum_{n=1}^{N-1} \left[\frac{U_0^2}{2\pi g} \left(\int_{\Gamma} d\eta \bar{\chi}_k(Q, t_n) \frac{\partial \tilde{G}(P, Q, t_N - t_n)}{\partial \xi} \right. \right. \\
&\quad \left. \left. - \tilde{G}(P, Q, t_N - t_n) \frac{\partial \bar{\chi}(Q, t_n)}{\partial \xi} \right) \right. \\
&\quad \left. + \frac{U_0}{\pi g} \int_{\Gamma} d\eta \bar{\chi}_k(Q, t_n) \frac{\partial \tilde{G}(P, Q, t_N - t_n)}{\partial t} \right]
\end{aligned}$$

Because $\partial \chi_k / \partial \xi$ is difficult to evaluate numerically, the term involving it is simplified based on a method used by Guevel and Bougis (1982). The term may be resolved into its components in the local ℓ - n - s coordinate system as shown in figure 1 and then reduced as follows:

$$\begin{aligned}
\int_{\Gamma} d\eta \frac{\partial \bar{\chi}}{\partial \xi} \tilde{G} &= \int_{\Gamma} d\eta (\underline{n} \cdot \underline{i}) \frac{\partial \bar{\chi}}{\partial n} \tilde{G} \\
&+ \int_{\Gamma} d\eta (\underline{s} \cdot \underline{i}) \frac{\partial \bar{\chi}}{\partial s} \tilde{G} + \int_{\Gamma} d\eta (\underline{\ell} \cdot \underline{i}) \frac{\partial \bar{\chi}}{\partial \ell} \tilde{G} \tag{54}
\end{aligned}$$

The first term is zero because $\partial \bar{\chi} / \partial n = 0$ on the body surface. For a wall sided body $(\underline{s} \cdot \underline{i}) = 0$ and the second

term equals zero. For the computed results in this paper, this term has been neglected for all cases based on the assumption that most bodies of interest are wall sided over most of their length. The third term can be integrated by parts to eliminate $\partial \bar{X} / \partial \xi$:

$$\begin{aligned}
 & \int_{\Gamma} d\eta \tilde{G}(P, Q, t-t_n) \frac{\partial \bar{X}_k(Q, t_n)}{\partial \xi} \\
 &= - \int_{\Gamma} d\eta \bar{X}_k(Q, t_n) \frac{\partial \tilde{G}(P, Q, t-t_n)}{\partial \xi} \quad (\underline{l} \cdot \underline{i}) \quad (55) \\
 & - \int_{\Gamma} d\ell \bar{X}_k(Q, t_n) \tilde{G}(P, Q, t-t_n) \frac{\partial}{\partial \ell} [(\underline{l} \cdot \underline{i}) (\underline{l} \cdot \underline{j})]
 \end{aligned}$$

At each time step equation (49) is solved using the same panel discretization used to solve for ψ_{1k} , ψ_{2k} . The line integral is evaluated by subdividing Γ into a series of straight line segments. The strength of \bar{X}_k on a line segment is assumed equal to the strength of the panel below it. The system of equations which must be solved at each time step has the form:

$$\sum_{m=1}^M A_{im} (\bar{X}_k(t_N))_m = B_i \quad i = 1, 2, \dots, M \quad (56)$$

where

M = number of quadrilateral elements

N = number of time steps

$(\bar{X}_k(t_N))_m$ = value of $\bar{X}_k(P, t)$ on the m^{th} panel at the t_N time step

$$\begin{aligned}
A_{im} &= 1 + \left\{ \frac{\Delta t U_0}{\pi} \int_{\Gamma_m} d\eta \frac{\partial}{\partial z} \frac{1}{r'} \right\} \quad i = m \\
&= \frac{1}{2\pi} \iint_{S_m} dS \underline{n}_m \cdot \nabla \left(\frac{1}{r} - \frac{1}{r'} \right) \\
&\quad + \left\{ \frac{\Delta t U_0}{\pi} \int_{\Gamma_m} d\eta \frac{\partial}{\partial z} \frac{1}{r'} \right\} \quad i \neq m
\end{aligned}$$

$$\begin{aligned}
B_i &= \frac{1}{2\pi} \sum_{m=1}^M \left\{ (n_k)_m \iint_{S_m} dS \tilde{G}(P, Q, t_N) \right. \\
&\quad \left. - (\psi_{1k})_m \iint_{S_m} dS \frac{\partial \tilde{G}(P, Q, t_N)}{\partial n_Q} \right) \\
&\quad + \frac{\Delta t}{2\pi} \sum_{n=1}^{N'} \left[(m_k)_m \iint_{S_m} dS \tilde{G}(P, Q, t_N - t_n) \right. \\
&\quad \left. - (\psi_{2k})_m \iint_{S_m} dS \frac{\partial \tilde{G}(P, Q, t_N - t_n)}{\partial n_Q} \right. \\
&\quad \left. - \iint_{S_m} dS (\bar{x}_k(t_n))_m \frac{\partial \tilde{G}(P, Q, t_N - t_n)}{\partial n_Q} \right] \} \\
&- \sum_{m^*} \Delta t \sum_{n=1}^{N-1} \left[\frac{U_0^2}{2\pi g} (\bar{x}_k(t_n))_{m^*} \right. \\
&\quad \times \left(\int_{\Gamma_{m^*}} d\eta \left(\frac{\partial \tilde{G}(P, Q, t_N - t_n)}{\partial \xi} + (\underline{l} \cdot \underline{i}) \frac{\partial \tilde{G}(P, Q, t_N - t_n)}{\partial l} \right) \right. \\
&\quad \left. + \int_{\Gamma_{m^*}} \tilde{G}(P, Q, t_N - t_n) \cdot d[(\underline{l} \cdot \underline{i})(\underline{l} \cdot \underline{j})] \right) \\
&\quad \left. + \frac{U_0}{\pi g} (\bar{x}_k(t_n))_{m^*} \int_{\Gamma_{m^*}} d\eta \frac{\partial \tilde{G}(P, Q, t_N - t_n)}{\partial t} \right]
\end{aligned}$$

Assuming that the variations along the waterline of the direction cosines of \underline{l} are small, the term involving them in B_i is neglected. Note that for A_{im} the line integral terms in large brackets are only used for panels on the free surface. Furthermore, m^* denotes that only the panels on the free surface are used in the summation for the line integral terms.

In the derivation of the above, use is made of the fact that

$$\begin{aligned}\bar{G}(P,Q,0) &= 0 \\ \frac{\partial \bar{G}(P,Q,0)}{\partial n} &= 0 \\ \frac{\partial \bar{G}(P,Q,0)}{\partial t} &= 2g \frac{\partial}{\partial z} \frac{1}{r'}\end{aligned}\quad (57)$$

Again the coefficient matrix A_{im} is independent of time. As in the zero speed case it is inverted only once at the beginning of the computation and then stored.

III.4 Numerical Evaluation of the Influence Coefficients

The evaluation of the coefficients A, B in the linear systems (47), (51) and (56) involves the surface integrals of the infinite fluid $\left(\frac{1}{r}\right)$ and memory (\bar{G}) parts of the Green function and their space derivatives, over each quadrilateral. The integrals of the infinite fluid $\left(\frac{1}{r}\right)$ terms are evaluated using the methods of Hess and Smith (1964). In their manner, a local coordinate

system (x', y', z') is assigned to each element such that the element lies on the plane $z'=0$ and its centroid is the local system origin. Then they replace the integral over the quadrilateral panel by the sum of four integrals over infinite strips, each strip being defined by one side of the panel. These integrals may be evaluated analytically giving the following exact formulas:

$$\iint \frac{\partial}{\partial x} \left(\frac{1}{r} \right) dS = - \sum_{\ell=1}^4 \frac{y'_{\ell+1} - y'_{\ell}}{d_{\ell}} \ln \left(\frac{r_{\ell} + r_{\ell+1} - d_{\ell}}{r_{\ell} + r_{\ell+1} + d_{\ell}} \right)$$

$$\iint \frac{\partial}{\partial y} \left(\frac{1}{r} \right) dS = \sum_{\ell=1}^4 \frac{x'_{\ell+1} - x'_{\ell}}{d_{\ell}} \ln \left(\frac{r_{\ell} + r_{\ell+1} - d_{\ell}}{r_{\ell} + r_{\ell+1} + d_{\ell}} \right)$$

$$\iint \frac{\partial}{\partial z} \left(\frac{1}{r} \right) dS = \sum_{\ell=1}^4 \left[\tan^{-1} \left(\frac{m_{\ell} e_{\ell+1} - h_{\ell+1}}{z' r_{\ell+1}} \right) - \tan^{-1} \left(\frac{m_{\ell} e_{\ell} - h_{\ell}}{z' r_{\ell}} \right) \right]$$

where

$$d_{\ell} = [(x'_{\ell+1} - x'_{\ell})^2 + (y'_{\ell+1} - y'_{\ell})^2]^{1/2}$$

$$m_{\ell} = (y'_{\ell+1} - y'_{\ell}) / (x'_{\ell+1} - x'_{\ell})$$

$$r_{\ell} = [(x' - x'_{\ell})^2 + (y' - y'_{\ell})^2 + z'^2]^{1/2}$$

$$e_{\ell} = z'^2 + (x' - x'_{\ell})^2$$

$$h_{\ell} = (y' - y'_{\ell})(x' - x'_{\ell})$$

The above exact integration formulas involve inverse tan and log functions whose evaluation is computationally time consuming. They are used only for values of r less

than twice the element maximum diagonal. For the values of r greater than four times the diagonal, the influence of the quadrilateral is approximated by a point source located at its centroid. For intermediate values of r a multipole expansion is used.

The surface integrals of the memory term \tilde{G} and its space derivatives are evaluated using coordinate mapping and Gauss quadrature. The arbitrary quadrilateral is first mapped into a unit square by a bilinear transformation. A Gauss product rule of any desired order is then used to numerically evaluate the integral. The details of the calculation are presented in Appendix D.

The line integral terms are evaluated by a one-dimensional trapezoidal rule along the waterline.

The development of a numerically efficient and accurate method to evaluate $\tilde{G}(P,Q,t-\tau)$ for arbitrary values of P,Q and $t-\tau$ is of key importance in the efficiency of this numerical method. For each time step, the evaluation of \tilde{G} and its derivatives is performed $M^2 \times N_G$ times where M is the number of panels and N_G the number of Gauss integration points on each panel. The most obvious choice to compute the Green function is numerical integration. This approach however, requires a major computational effort and must be avoided whenever a more efficient algorithm can be developed. More efficient numerical techniques have been developed and may be used

for any combination of P, Q and $t-\tau$ except for the special case $R=z=\zeta=0$. For this case \tilde{G} is unbounded since the integral in eq. (5) doesn't exist. This case however never occurs in the computation scheme.

From equation (5) \tilde{G} is:

$$\tilde{G}(P, Q, t-\tau) = 2 \int_0^{\infty} dk \sqrt{kg} \sin(\sqrt{kg} (t-\tau)) e^{k(z+\zeta)} J_0(kR)$$

An equivalent form more convenient for numerical evaluation is obtained by making the substitution $\lambda=kr'$ where $r'^2 = (x-\xi)^2 + (y-\eta)^2 + (z+\zeta)^2$ giving:

$$\tilde{G} = 2 \frac{\sqrt{g}}{\sqrt{r'^3}} \int_0^{\infty} d\lambda \sqrt{\lambda} \sin(\beta\sqrt{\lambda}) e^{-\lambda\mu} J_0(\lambda\sqrt{1-\mu^2}) \quad (58)$$

where

$$\beta = \sqrt{g/r'} (t-\tau)$$

$$\mu = - \left(\frac{z+\zeta}{r'} \right) = \frac{1}{\sqrt{1+R^2/(z+\zeta)^2}}$$

Except for the multiplicative factor $2 \frac{\sqrt{g}}{\sqrt{r'^3}}$, \tilde{G} is only a function of the two parameters μ and β . The parameter μ relates the depth of submergence to the horizontal distance R and ranges in value between 0 and 1. The parameter β is related to the phase of the generated waves.

For the special case $\mu=0$ which corresponds to having both the source and the field points on the free surface, \tilde{G} may be expressed in terms of the Bessel functions of

orders $\pm 1/4$ and $\pm 3/4$. The final form is given by Wehausen and Laitone (1960) eq. 22.21:

$$\tilde{G} = \frac{\sqrt{g}}{\sqrt{r'^3}} \frac{\pi \beta^3}{8\sqrt{2}} \left(J_{1/4}\left(\frac{\beta^2}{8}\right) J_{-1/4}\left(\frac{\beta^2}{8}\right) + J_{3/4}\left(\frac{\beta^2}{8}\right) J_{-3/4}\left(\frac{\beta^2}{8}\right) \right)$$

For the special case $\mu=1$, the Bessel function J_0 is equal to 1 and the integral giving \tilde{G} is a Fresnel type integral. The final expression for \tilde{G} , in that special case, may be found in Abramowitz and Stegun (1964) eq. 7.4.7.:

$$\tilde{G} = - \frac{\sqrt{g}}{\sqrt{r'^3}} \left\{ ((-2+\beta^2) e^{-\beta^2/4} \int_0^{\beta/2} e^{-t^2} dt) - \beta \right\}$$

Efficient algorithms for evaluating the Dawson integral

$$e^{-\beta^2/4} \int_0^{\beta/2} e^{-t^2} dt$$

are given by Cody, Paciorek and Thacher (1970). The algorithms that they use are well behaved for all real and positive values of β .

Returning now to the general case one may observe that because of the sine and the Bessel function, the integrand is highly oscillatory and ordinary quadrature formulas are inappropriate. Depending on the size of the two non-dimensional parameters μ and β , different techniques are used to evaluate the integral (58). For μ greater than .7 a Filon integration rule is used. For values of

μ less than .7 either a power series expansion or an asymptotic expansion are used depending on the value of β as shown in Figure (2). The sections that follow describe the three algorithms used to evaluate \bar{G} .

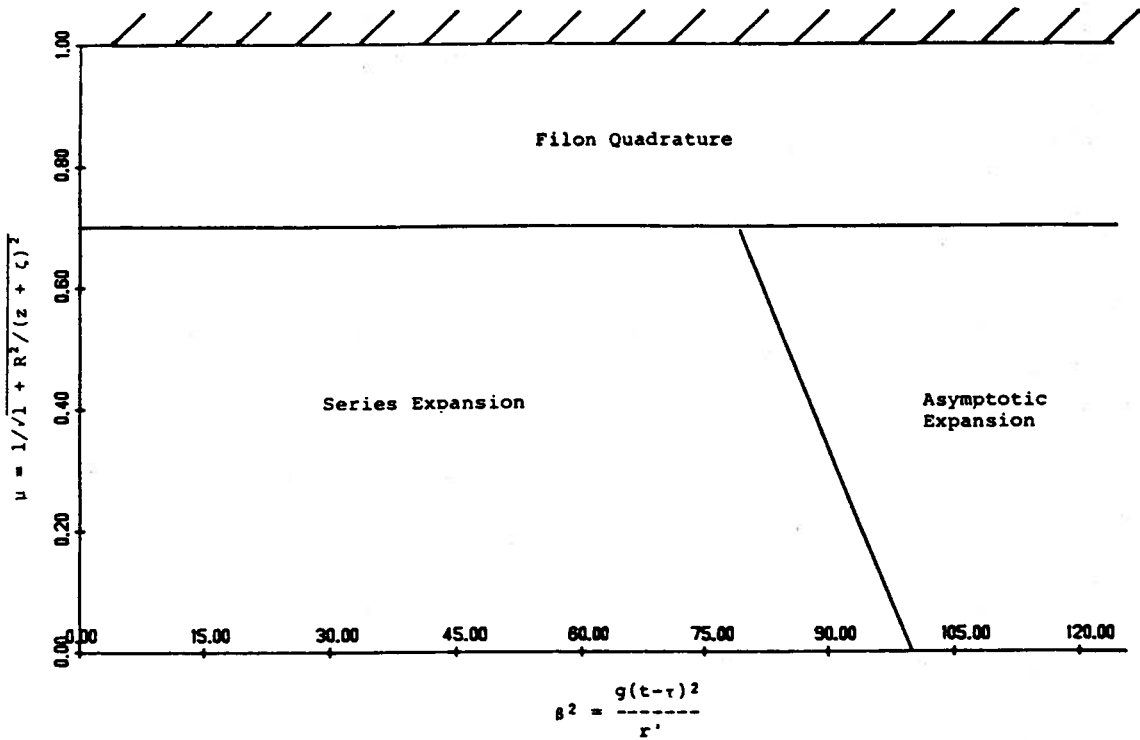


Figure 2: Computational Domain for \bar{G}

Filon Quadrature Rule.

For μ greater than .7 the exponential factor in the integral (58) causes the integrand to decay fast enough that a numerical quadrature formula may be used efficiently. In order to truncate the oscillatory tail of

the Bessel function we add and subtract the leading term of its asymptotic expansion. This gives:

$$\begin{aligned} \bar{G} = & 2 \frac{\bar{g}}{\sqrt{r}^3} \int_0^\infty d\lambda \sin(\beta\sqrt{\lambda}) e^{-\lambda\mu} [\sqrt{\lambda} J_0(\lambda\sqrt{1-\mu^2}) \\ & - \frac{1}{(1-\mu^2)^{1/4}} \frac{\bar{2}}{\sqrt{\pi}} \cos(\lambda\sqrt{1-\mu^2} - \frac{\pi}{4})] \\ & + 2 \frac{\bar{2g}}{\sqrt{\pi r}^3} \frac{1}{(1-\mu^2)^{1/4}} \int_0^\infty d\lambda \sin(\beta\sqrt{\lambda}) e^{-\lambda\mu} \cos(\lambda\sqrt{1-\mu^2} - \frac{\pi}{4}) \end{aligned}$$

The second integral can be evaluated analytically with the final result:

$$\begin{aligned} \bar{G} = & 2 \frac{\bar{g}}{\sqrt{r}^3} \int_0^\infty d\lambda \sin(\beta\sqrt{\lambda}) e^{-\lambda\mu} [\sqrt{\lambda} J_0(\lambda\sqrt{1-\mu^2}) \\ & - \frac{\bar{2}}{\sqrt{\pi}} (1-\mu^2)^{-1/4} \cos(\lambda\sqrt{1-\mu^2} - \frac{\pi}{4})] \\ & + \frac{\bar{2g}}{\sqrt{r}^3} \frac{\beta}{(1-\mu^2)^{1/4}} e^{-\beta^2\mu/4} \sin(\frac{\beta^2\sqrt{1-\mu^2}}{4} + \frac{3\theta}{2}) \end{aligned}$$

where $\theta = \sin^{-1}(\mu)$

By setting

$$k^2 = \lambda\sqrt{1-\mu^2}, \quad \gamma = \beta/(1-\mu^2)^{1/4}$$

$$\bar{G} = 4 \frac{\bar{g}}{\sqrt{r}^3} \frac{1}{(1-\mu^2)^{3/4}} \int_0^\infty dk k \sin(\gamma k) e^{-k^2\mu/\sqrt{1-\mu^2}}$$

$$\begin{aligned}
& \left[k J_0(k^2) - \frac{\sqrt{2}}{\sqrt{\pi}} \cos(k^2 - \pi/4) \right] \\
& + \frac{\sqrt{2g}}{\sqrt{r'^3}} \frac{1}{(1-\mu^2)^{1/4}} e^{-\beta^2 \mu/4} \sin\left(\frac{\beta^2 \sqrt{1-\mu^2}}{4} + \frac{3\theta}{2}\right) \\
= & 4 \frac{\bar{g}}{\sqrt{r'^3}} \frac{1}{(1-\mu^2)^{3/4}} \int_0^{\infty} dk k \sin(\gamma k) e^{-k\mu/\sqrt{1-\mu^2}} f(k) \\
& + \frac{\sqrt{2g}}{\sqrt{r'^3}} \frac{\beta}{(1-\mu^2)^{1/4}} e^{-\beta^2 \mu/4} \sin\left(\frac{\beta^2 \sqrt{1-\mu^2}}{4} + \frac{3\theta}{2}\right)
\end{aligned}$$

The infinite integral is truncated at a value $k=k_{\max}$ where the factor

$$k f(k) e^{-k\mu/\sqrt{1-\mu^2}}$$

is less than 10^{-7} . The finite integral is then subdivided into $2N$ subintervals of equal length h where h is chosen equal to 0.05. In order to save computer time, the function

$$f(k) = k J_0(k^2) - \frac{\sqrt{2}}{\sqrt{\pi}} \cos\left(k^2 - \frac{\pi}{4}\right)$$

is evaluated only once and tabulated for the integration points $k=nh$ ($n=0,1,2, \dots$.)

The partial integrand

$$g(k) = k f(k) e^{-k\mu/\sqrt{1-\mu^2}}$$

is then approximated by a parabola obtained by

interpolation at the mesh points. The resulting integrals of the form

$$\int_{k_1}^{k_2} (c_2 k^2 + c_1 k + c_0) \sin(\gamma k) dk$$

may be evaluated analytically leading to a formula similar to that first presented by Filon (1929):

$$\begin{aligned} \bar{G} = & 4 \frac{\bar{g}}{\sqrt{r'}^3} \frac{h}{(1-\mu^2)^{3/4}} \left[-\alpha_1 g(k_{\max}) \cos(\gamma k_{\max}) + \right. \\ & \left. + \alpha_2 S_{2n} + \alpha_3 S_{2n-1} \right] \\ & + \frac{\sqrt{2g}}{\sqrt{r'}^3} \frac{\beta}{(1-\mu^2)^{1/4}} e^{-\beta^2 \mu/4} \sin\left(\frac{\beta^2 \sqrt{1-\mu^2}}{4} + \frac{3\theta}{2}\right) \end{aligned} \quad (59)$$

The constants α_1 , α_2 , α_3 are defined as:

$$\alpha_1 = (\delta^2 + \delta \sin\delta \cos\delta - 2\sin^2\delta)/\delta^3$$

$$\alpha_2 = 2 [\delta(1+\cos^2\delta) - 2\sin\delta\cos\delta]/\delta^3$$

$$\alpha_3 = 4 (\sin\delta - \delta \cos\delta)/\delta^3$$

where

$$\delta = \gamma \cdot h$$

The sums S_{2N} and S_{2N-1} are given by the formulae:

$$S_{2N} = g(2h) \sin(2h\gamma) + g(4h)\sin(4h\gamma) + \dots$$

$$+ \frac{1}{2} g(k_{\max}) \sin(k_{\max}\gamma)$$

$$S_{2N-1} = g(h) \sin(h\gamma) + g(3h)\sin(3h\gamma) + \dots$$

$$+ g(k_{\max}-h) \sin((k_{\max}-h)\gamma)$$

Formula (59) retains uniform accuracy even when γ is so large that many oscillations occur within the step size

$h=0.05$.

Series expansion.

Following Lamb (1932), for small values of β the $\sin(\beta\sqrt{\lambda})$ factor may be expanded into a power series to produce:

$$\tilde{G} = 2 \frac{g}{\sqrt{r'^3}} \int_0^{\infty} d\lambda e^{-\lambda\mu} J_0(\lambda\sqrt{1-\mu^2}) \sqrt{\lambda} \sum_{n=1}^{\infty} \frac{(\beta\sqrt{\lambda})^{2n-1} (-1)^{n-1}}{(2n-1)!}$$

Using the formula

$$\int_0^{\infty} \lambda^n e^{-\lambda\mu} J_0(\lambda\sqrt{1-\mu^2}) d\lambda = n! P_n(\mu)$$

where $P_n(\mu)$ is the Legendre polynomial of order n , each of the terms of the power series may be integrated analytically with the final result:

$$\begin{aligned} \tilde{G} = 2\sqrt{g/r'^3} \beta & \left[P_1(\mu) - \frac{2!}{3!} P_2(\mu) \beta^2 \right. \\ & \left. + \frac{3!}{5!} P_3(\mu) \beta^4 - \frac{4!}{7!} P_4(\mu) \beta^6 + \dots \right] \end{aligned} \quad (60)$$

Using double precision and enough terms, this series has been found to have an error less than 10^{-6} for the region shown in Figure (2). The Legendre polynomial $P_n(\mu)$ is evaluated from $P_{n-2}(\mu)$ and $P_{n-1}(\mu)$ using the forward recursion formula.

Asymptotic expansion

For large values of β the series expansion (60) of \tilde{G} converges very slowly and there is a loss in accuracy

due to roundoff errors. In this case, it is more efficient to develop an asymptotic representation of \bar{G} in negative powers of β . Replacing the Bessel function J_0 by its integral representation and reversing the orders of integration gives:

$$\bar{G} = \frac{2}{\pi} \frac{\bar{g}}{\sqrt{r}^3} \operatorname{Re} \left[\int_{-\pi/2}^{\pi/2} d\phi \int_0^{\infty} d\lambda \sqrt{\lambda} \sin(\beta\sqrt{\lambda}) e^{-(\mu-i\sqrt{1-\mu^2}\cos\phi)\lambda} \right]$$

where Re denotes that the real part of the above must be taken. The inner integral can be expressed in terms of the Dawson integral (Abramowitz and Stegun (1964) eq. 7.4.7) with the complex argument

$$\left(Z = \frac{\beta}{2 \sqrt{(\mu-i\sqrt{1-\mu^2}\cos\phi)}} \right) :$$

$$\int_0^{\infty} d\lambda \sqrt{\lambda} \sin(\beta\sqrt{\lambda}) e^{-\lambda(\mu-i\sqrt{1-\mu^2}\cos\phi)} = \frac{\operatorname{DDAW}(Z)}{(\mu-i\sqrt{1-\mu^2}\cos\phi)^{3/2}} - \frac{2 Z^2}{(\mu-i\sqrt{1-\mu^2}\cos\phi)^{3/2}} \operatorname{DDAW}(Z) + \frac{Z}{(\mu-i\sqrt{1-\mu^2}\cos\phi)^{3/2}} \quad (61)$$

where DDAW is the Dawson integral defined as

$$\operatorname{DDAW}(Z) = e^{-Z^2} \int_0^Z e^{t^2} dt$$

Because μ has values between 0 and 1, when the nondimensional parameter β is large, the complex argument Z of the Dawson integral has a large modulus. As a result it may be approximated by the large argument expansion of the Dawson integral (Gauchi 1970):

$$\text{DDAW}(Z) = \frac{1}{2Z} + \frac{1}{2^2 Z^3} + \frac{3}{2^3 Z^5} + \frac{15}{2^4 Z^7} + \dots - \frac{\sqrt{\pi} e^{-Z^2}}{2i} \quad (62)$$

Substituting (62) into (61) we may write:

$$\begin{aligned} & \int_0^{\infty} d\lambda \sqrt{\lambda} \sin(\beta\sqrt{\lambda}) e^{-\lambda(\mu - i\sqrt{1-\mu^2} \cos\phi)} = \\ & = \left[(1 - 2Z^2) \left(\frac{1}{2Z} + \frac{1}{2^2 Z^3} + \frac{3}{2^3 Z^5} + \frac{15}{2^4 Z^7} + \dots - \frac{\sqrt{\pi} e^{-Z^2}}{2i} \right) \right. \\ & \left. + Z \right] / (\mu - i\sqrt{1-\mu^2} \cos\phi)^{3/2} = \\ & = \left[-\frac{1}{2Z^3} - \frac{3}{2Z^5} - \frac{45}{2^3 Z^7} - \dots \right. \\ & \left. - (1-2Z^2) \frac{\sqrt{\pi} e^{-Z^2}}{2i} \right] / (\mu - i\sqrt{1-\mu^2} \cos\phi)^{3/2} \quad (63) \end{aligned}$$

Replacing the inner integral from (63) into the expression (61) for \tilde{G} gives:

$$\begin{aligned} \tilde{G} &= \frac{2}{\pi} \frac{\overline{g}}{\sqrt{r'^3}} \operatorname{Re} \int_{-\pi/2}^{\pi/2} d\phi \left[-\frac{1}{2Z^3} - \frac{3}{2Z^5} - \frac{45}{2^3 Z^7} \right. \\ & \left. - (1-2Z^2) \frac{\sqrt{\pi} e^{-Z^2}}{2i} (\mu - i\sqrt{1-\mu^2} \cos\phi)^{3/2} \right] \\ &= \frac{2}{\pi} \frac{\overline{g}}{\sqrt{r'^3}} \operatorname{Re} \left[\int_{-\pi/2}^{\pi/2} d\phi \left[-\frac{4}{\beta^3} - \frac{48}{\beta^5} (\mu - i\sqrt{1-\mu^2} \cos\phi) - \right. \right. \end{aligned}$$

$$\begin{aligned}
& - \frac{180}{\beta'} (\mu - i\sqrt{1-\mu^2} \cos\phi)^2 - \dots \\
& - \frac{\sqrt{\pi}}{2i} \left[(\mu - i\sqrt{1-\mu^2} \cos\phi)^{-3/2} - 2\beta^2 (\mu - i\sqrt{1-\mu^2} \cos\phi)^{-5/2} \right] \\
& \times e^{-\frac{\beta^2}{4(\mu - i\sqrt{1-\mu^2} \cos\phi)}}] = \\
& = 2 \frac{\overline{g}}{\sqrt{r'^3}} \left[\left(-\frac{4}{\beta^3} - \frac{48\mu}{\beta^5} - \frac{360}{\beta'} (3\mu^2-1) \dots \right) - \right. \\
& - \operatorname{Re} \left[\frac{1}{\sqrt{\pi}i} \frac{\overline{g}}{\sqrt{r'^3}} \int_{-\pi/2}^{\pi/2} d\phi (\mu - i\sqrt{1-\mu^2} \cos\phi)^{-3/2} \right. \\
& \left. \left. - 2\beta^2 (\mu - i\sqrt{1-\mu^2} \cos\phi)^{-5/2} \right] e^{-\frac{\beta^2}{4(\mu - i\sqrt{1-\mu^2} \cos\phi)}} \right] = \\
& = 2 \frac{\overline{g}}{\sqrt{r'^3}} \left[\left(-\frac{4}{\beta^3} - \frac{48\mu}{\beta^5} - \frac{360}{\beta'} (3\mu^2-1) \dots \right) - \right. \\
& - \operatorname{Re} \left[\frac{1}{\sqrt{\pi}i} \int_0^{\pi/2} d\phi [(\mu - i\sqrt{1-\mu^2} \cos\phi)^{-3/2} - \right. \\
& \left. \left. - 2\beta^2 (\mu - i\sqrt{1-\mu^2} \cos\phi)^{-5/2} \right] e^{-\frac{\beta^2}{4(\mu - i\sqrt{1-\mu^2} \cos\phi)}} \right] \quad (64)
\end{aligned}$$

The main contribution to the integral term comes from the neighborhood of the end point $\phi=0$ where the

exponential is stationary. A systematic series expansion around that point gives the asymptotic behavior of the integral for large β . The details of the asymptotic analysis may be found in Appendix E. The final result is:

$$\begin{aligned}
\bar{G} = & 2 \frac{\overline{g}}{\sqrt{r}^3} \left[\left(-\frac{4}{\beta^3} - \frac{48\mu}{\beta^5} - \frac{360}{\beta^7} (3\mu^2-1) \dots \right) + \right. \\
& + \frac{e^{-\beta^2\mu/4}}{\sqrt{2}} \left(\frac{\beta}{(1-\mu^2)^{1/4}} \sin\left(\frac{\beta^2\sqrt{1-\mu^2}}{4} + \frac{3\theta}{2} \right) \right. \\
& + \frac{1}{2\beta(1-\mu^2)^{3/4}} \cos\left(\frac{\beta^2\sqrt{1-\mu^2}}{4} - \frac{\theta}{2} \right) \\
& + \frac{1}{\beta^3(1-\mu^2)^{3/4}} \sin\left(\frac{\beta^2\sqrt{1-\mu^2}}{4} - \frac{3\theta}{2} \right) \\
& - \frac{9}{8\beta^3(1-\mu^2)^{5/4}} \sin\left(\frac{\beta^2\sqrt{1-\mu^2}}{4} - \frac{5\theta}{2} \right) - \\
& - \frac{9}{\beta^5(1-\mu^2)^{3/4}} \cos\left(\frac{\beta^2\sqrt{1-\mu^2}}{4} - \frac{7\theta}{2} \right) \\
& \left. + \frac{24}{\beta^5(1-\mu^2)^{3/4}} \cos\left(\frac{\beta^2\sqrt{1-\mu^2}}{4} - \frac{5\theta}{2} \right) \right] + O(\beta^{-7}) \quad (65)
\end{aligned}$$

where

$$\theta = \sin^{-1}(\mu)$$

Because of the exponential factor $e^{-\beta^2 \mu/4}$ the contribution of the integral term is significant only for small μ , that is close to the free surface.

An asymptotic series equivalent to (65) has been derived by Newman (1985) by first expanding the Bessel function J_0 for large arguments and evaluating the resulting integrals by the method of stationary phase.

CHAPTER IV
NUMERICAL RESULTS

IV.1 Numerical Evaluation of the Force Coefficients
in the Time and Frequency Domain for a Sphere, a
Cylinder and a Series 60 Ship.

IV.1.a Case of Zero Forward Speed

A sphere in heave was chosen as the first test problem for the numerical method. Figure 3 shows the nondimensional memory function $K(t)/\rho \frac{2\pi}{3} R^3$, for a heaving sphere versus nondimensional time, $t/\sqrt{g/R}$, where R is the radius of the sphere. The solid curve is obtained by Fourier transforming the frequency-domain results of Barakat (1962). The asterisks and crosses show the numerical results using the source or potential methods respectively. For the numerical results only 12 panels were used on 1/4 of the body. This small number of panels illustrates the errors associated with the numerical solution.

Figure 3 illustrates that even with a small number of panels either the source or potential methods give reasonable results. One of the major problems of this method is the oscillatory tail which occurs in the memory functions at large times. This oscillatory component

persists indefinitely in time and as Figure 3 indicates, is much smaller for the potential method than for the source method.

Adachi and Ohmatsu (1979, 1980) examined the two-dimensional problem and showed that the oscillatory error in the time domain is the equivalence of the irregular frequencies in the frequency domain. The irregular frequencies in the frequency domain are eigensolutions of the interior problem. They satisfy the linearized free surface condition and a Dirichlet condition $\phi=0$ on the body surface. At these resonant frequencies ω_j the solution in the frequency domain has a singularity of the type $1/\omega-\omega_j$. The Fourier transform of this singular error gives the effect of each irregular frequency in the time domain as $\frac{e^{i\omega_j t}}{2i}$. In fact, as the present calculations indicate only the lowest eigenfrequency affects the solution. Hulme (1982) gives the lowest irregular frequency for an oscillating sphere in heave as $\omega_1 = 5.01$ rad/sec. The oscillatory error in Figure 3 has an approximate frequency of 5.03 rad/sec that is very close to ω_1 .

Adachi and Ohmatsu show that using the source method the oscillatory error cannot be eliminated regardless of the number of panels or the size of the time step. However, using orthogonality arguments they show that analytically the potential method has a solution which is

free of the oscillatory error. Numerically this might not be the case because of computational errors, but at least the potential method should converge to the proper solution given sufficient numerical accuracy.

Figure 3 verifies that the potential method does indeed give a better solution. For the same number of panels and time step size the potential method has a significantly smaller amplitude of oscillation (f^*) than the source method. The potential method also appears more accurate over most of the range. Thus, even though the potential method requires slightly more computational effort than the source method, it seems to be worthwhile.

Figure 4 presents the same results as figure 3 except that the numerical calculations were made using the potential method with 65 panels on the $1/4$ sphere and a nondimensional time step of $\Delta t^* = \Delta t \sqrt{g/R} = 0.05 \sqrt{g/R}$. The agreement between the analytic result and the calculations is now excellent. The amplitude of the oscillatory error is not zero, but it is small enough for practical calculations. The amplitude of the oscillatory error could be made smaller by taking more panels and a smaller time step.

Figures 5 and 6 show the added mass and damping as a function of nondimensional frequency for a sphere in heave. The numerical results were obtained by Fourier transforming the results of figure 4 according to equation (40). The

analytic results are from Barakat (1962). It should be noted that even though there is a small oscillatory error in the tail of figure 4, because of the discretized form of the Fourier transform it does not affect the added mass and damping predictions.

Figure 7 presents the nondimensional memory function for a right circular cylinder in heave. The radius to draft ratio (R/T) is 2.0. The solid curve was computed by Newman (1985) using ring sources and a one-dimensional integral equation. The results computed by the present three-dimensional theory were obtained using a cosine spacing of 31 panels on the bottom and 25 panels on the side of a 1/4-body. The nondimensional time step was again $\Delta t^* = .05\sqrt{g/R}$. The slight difference between the computed results and those of Newman are apparently due to the difficulty of properly modeling the flow around the sharp corner where the bottom meets the side. The best agreement was obtained by using a cosine spacing of the panels and by placing a small panel at an angle of 45° in the corner, rather than having the side and bottom panels meeting at right angles.

Figure 8 shows the nondimensional memory function for a sphere in sway. The numerical results were computed using 37 panels on a 1/4 sphere and a nondimensional time step of $\Delta t^* = .05\sqrt{g/R}$. The analytic curve was obtained by an inverse Fourier transform of the frequency domain

results of Hulme (1982). As with the heave results, the agreement is again excellent.

Finally, the method was used to calculate the added mass and damping of a Series 60 ship forced to oscillate in heave and pitch. The Series 60 model is a parent form ($L/B = 7.0$, $B/T = 2.5$, $LCB/L = 5\%$ forward) for the $C_B = 0.70$ series. This model has been tested by Gerritsma (1966) and Gerritsma and Beukelman (1964). In addition, Chang (1977), Inglis (1980) and Inglis and Price (1982) have presented numerical results using frequency-domain calculations.

As Figure 9 indicates, at large times there is an oscillatory component similar to that observed in the case of a sphere in heave. As in all the other cases, the potential method has less oscillatory error than the source method. The oscillatory error may be further reduced by increasing the number of panels and time steps. The final discretized model that was used in the computations is shown in Figure 10. There are 108 panels on the half-body. The panels are smaller near the ends because these areas are critical for the pitch calculations.

Figures 11-13 show the nondimensional added mass and damping coefficients (A_{jk} and B_{jk}) for the Series 60 ship as a function of non-dimensional frequency. Five different sets of data are presented. The solid lines are the results computed by time-domain analysis using the

potential method presented in this paper. For the calculations 108 panels on the half-body were used and the time step size was $\Delta t^* = 0.6264$. The small-dash curves are the experimental results of Gerritsma (1966) for zero forward speed and Gerritsma and Beukelman (1964) for a Froude number of .2. The large-dash curves are strip theory results. The strip theory results were computed using the coefficients of Salvesen, Tuck and Faltinsen (1970) and a source distribution technique to solve the two-dimensional problem. The results computed by three-dimensional methods in the frequency domain using source panel techniques are shown as crosses and asterisks. The crosses are the results of Inglis (1980) for zero forward speed and Inglis and Price (1982) for a Froude number of .2. The results are for their IP2 method which corresponds to the method presented in this paper. The asterisks were presented by Chang (1977). Chang's results are plotted in dimensional form and no model length or density are given in the paper. To nondimensionalize Chang's results a model length of 10 ft (3.048 m) was used. Note that not all of the coefficients were plotted by Chang.

Figure 11 shows the added mass and damping in heave for zero forward speed. As can be seen all the results agree reasonably well. For the added mass the present calculations fall between those of Chang and Inglis. The

Barakat (1962) _____
 Time-Domain Computations
 Source Method _____
 12-Panels (1/4-body) _____
 Potential Method _____
 12-Panels (1/4-body) _____

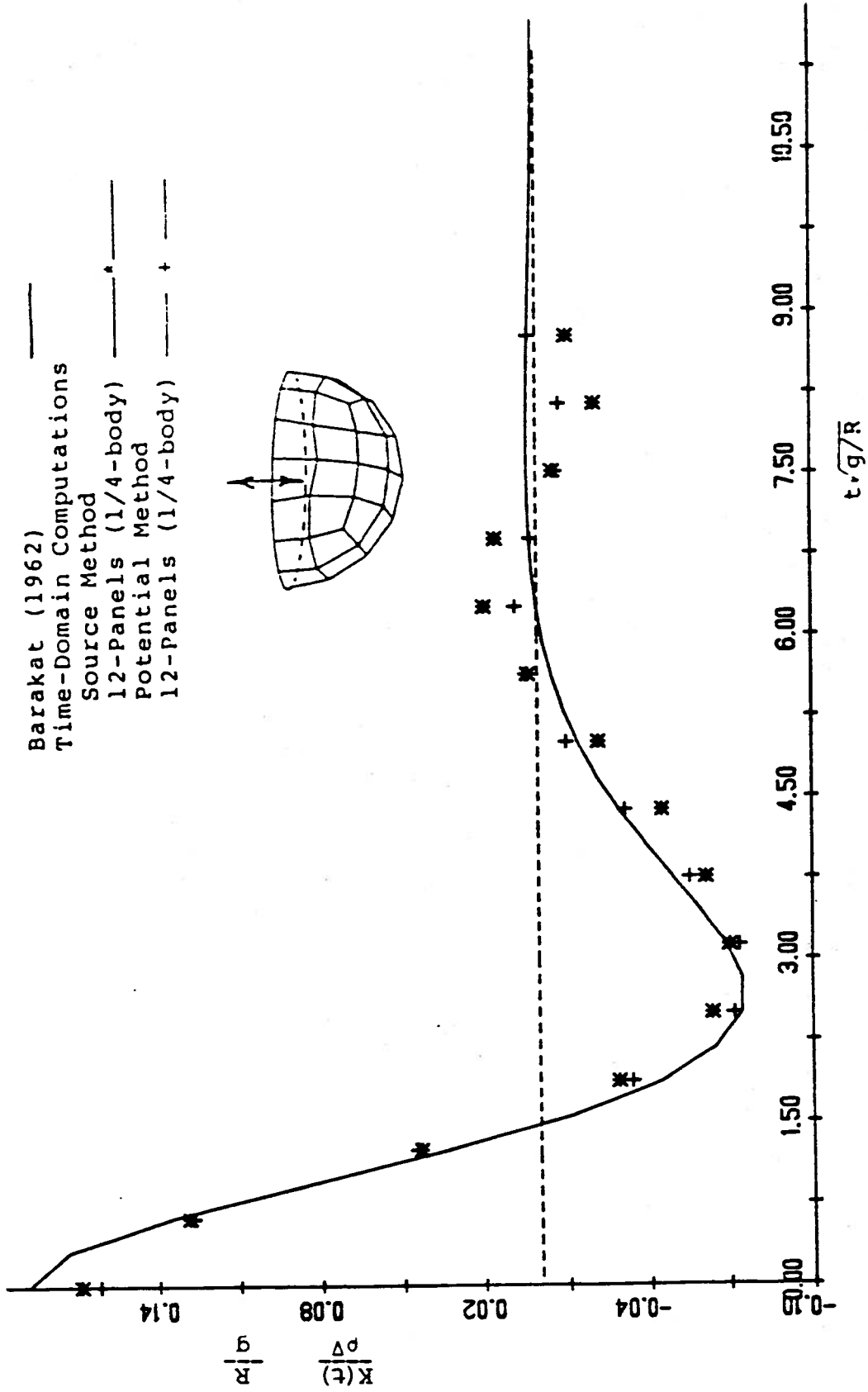
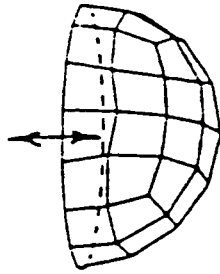


Figure 3.

Nondimensional Memory Function for Heave Force on a Hemisphere versus Nondimensional Time

Barakat (1962)
 Time-Domain Computations
 Potential Method
 65-Panels (1/4-body) + + +

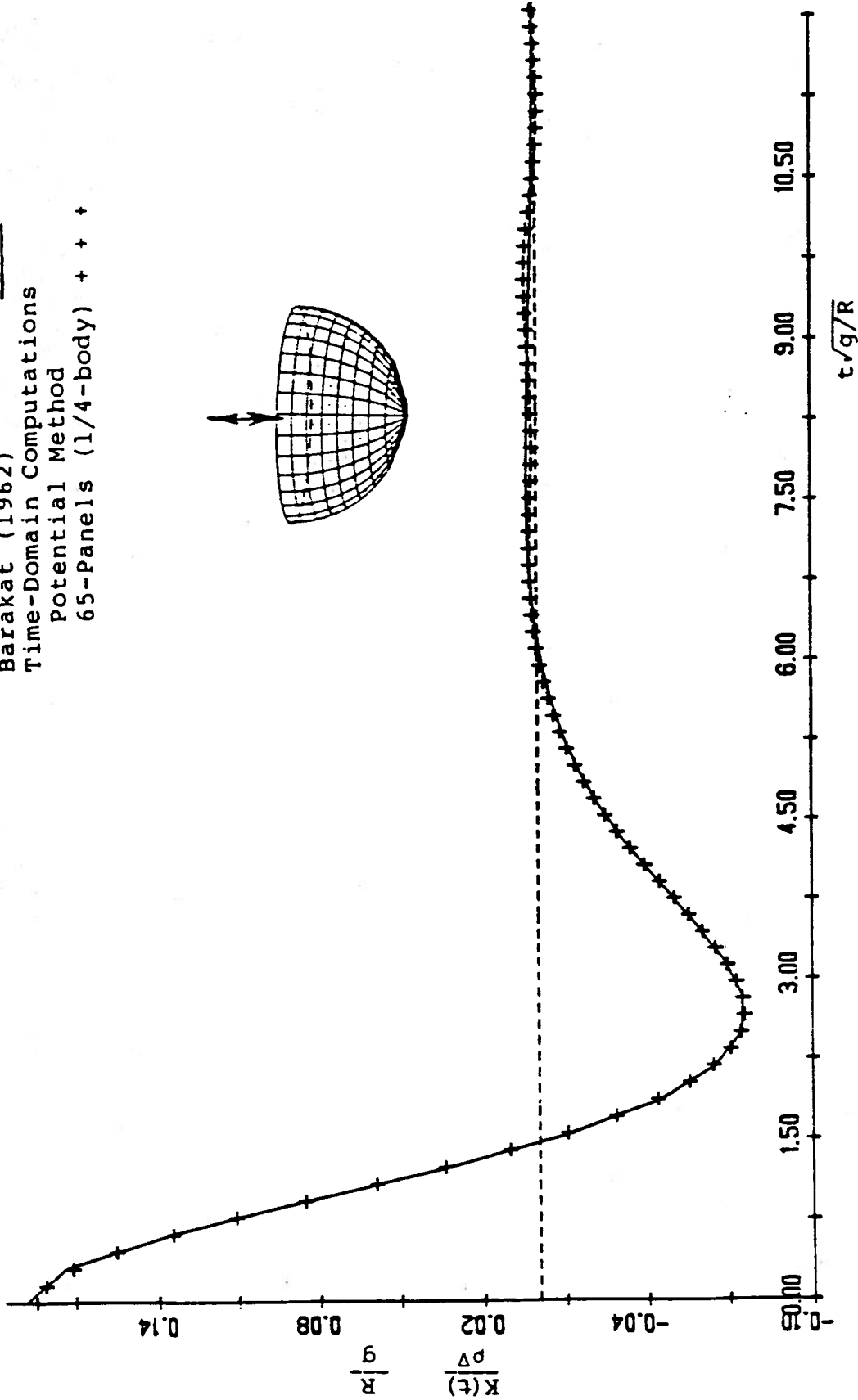
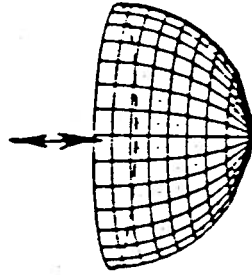
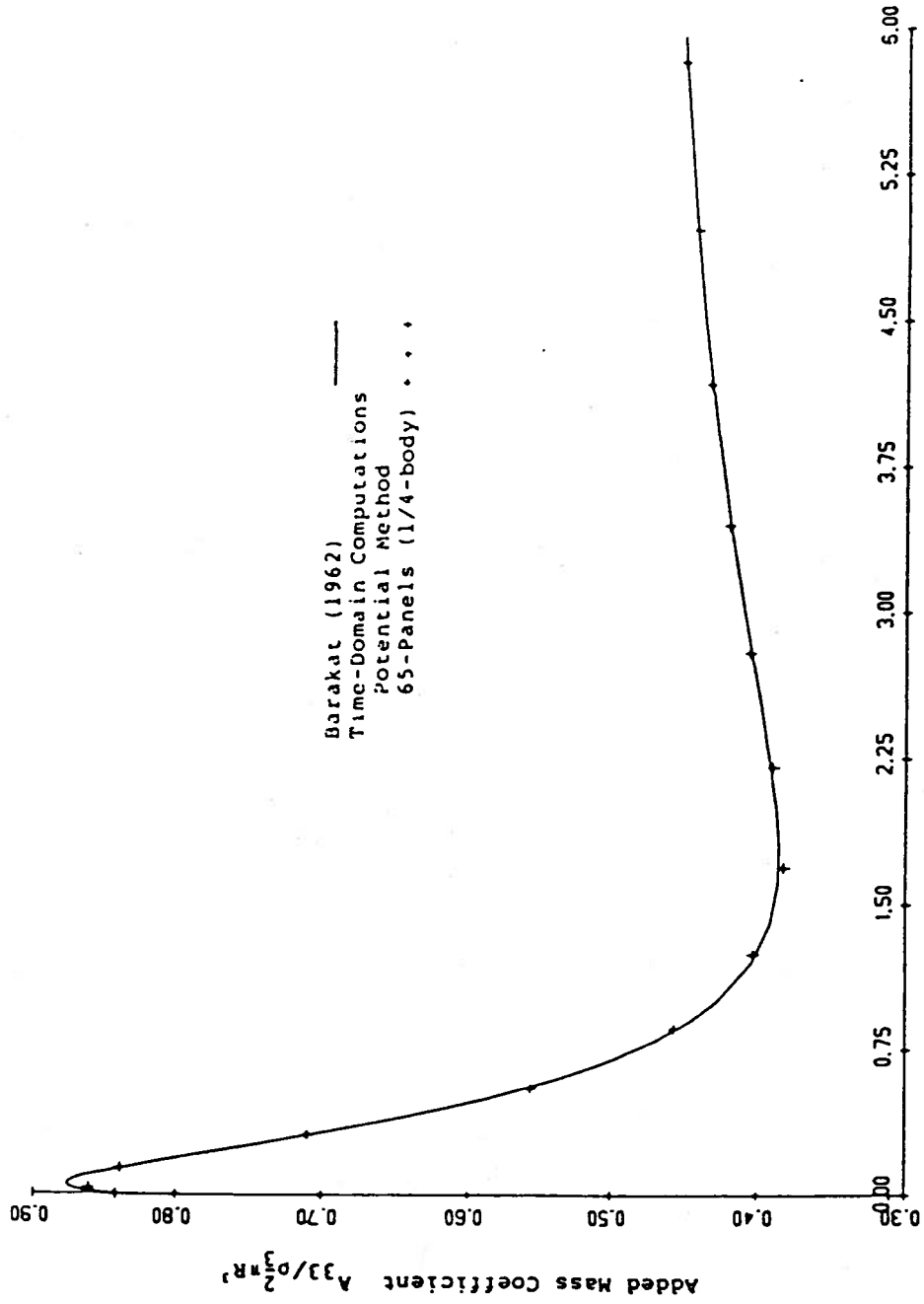


Figure 4.

Nondimensional Memory Function for Heave Force on a Hemisphere versus Nondimensional Time



$\frac{\omega R}{\eta}$

Figure 5.

Nondimensional Added Mass Coefficient for a Sphere in Heave versus Nondimensional Frequency

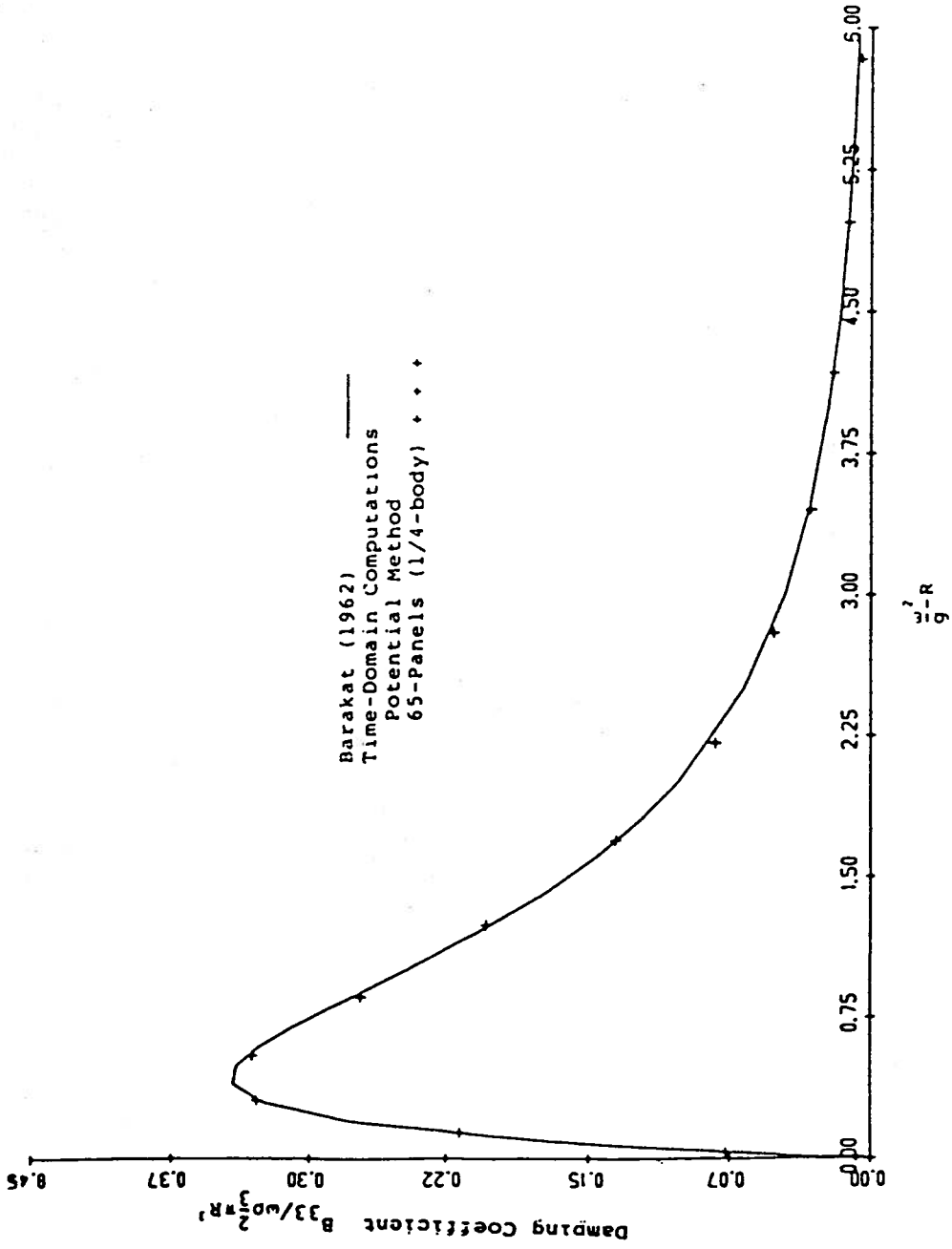


Figure 6.
 Nondimensional Damping Coefficient for a Sphere in Heave versus Nondimensional Frequency

Newman (1985)
 Time-Domain
 Potential Method
 31+25 Panels (1/4-body) + + + +

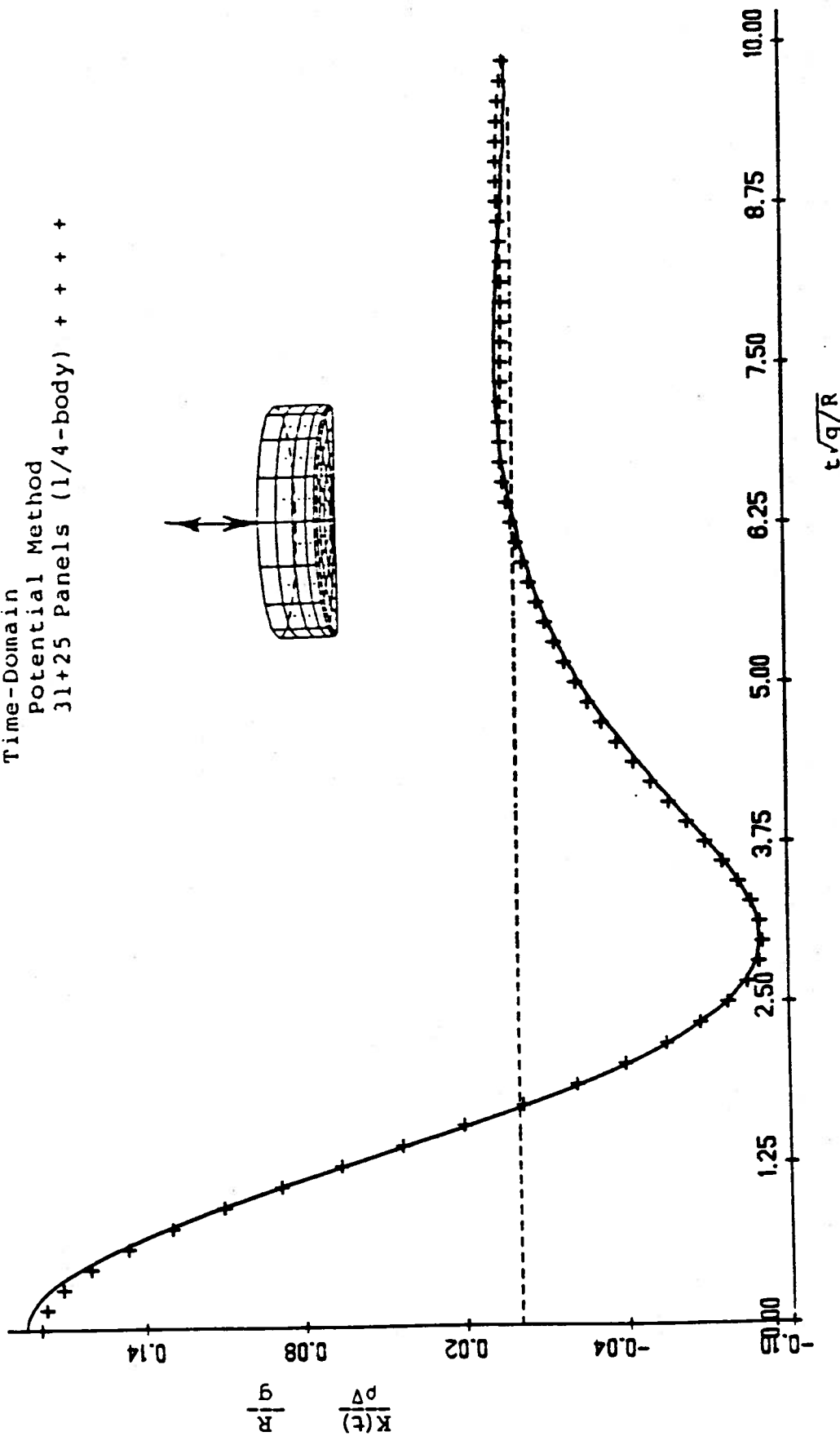
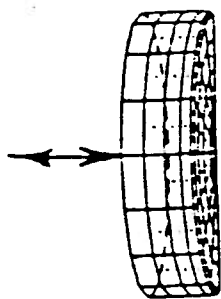


Figure 7.

Nondimensional Memory Function for a Right Circular Cylinder in Heave versus Nondimensional Time

Hulme (1982)
 Time-Domain Equations
 Potential Method
 37-Panels (1/4-body) + + +

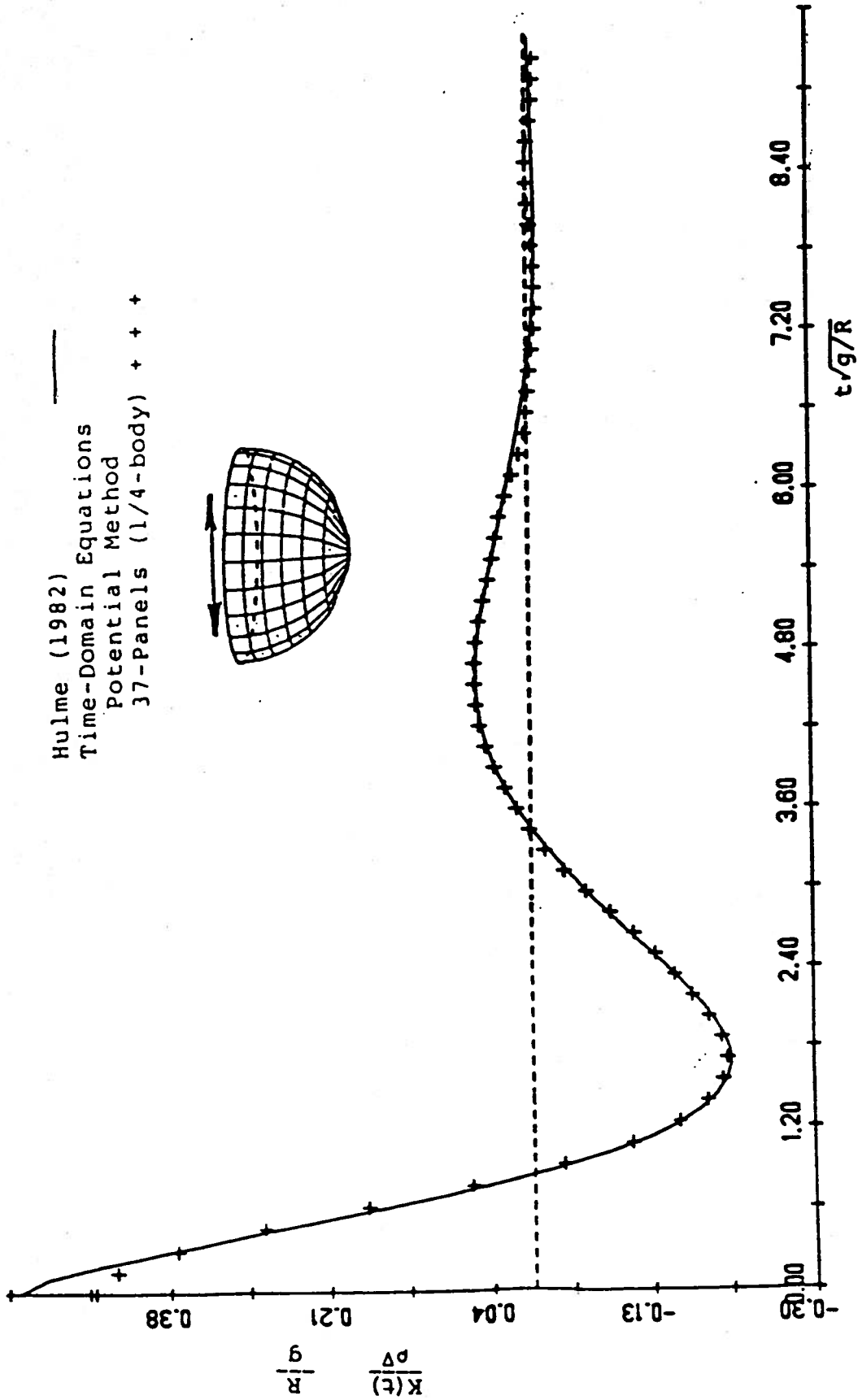
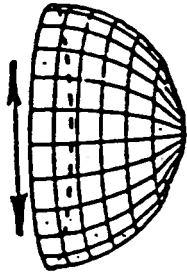


Figure 8.

Non-dimensional Memory Function for Sway Force on a Hemisphere versus Non-dimensional Time

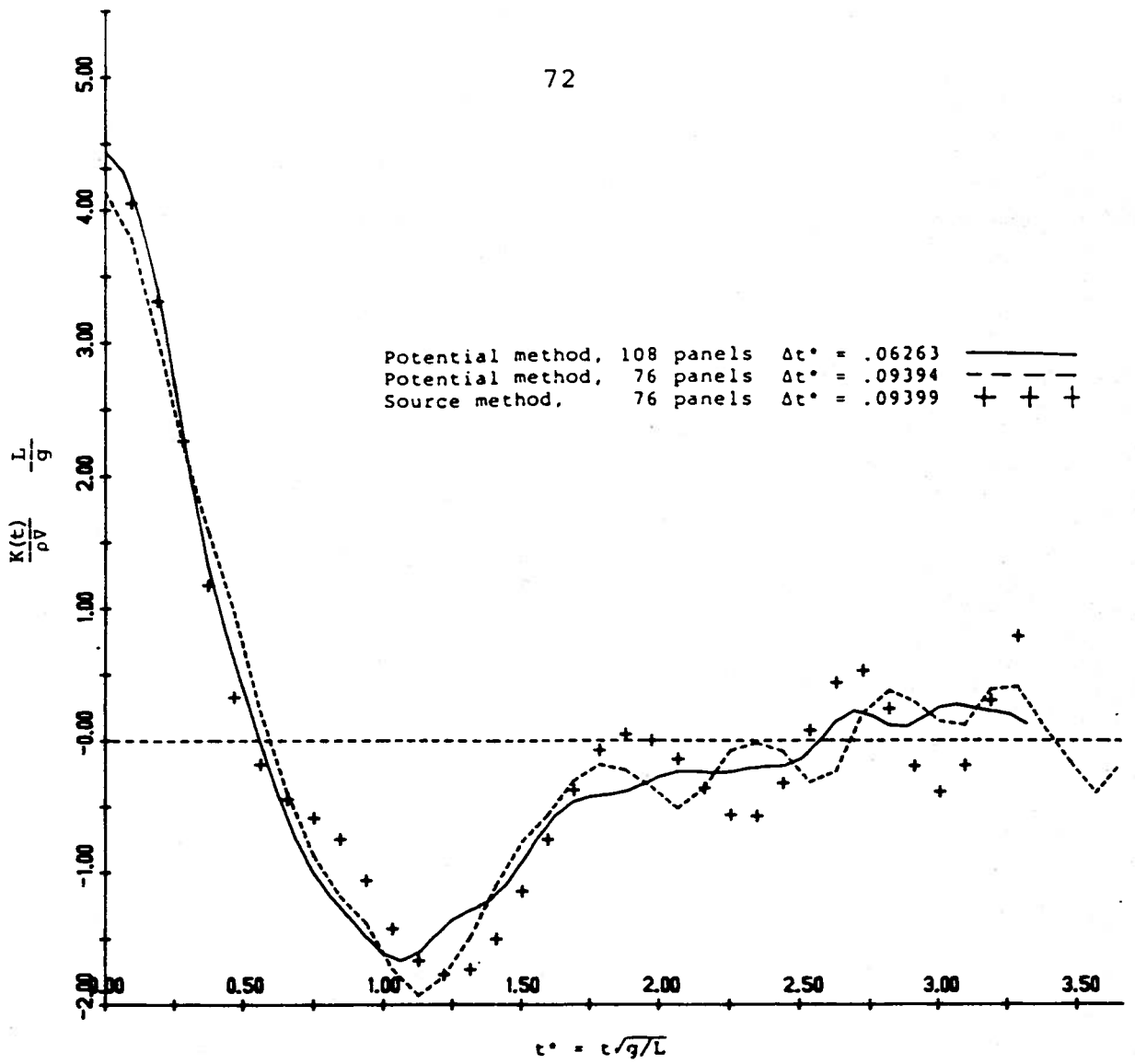


Figure 9

Memory Function for Heave Force on a Series 60
 ($C_B = .70$) Model at $F_n = 0$



Figure 10. Panel Distribution

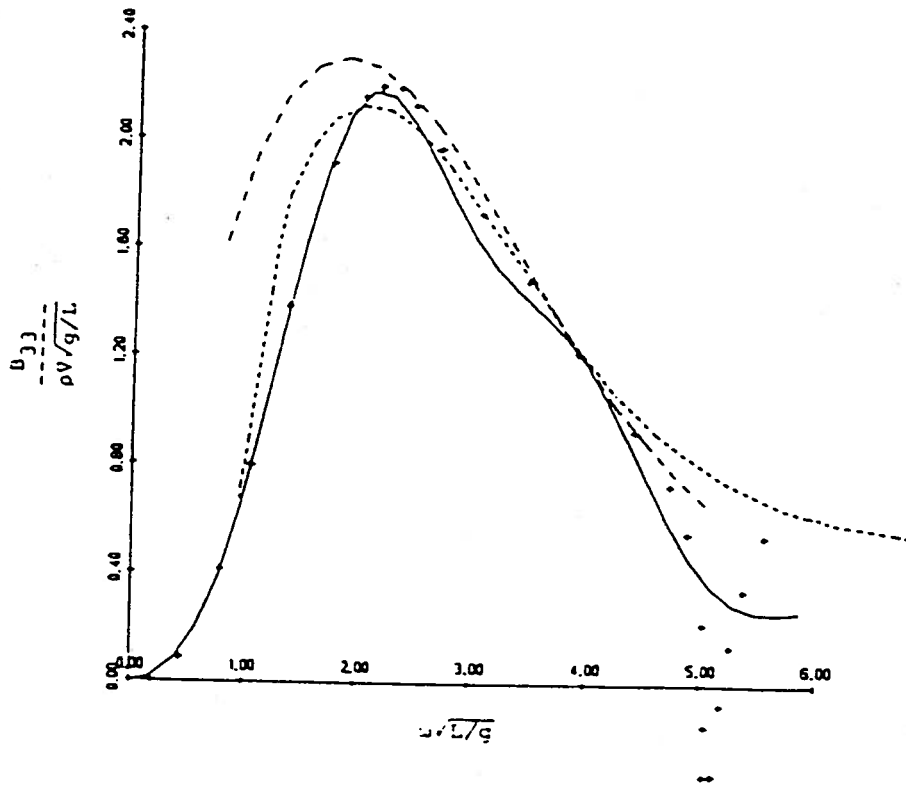
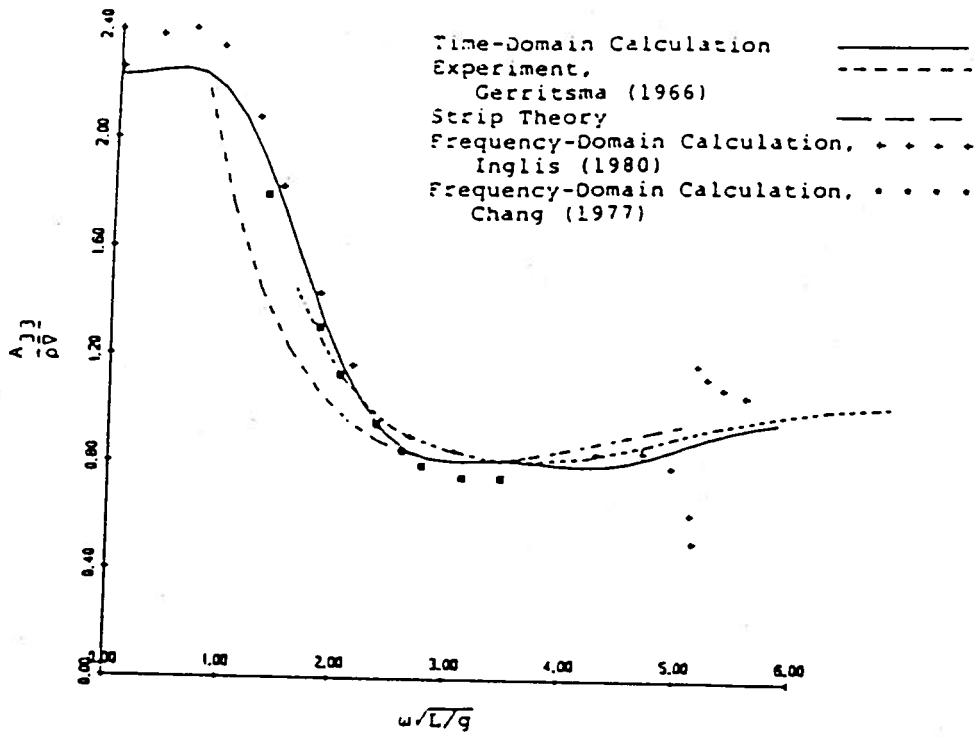


Figure 11. Heave Added Mass and Damping Coefficients for a Series 60 ($C_B = .70$) Model at $F_n = 0$

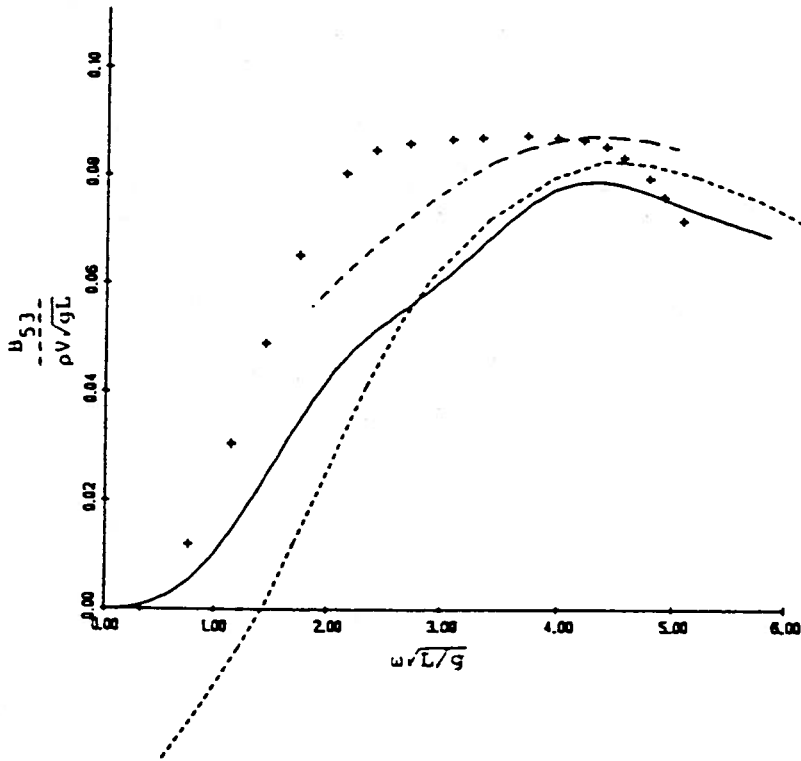
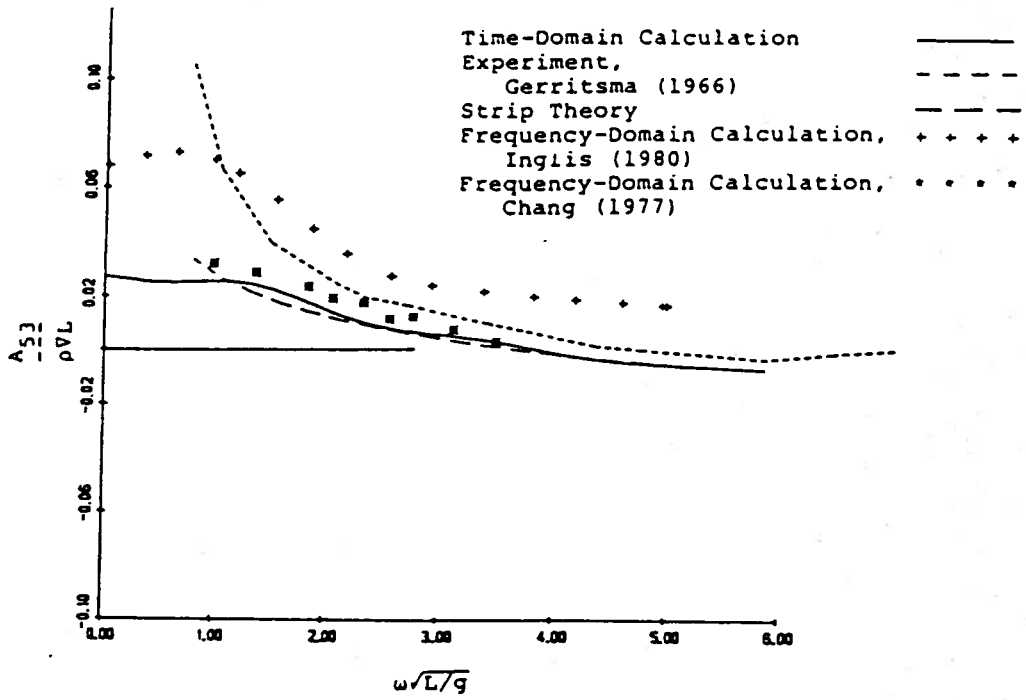


Figure 12. Heave-Pitch Cross Coupling Coefficients for a Series 60 ($C_B = .70$) Model at $F_n = 0$

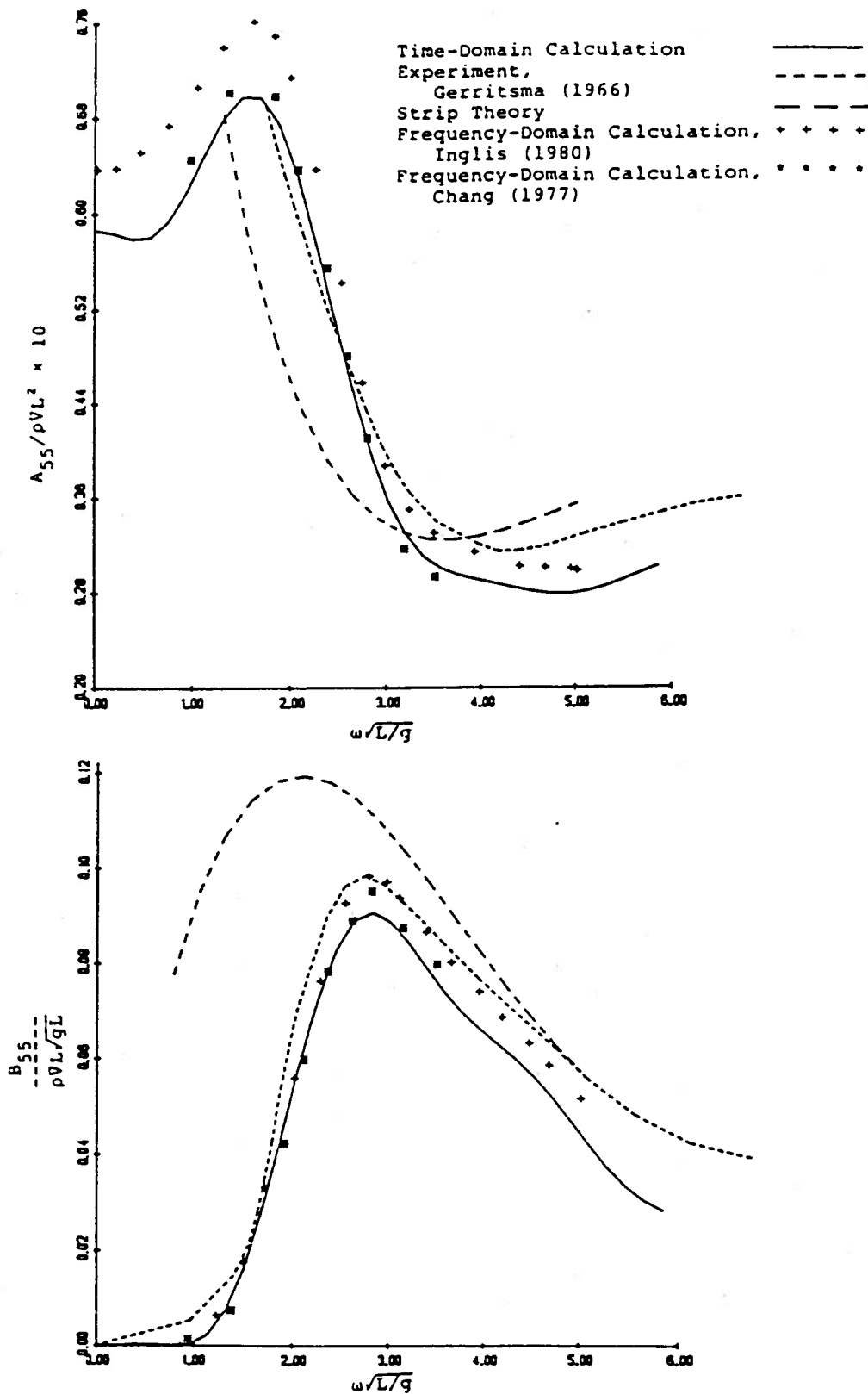


Figure 13. Pitch Added Mass and Damping Coefficients for a Series 60 ($C_B = .70$) Model at $F_n = 0$

singularity in Inglis' results around $\omega^* = 5.0$ is the irregular frequency in the frequency domain calculation. The time domain calculations also exhibit erratic behavior in this region. Similar to the case of the sphere the time domain predictions may be improved by increasing the number of panels and time steps.

Figure 12 presents the cross-coupling coefficient between heave and pitch. At zero forward speed $A_{35} = A_{53}$ and $B_{35} = B_{53}$; thus only A_{35} and B_{35} are plotted. The differences in the computed values of A_{35} , B_{35} and A_{53} , B_{53} are less than 3% in all cases. The cross-coupling coefficients are the most sensitive measures of the numerical accuracy of the program because they involve taking the differences between the two ends of the model, which have been exaggerated due to a multiplication by the lever arm. The reason Inglis' results are so much larger than the others is not known. Note that both the present results and the experimental results cross zero and become negative.

The pitch added mass and damping is presented in figure 13. As with heave the time-domain curves are not smooth at high frequencies due to a presumed small number of panels and too big a time step size. Similar to A_{35} , Inglis' results for A_{55} are too large around the peak values.

IV. 1.b Case of Non-zero Forward Speed

In solving the forward speed problem two simplifications have been made. The first is that \underline{m} has been approximated by

$$\underline{m} = (0, 0, 0, 0, +U_0 n_3, -U_0 n_2) \quad (66)$$

The approximation (66) is equivalent to neglecting the effects of the steady perturbation velocities on the body boundary condition. This approximation was made because of the difficulty of determining ϕ_0 . The use of the complete value for m_j , as given in equation (3) would not alter the time-domain computer program; it would nearly require different input values.

The second simplifying assumption is that in the computation for the hydrodynamic pressure the steady velocity vector, \underline{W} , can be approximated by the free stream-vector:

$$\underline{W} = (-U_0, 0, 0) \quad (67)$$

This assumption is consistent with neglecting the steady perturbation potential in the body boundary condition. The elimination of the steady perturbation velocities in equations (66) and (67) greatly eases the computational burden but it does not affect the time-domain analysis procedure.

The added mass and damping coefficients for the ship moving at a constant forward speed of Froude number equal to .2 are shown in figures 14 and 15. The computational time for these results is almost the same as for the zero forward speed case. The additional calculations which

must be made to include the line integral terms has very little effect on the total computer time. Arbitrarily deleting the line integral term from the calculations alters the results a maximum of 20%. Most of the alteration to the memory function curve due to the effect of the line integrals occurs around the peak of the curve and at large time.

The forward speed results all suffer from oscillations in the memory function at large time. This is the same problem as discussed in reference to figure 9. The same paneling was used for both $F_n = 0$ and $F_n = .2$. While the paneling was sufficient for the zero speed case, it apparently needs further refinement in the forward speed case. In addition the time step size and maximum time for the calculations has to be adjusted in order to improve the predictions. As can be seen in figures 14 and 15 the oscillations in the tail of the memory functions has lead to oscillations in the added mass and damping coefficients.

The heave added mass and damping is shown in figure 14. For the added mass all the results agree reasonably well; the damping shows a much larger spread between the various predictions. The hook at high frequency in the time-domain analysis curve is false and is the result of the oscillatory tail.

The pitch added inertia, pitch damping, and heave-pitch cross-coupling curves all show strong influences of

the oscillatory tail and need further investigation. When compared to the other theoretical calculations and to the experiments the time-domain predictions all have the correct magnitude, but the curves are not smooth. As an example, figure 15 shows the added mass and damping in pitch. The time-domain curves are not shown in the low frequency range because the results in that region depend on the arbitrary method of closure of the memory function at large time. A closure technique was necessary because the computer run was inadvertently stopped before the memory function return to zero. Lack of time and computer funds prevents a re-run. As can be seen the results are in the proper range. The oscillations and low frequency results can be improved by better numerical techniques at large time.

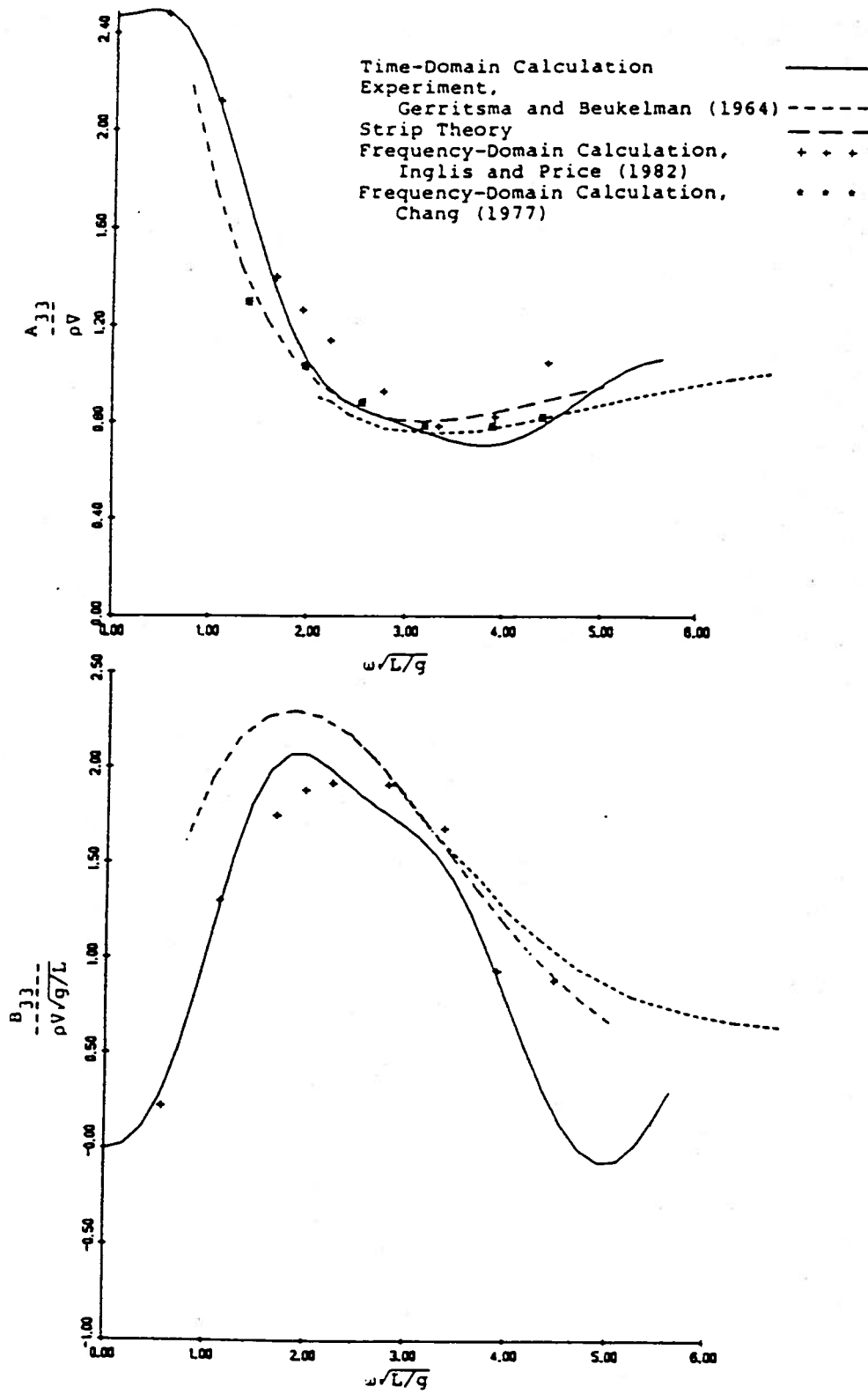


Figure 14. Heave Added Mass and Damping Coefficients for a Series 60 ($C_B = .70$) Model at $F_n = .2$

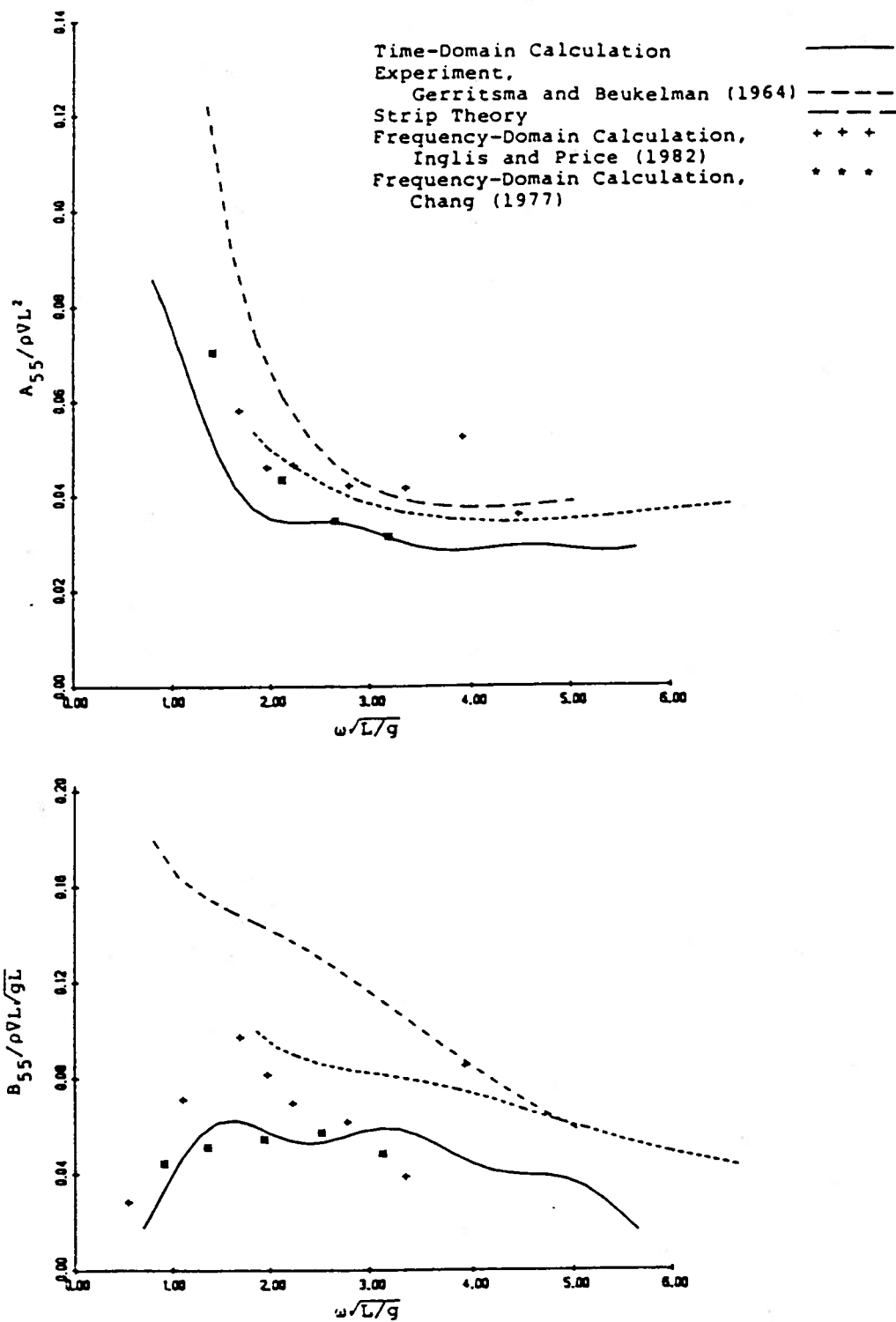


Figure 15. Pitch Added Mass and Damping Coefficients for a Series 60 ($C_B = .70$) Model at $F_n = .2$

IV.2 Motion of a Freely Floating Sphere

As an example of the use of the impulse response function, the problem of the transient motion of a floating sphere in heave is investigated. The sphere is in equilibrium floating on its meridian. At $t = 0$ it is assumed to be released from a small initial displacement in heave. The velocity of the sphere at $t = 0$ is zero.

The equation of motion for the sphere is

$$M\ddot{\zeta}_3(t) = -\rho g A \zeta_3(t) + F_{33}(t) \quad (68)$$

where

M = mass of sphere

$$= \rho \times \frac{2}{3}\pi R^3$$

R = radius of sphere

A = waterplane area of sphere

$$= \pi R^2$$

$\zeta_3(t)$ = heave amplitude

$F_{33}(t)$ = vertical hydrodynamic force acting on the sphere.

Using equation (36) and bringing all terms to the left-hand side of (68) the following integral-differential equation for the heave motion can be found:

$$(M + \mu_{33})\ddot{\zeta}_3(t) + \int_0^t d\tau K_{33}(t - \tau) \dot{\zeta}_3(\tau) + \rho g A \zeta_3(t) = 0 \quad (69)$$

subject to $\zeta_3(0) = h$

$$\dot{\zeta}_3(0) = 0$$

Equation (69) could be solved by a time-stepping numerical scheme. However for this simple problem it is much easier to use the standard Laplace transform technique. Taking the Laplace transform of (69) and solving for the Laplace transform of the heave motion ζ_3^* yields

$$\zeta_3^*(s) = \frac{s(M + \mu_{33})h + K_{33}^*(s)h}{(M + \mu_{33})s^2 + sK_{33}^*(s) + \rho g A} \quad (70)$$

where s = Laplace transform variable

$\zeta_3^*(s)$ = Laplace transform of $\zeta_3(t)$

$K_{33}^*(s)$ = Laplace transform of $K_{33}(t)$

h = initial displacement of sphere

The actual time history is found by taking the inverse transform of (70). As shown in Kotik and Lurye (1964, 1968), because $\zeta(t)$ and $K_{33}(t)$ are zero for $t < 0$, the Laplace transform can be evaluated using Fourier transforms with $s = i\omega$. For the numerical results presented in figure 16 a Fast Fourier transform routine was used to compute the transforms and their inverses.

Figure 16 shows the nondimensional heave displacement $(\zeta_3(t)/h)$ versus nondimensional time $(t\sqrt{g/R})$ for a sphere released from an initial displacement h . The results computed by the techniques presented in this paper agree with those of Kotik and Lurye to within the accuracy

of their graph. Kotik and Lurye also used the Fourier transform technique, but they find the added mass and damping analytically using asymptotic methods and the Kramers-Kronig relations.

Also shown in figure 16 are the results of a simple experiment carried out at the Ship Hydrodynamics Laboratory of The University of Michigan. A .508 m diameter sphere was suspended over the towing tank and released. The sphere model was built with wall sides from the waterline upward. The heave motion was measured by a sonic wave probe placed over the model; a technique which gives a resolution in vertical heave motion of .25 mm. The analogue signal for the heave displacement was digitized at a rate of 101 samples per second and stored in a computer for subsequent data analysis. The model was released by the cutting of a thin suspension wire. The precise starting time was obtained by examination of the digital record, which showed a small "blip" when the wire was cut. The starting time was thus known to within $\pm .005$ of a sec.

Several initial displacements were run. Within experimental accuracy the responses were linear with h up until about a 2.5 cm initial displacement. The results shown in figure 8 are for an initial displacement of 2.51 cm. As can be seen the agreement between theory and experiment is excellent. The experimental record was stopped after $t/\sqrt{g/R} = 32.00$ due to wall reflections

causing changes in the response. As can be seen in figure 16 the experimental results agree extremely well with the analytic predictions made by the methods presented in this paper or those of Kotik and Lurye (1968).

Bailey, Griffiths and Maskell (1976) conducted similar experiments but on spheres of 5 and 10 cm in diameter. They measured the vertical displacement from photographs taken at 18 frames per second. Bailey et al did not compare their results to the analytic predictions of Kotik and Lurye (1968) but a simple comparison shows they do not agree very well. The peak amplitudes in their experimental curves are lower than the analytic results by 10 to 35%. The phases can not be compared because Bailey et al do not list the nondimensionalization used for the time scale. Presumably the results of Bailey et al are low because of the small sphere diameter and the effects of viscosity and surface tension.

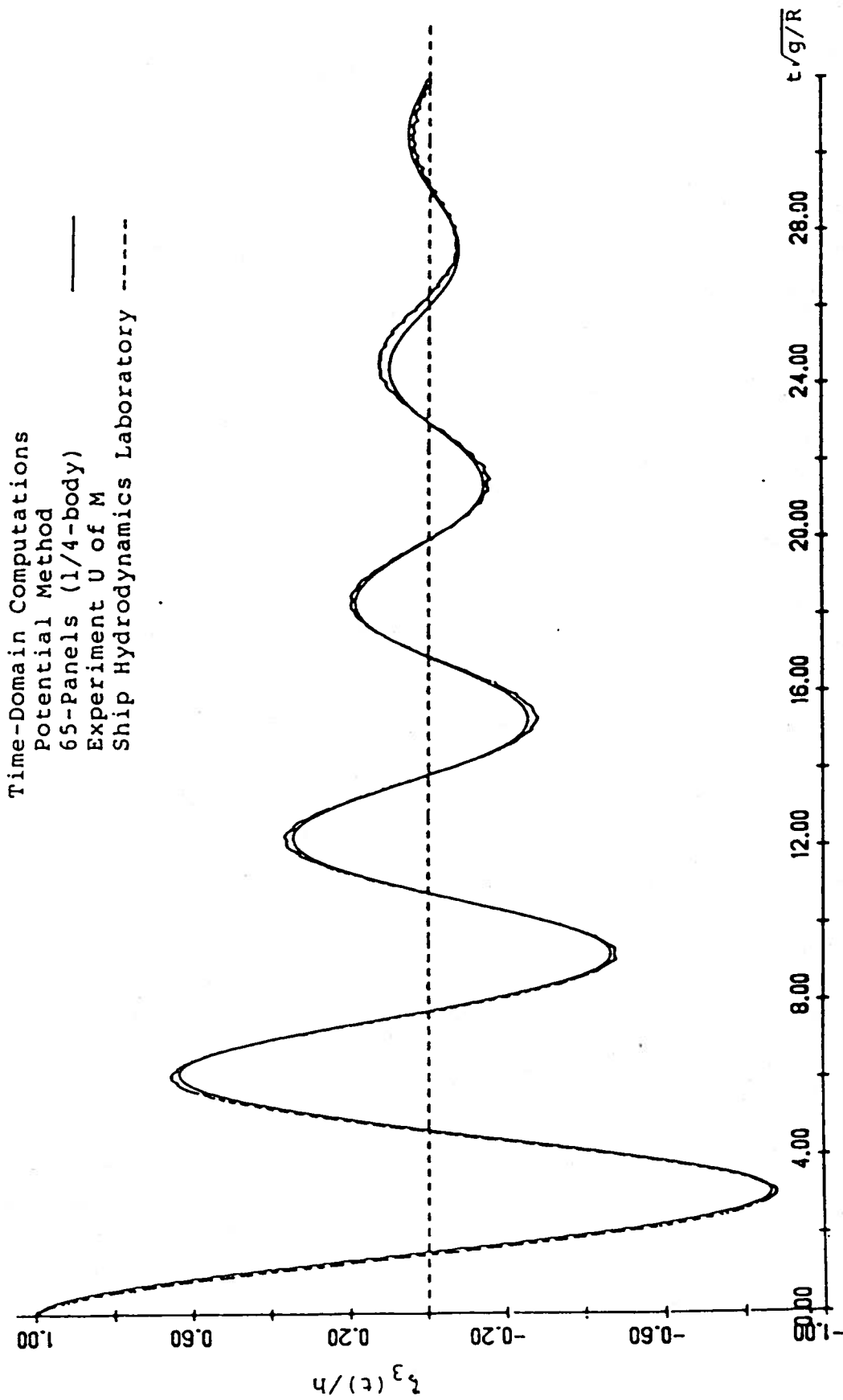


Figure 16.

Nondimensional Heave Displacement versus Nondimensional Time for a Hemisphere Released From a Height h

CHAPTER V
CONCLUSIONS

The use of time-domain analysis has been shown to be a viable alternative to the frequency-domain approach for solving the radiation problem. As compared to a frequency domain formulation, the time-domain technique can be extended from zero to constant forward speed with only minor modifications. The computer time for the forward speed case is only slightly larger than the zero speed case. On the other hand, the extension of the frequency domain solution to include forward speed is very difficult. Furthermore the present method may be extended to the more general case of nonconstant forward speed and a curved trajectory.

The major disadvantages of the time domain analysis are all related to the behavior of the memory functions at large time. Related to the irregular frequencies in the frequency domain, an oscillatory error appears in the tail of the time-domain memory function as it approaches zero at large time. By solving for the velocity potential directly, the oscillatory error can presumably be made as small as necessary by using time steps and quadrilateral elements which are sufficiently small. Unfortunately, this

greatly increases the computer time. Variable time step size and/or asymptotic analysis can make this analysis more efficient for practical calculations. Finally, in order for this method to be complete the diffraction problem must be formulated and solved in the time-domain. This requires determining the diffraction force exerted on a stationary body by some kind of transient wave input.

APPENDICES

APPENDIX A

Extension of the theory to Ship Maneuvering.

The theory developed in Chapter II may be extended to include a more general case of an unsteady maneuver of a surface ship. Although the analysis for this case follows a similar manner, the computational effort increases considerably. Also in this case, viscous effects are important and neglecting them may affect the results significantly.

It is convenient to employ a coordinate system $Oxyz$ fixed to the ship. Since the path of a surface ship is restrained to the horizontal plane, the coordinates $X(t)$ and $Y(t)$ of O and the heading angle ψ define its position at any time as shown in figure A1. In order to convert the equations to the moving axes we first need to find the relationship of the moving frame $Oxyz$ to a coordinate frame $O_0x_0y_0z_0$ fixed in space. This relationship between the coordinate frames is:

$$\begin{aligned}x &= [x_0 - X(t)]\cos\psi + [y_0 - Y(t)]\sin\psi \\y &= - [x_0 - X(t)]\sin\psi + [y_0 - Y(t)]\cos\psi \\z &= z_0\end{aligned}\tag{A1}$$

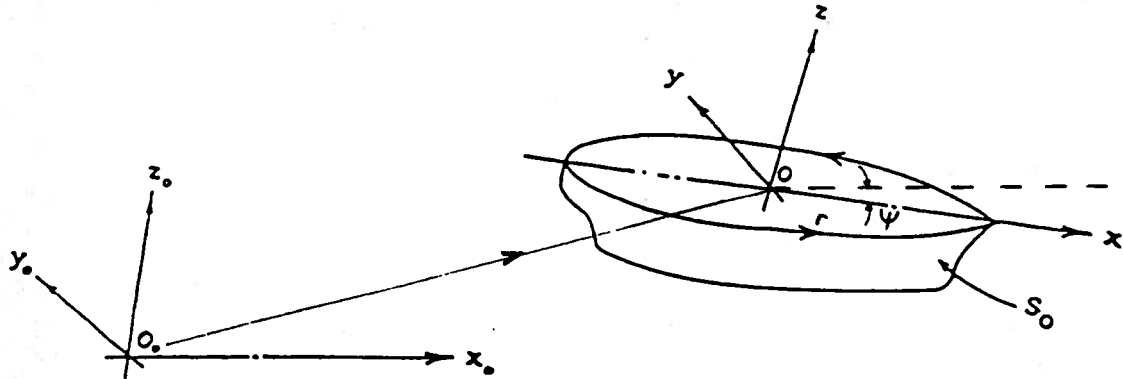


Figure A-1: Coordinate System for a Maneuvering Ship

Using the relations (A1) we may write the free surface condition in the moving frame as:

$$\left(\frac{\partial}{\partial t} - f_1(t) \frac{\partial}{\partial x} - f_2(t) \frac{\partial}{\partial y} \right)^2 \phi + g \frac{\partial \phi}{\partial z} = 0 \text{ on } z = 0 \tag{A2}$$

where

$$f_1(t) = - \frac{\partial x}{\partial t} = - \left[- \frac{\partial X}{\partial t} \cos \psi + X \sin \psi \frac{\partial \psi}{\partial t} - \frac{\partial Y}{\partial t} \sin \psi - Y \sin \psi \frac{\partial \psi}{\partial t} \right]$$

$$f_2(t) = - \frac{\partial y}{\partial t} = - \left[- \frac{\partial X}{\partial t} \sin \psi + X \cos \psi \frac{\partial \psi}{\partial t} - \frac{\partial Y}{\partial t} \cos \psi - Y \sin \psi \frac{\partial \psi}{\partial t} \right]$$

Since the ship follows a prescribed path \$f_1, f_2\$ are given functions of time. In the special case of a straight

trajectory by setting $\frac{\partial X}{\partial t} = U_0$, $\frac{\partial Y}{\partial t} = 0$ and $\psi = 0$ the free surface condition (A2) simply reduces to equation (2) of Chapter II.

For this problem the appropriate Green function is:

$$G(P, Q, t, \tau) = \left(\frac{1}{r} - \frac{1}{r'} \right) \delta(t - \tau) + H(t - \tau) \\ \times 2 \int_0^{\infty} dk \sqrt{kg} \sin(\sqrt{kg}(t - \tau)) e^{k(z + \zeta)} J_0(kR) \quad (A3)$$

where

$$P = (x, y, z)$$

$$Q = (\xi, \eta, \zeta)$$

$$r^2 = (x - \xi)^2 + (y - \eta)^2 + (z - \zeta)^2$$

$$r'^2 = (x - \xi)^2 + (y - \eta)^2 + (z - \zeta)^2$$

$$R^2 = \left(x - \xi + \int_{\tau}^t f_1(\tau) d\tau \right)^2 + \left(y - \eta + \int_{\tau}^t f_2(\tau) d\tau \right)^2$$

The integrated form of G is given by Wehausen and Laitone (1960) as the potential for a source of variable strength following an arbitrary path. Note that while in the special case of constant forward speed one may express G a function of $t - \tau$, in this more general case this is no longer true. As a result, in this general case the linear system which is used to model the ship motions is no longer time invariant.

As in the case of constant forward speed applying Green's theorem to the fluid domain gives:

$$\begin{aligned} \phi(P,t) = & -\frac{1}{4\pi} \int_0^t d\tau \iint_S dS \left(\phi(Q,\tau) \frac{\partial G(P,Q,t,\tau)}{\partial n_Q} \right. \\ & \left. - G(P,Q,t,\tau) \frac{\partial \phi(Q,\tau)}{\partial n_Q} \right) \end{aligned} \quad (A4)$$

The contribution from the integral over the free surface on the right hand side of (A4) may be reduced to a line integral. From (A2) on the free surface $z=0$ we have:

$$\frac{\partial}{\partial n} \equiv \frac{\partial}{\partial \zeta} = -\frac{1}{g} \left(\frac{\partial}{\partial \tau} - f_1(\tau) \frac{\partial}{\partial \xi} - f_2(\tau) \frac{\partial}{\partial \eta} \right)^2$$

In view of the above, the contribution to (A4) from the free surface is:

$$\begin{aligned} \phi_F = & \frac{1}{4\pi g} \int_0^t d\tau \iint_{S_F} dS \left[\phi(Q,\tau) \left(\frac{\partial}{\partial \tau} - f_1(\tau) \frac{\partial}{\partial \xi} - f_2(\tau) \frac{\partial}{\partial \eta} \right)^2 \right. \\ & G(P,Q,t,\tau) \\ & \left. - G(P,Q,t,\tau) \left(\frac{\partial}{\partial \tau} - f_1(\tau) \frac{\partial}{\partial \xi} - f_2(\tau) \frac{\partial}{\partial \eta} \right)^2 \phi(Q,\tau) \right] \\ = & \phi_{F1} + \phi_{F2} + \phi_{F3} + \phi_{F4} \end{aligned} \quad (A5)$$

where

$$\begin{aligned} \phi_{F1} = & \frac{1}{4\pi g} \int_0^t d\tau \iint_{S_F} dS \left[\phi(Q,\tau) G_{\tau\tau}(P,Q,t,\tau) \right. \\ & \left. - G(P,Q,t,\tau) \phi_{\tau\tau}(Q,\tau) \right] \\ = & \frac{1}{4\pi g} \iint_{S_F} dS \int_0^t d\tau \frac{\partial}{\partial \tau} \left[\phi(Q,\tau) G_{\tau}(P,Q,t,\tau) \right. \\ & \left. - G(P,Q,t,\tau) \phi_{\tau}(Q,\tau) \right] \end{aligned}$$

$$= \frac{1}{4\pi g} \iint_{S_F} dS [\phi(Q, \tau) G_\tau(P, Q, t, \tau) - G(P, Q, t, \tau) \phi_\tau(Q, \tau)] \Big|_0^t \quad (A6)$$

Assuming zero initial conditions for ϕ and ϕ_τ the last expression is zero at both limits. The ϕ_{F2} term is:

$$\begin{aligned} \phi_{F2} &= \frac{1}{4\pi g} \int_0^t d\tau \iint_{S_F} dS (f_1^2 G_{\xi\xi} \phi - f_1^2 \phi_{\xi\xi} G \\ &+ f_2^2 G_{\eta\eta} \phi - f_2^2 \phi_{\eta\eta} G) \\ &= \frac{1}{4\pi g} \int_0^t d\tau \iint_{S_F} dS [f_1^2 \frac{\partial}{\partial \xi} (G_\xi \phi - \phi_\xi G) \\ &+ f_2^2 \frac{\partial}{\partial \eta} (G_\eta \phi - \phi_\eta G)] \end{aligned}$$

Applying Stokes' theorem we get:

$$\begin{aligned} \phi_{F2} &= - \frac{1}{4\pi g} \int_0^t d\tau [f_1^2(\tau) \int_\Gamma d\eta (G_\xi \phi - \phi_\xi G) \\ &- f_2^2(\tau) \int_\Gamma d\xi (G_\eta \phi - \phi_\eta G)] \quad (A7) \end{aligned}$$

Where Γ is the intersection of the mean hull surface S_0 and the plane $z=0$.

The ϕ_{F3} term is:

$$\begin{aligned} \Phi_{F3} = & \frac{1}{4\pi g} \int_0^t d\tau \iint_{S_F} dS (-f_1 G_{\xi\tau} \phi - f_{1\tau} G_{\xi} \phi \\ & + f_1 \phi_{\xi\tau} G + f_{1\tau} \phi_{\xi} G - f_1 G_{\xi\tau} \phi + f_1 \phi_{\xi\tau} G - f_2 G_{\eta\tau} \phi \\ & - f_{2\tau} G_{\eta} \phi + f_2 \phi_{\eta\tau} G + f_{2\tau} \phi_{\eta} G - f_2 G_{\eta\tau} \phi + f_2 \phi_{\eta\tau} G) \end{aligned}$$

Integrating by parts with respect to time gives:

$$\begin{aligned} \Phi_{F3} = & \frac{1}{4\pi g} \int_0^t d\tau \iint_{S_F} dS \left(-\phi \frac{\partial}{\partial \tau} (f_1 G_{\xi\tau}) + G \frac{\partial}{\partial \tau} (f_1 \phi_{\xi\tau}) \right. \\ & - f_1 G_{\xi\tau} \phi + f_1 \phi_{\xi\tau} G \\ & - \phi \frac{\partial}{\partial \tau} (f_2 G_{\eta\tau}) + G \frac{\partial}{\partial \tau} (f_2 \phi_{\eta\tau}) - f_2 G_{\eta\tau} \phi + f_2 \phi_{\eta\tau} G) = \\ & \frac{1}{4\pi g} \int_0^t d\tau \iint_{S_F} dS (f_1 \phi_{\tau} G_{\xi} - f_1 \phi_{\xi} G_{\tau} - f_1 G_{\xi\tau} \phi \\ & + f_1 \phi_{\xi\tau} G + f_2 \phi_{\tau} G_{\eta} - f_2 \phi_{\eta} G_{\tau} - f_2 G_{\eta\tau} \phi + f_2 \phi_{\eta\tau} G = \\ & = \frac{1}{4\pi g} \int_0^t d\tau \iint_{S_F} dS \left[-f_1 \frac{\partial}{\partial \xi} (G_{\tau} \phi - \phi_{\tau} G) \right. \\ & \left. - f_2 \frac{\partial}{\partial \eta} (G_{\tau} \phi - \phi_{\tau} G) \right] \end{aligned}$$

Again the above expression may be simplified by using Stokes' theorem:

$$\begin{aligned} \phi_{F3} &= \frac{1}{4\pi g} \int_0^t d\tau \left[f_1(\tau) \int_{\Gamma} dn (G_{\tau} \phi - \phi_{\tau} G) \right. \\ &\quad \left. - f_2(\tau) \int_{\Gamma} d\xi (G_{\tau} \phi - \phi_{\tau} G) \right] \end{aligned} \quad (A8)$$

Finally the ϕ_{F4} term is:

$$\begin{aligned} \phi_{F4} &= \frac{1}{4\pi g} \int_0^t d\tau \iint_{S_F} dS (2f_1 f_2 G_{\xi n} \phi - 2f_1 f_2 \phi_{\xi n} G) \\ &= \frac{1}{4\pi g} \int_0^t d\tau \iint_{S_F} dS 2f_1 f_2 \left[\frac{\partial}{\partial \xi} (G_{\xi} \phi) - \frac{\partial}{\partial n} (\phi_n G) \right] \end{aligned}$$

Stokes theorem gives:

$$\phi_{F4} = \frac{1}{4\pi g} \int_0^t d\tau 2f_1(\tau)f_2(\tau) \left[\int_{\Gamma} dn G_{\xi} \phi + \int_{\Gamma} d\xi \phi_n G \right]$$

Integrating the last integral by parts gives the result:

$$\phi_{F4} = \frac{1}{4\pi g} \int_0^t d\tau 2f_1(\tau)f_2(\tau) \left[\int_{\Gamma} dn G_{\xi} \phi + \int_{\Gamma} d\xi G_n \phi \right] \quad (A9)$$

Combining equations (A4), (A5), (A6), (A7), (A8) and (A9) we may express the potential at any point P in the fluid domain as:

$$\begin{aligned} \phi(P, t) &= - \frac{1}{4\pi g} \int_0^t d\tau \iint_{S_O} dS \left(\phi \frac{\partial G}{\partial n} - G \frac{\partial \phi}{\partial n} \right) \\ &\quad + \frac{1}{4\pi g} \int_0^t d\tau \int_{\Gamma} dn [f_1^2(\tau) \left(G \frac{\partial \phi}{\partial \xi} - \phi \frac{\partial G}{\partial \xi} \right) \end{aligned}$$

$$\begin{aligned}
& - f_1(\tau) \left(G \frac{\partial \phi}{\partial \tau} - \phi \frac{\partial G}{\partial \tau} \right) - 2 f_1(\tau) f_2(\tau) \phi \frac{\partial G}{\partial \xi} \\
& - \frac{1}{4\pi g} \int_0^t d\tau \int_{\Gamma} d\xi \left[f_2^2(\tau) \left(G \frac{\partial \phi}{\partial \eta} - \phi \frac{\partial G}{\partial \eta} \right) \right. \\
& \left. - f_2(\tau) \left(G \frac{\partial \phi}{\partial \tau} - \phi \frac{\partial G}{\partial \tau} \right) - 2 f_1(\tau) f_2(\tau) \phi \frac{\partial G}{\partial \eta} \right] \quad (A10)
\end{aligned}$$

This expression states that the fluid flow resulting from an arbitrary maneuver of the ship may be represented by a distribution of sources and dipoles over the mean hull surface S_0 and the line Γ which is the intersection of S_0 with the plane $z=0$. The special case of a ship moving at a constant forward speed in the x direction may be recast by setting $f_1(\tau) = U_0$ and $f_2(\tau) = 0$. In that special case equation (A10) becomes identical to equation (II.14) which was used in the numerical computation scheme.

Equation (A10) may be reduced to a pure source distribution of density $\sigma(Q, \tau)$ by defining a fictitious interior flow and subtracting it from the original equation (A10). The final result is equivalent to equation (II.15):

$$\begin{aligned}
\phi(P, t) &= - \frac{1}{4\pi} \int_0^t d\tau \iint_{S_0} dS G(P, Q, t, \tau) \sigma(Q, \tau) \\
& - \frac{1}{4\pi g} \int_0^t d\tau f_1^2(\tau) \int_{\Gamma} d\eta n_1 G(P, Q, t, \tau) \sigma(Q, \tau) \\
& + \frac{1}{4\pi g} \int_0^t d\tau f_2^2(\tau) \int_{\Gamma} d\xi n_2 G(P, Q, t, \tau) \sigma(Q, \tau) \quad (A11)
\end{aligned}$$

Where n_1, n_2 are the x and y components of the normal respectively.

The mathematical model described in this Appendix may be used to analyze the flow pattern created by a ship maneuver. In this general case however, since the ship speed and direction changes with time, an impulse response function can no longer be used. The method appropriate for this case, is to solve the hydrodynamic problem in conjunction with the dynamic equations as an initial value problem.

APPENDIX B

Derivation of the Integral Equations for the components of the potential ψ_{1k} , χ_k .

In equation (20) the potential is written as the sum of two parts:

$$\phi_k(P, t) = \psi_{1k}(P)\delta(t) + \chi_k(P, t) \quad (B1)$$

Substituting $\phi_k(P, t)$ from equation (B1) into the governing equation (14) gives:

$$\begin{aligned} \psi_{1k}(P)\delta(t) + \chi_k(P, t) = & -\frac{1}{4\pi} \int_0^t d\tau \iint_{S_0} dS [(\psi_{1k} \delta(\tau) + \chi_k(\tau)) \\ & \left(\frac{\partial}{\partial n_Q} \left(\frac{1}{r} - \frac{1}{r'} \right) \delta(t-\tau) + \frac{\partial \tilde{G}(t-\tau)}{\partial n_Q} \right) \\ & \left(\left(\frac{1}{r'} - \frac{1}{r} \right) \delta(t-\tau) + \tilde{G}(t-\tau) \right) \left(\frac{\partial \psi_{1k}}{\partial n_Q} \delta(\tau) + \frac{\partial \chi_k}{\partial n_Q} \right)] + \\ & + \frac{1}{4\pi g} \int_0^t d\tau \int_{\Gamma} dn \{ U_0^2 \left[\left(\frac{1}{r} - \frac{1}{r'} \right) \delta(t-\tau) + \tilde{G}(t-\tau) \right] \right. \\ & \left. \left(\frac{\partial}{\partial \xi} \psi_{1k}(P)\delta(\tau) + \frac{\partial \chi_k(P, \tau)}{\partial \xi} \right) \right. \\ & \left. - \left(\frac{\partial}{\partial \xi} \left(\frac{1}{r} - \frac{1}{r'} \right) \delta(t-\tau) + \frac{\partial \tilde{G}(t-\tau)}{\partial \xi} \right) (\psi_{1k} \delta(\tau) + \chi_k(\tau)) \right] - \end{aligned}$$

$$\begin{aligned}
& - U_0 \left[\left(\frac{1}{r} - \frac{1}{r'} \right) \delta(t-\tau) + \tilde{G}(t-\tau) \right] \left(\psi_{1k} \frac{\partial}{\partial \tau} \delta(t-\tau) + \frac{\partial}{\partial \tau} \chi_k(\tau) \right) - \\
& - \left[\left(\frac{1}{r} - \frac{1}{r'} \right) \frac{\partial}{\partial \tau} \delta(t-\tau) + \frac{\partial}{\partial \tau} \tilde{G}(t-\tau) \right] \left(\psi_{1k} \delta(\tau) + \chi_k(\tau) \right) \Big\} \\
& \hspace{20em} (B1)
\end{aligned}$$

The line integral terms may be simplified by observing that on the free surface $\frac{1}{r} - \frac{1}{r'} = 0$ and $\psi_{1k} = 0$. This gives:

$$\begin{aligned}
\psi_{1k}(P)\delta(t) + \chi_k(P,t) &= - \frac{1}{4\pi} \int_0^t d\tau \iint_{S_0} dS \left[(\psi_{1k} \delta(\tau) + \chi_k(\tau)) \right. \\
& \times \left. \left(\frac{\partial}{\partial n_Q} \left(\frac{1}{r} - \frac{1}{r'} \right) \delta(t-\tau) + \frac{\partial \tilde{G}(t-\tau)}{\partial n_Q} \right) \right. \\
& - \left. \left(\frac{1}{r} - \frac{1}{r'} \right) \delta(t-\tau) + \tilde{G}(t-\tau) \right] \left(\frac{\partial \psi_{1k}}{\partial n_Q} \delta(\tau) + \frac{\partial \chi_k}{\partial n_Q} \right) \\
& + \frac{1}{4\pi g} \int_0^t d\tau \int_{\Gamma} d\eta \left[U_0^2 \left(\tilde{G}(t-\tau) \frac{\partial \chi_k(\tau)}{\partial \xi} - \frac{\partial \tilde{G}(t-\tau)}{\partial \xi} \chi_k(\tau) \right) \right. \\
& - \left. U_0 \left(\tilde{G}(t-\tau) \frac{\partial \chi_k(\tau)}{\partial \tau} - \frac{\partial \tilde{G}(t-\tau)}{\partial \tau} \chi_k(\tau) \right) \right] \hspace{2em} (B2)
\end{aligned}$$

In order to get an integral equation for the values of the potential on the body surface let P approach the body surface. Then, as is well known, the surface integrals have a $\frac{1}{2}(\psi_{1k}\delta(\tau) + \chi_k(\tau))$ contribution. The final result is that the 4π becomes a 2π and the surface integrals are assumed to exclude the singularity. Since

$$\frac{\partial \psi_{1k}}{\partial n} = n_k \quad \text{and} \quad \frac{\partial \chi_k}{\partial n} = m_k \quad \text{from equation (21)}$$

equation (B2) becomes:

$$\begin{aligned} \psi_{1k}(P)\delta(t) + \chi_k(P,t) = & -\frac{1}{2\pi} \int_0^t d\tau \iint_{S_0} dS [(\psi_{1k}\delta(\tau) + \chi_k(\tau)) \\ & \times \left(\frac{\partial}{\partial n_Q} \left(\frac{1}{r} - \frac{1}{r'} \right) \delta(t-\tau) + \frac{\partial \tilde{G}(t-\tau)}{\partial n_Q} \right) \\ & - \left(\left(\frac{1}{r} - \frac{1}{r'} \right) \delta(t-\tau) + \tilde{G}(t-\tau) \right) (n_k \delta(\tau) + m_k)] + \\ & + \frac{1}{4\pi g} \int_0^t d\tau \int_{\Gamma} d\eta [U_0^2 \left(\tilde{G}(t-\tau) \frac{\partial \chi_k(\tau)}{\partial \xi} - \frac{\partial \tilde{G}(t-\tau)}{\partial \xi} \chi_k(\tau) \right) + \\ & - U_0 \left(\tilde{G}(t-\tau) \frac{\partial \chi_k(\tau)}{\partial \tau} - \frac{\partial \tilde{G}(t-\tau)}{\partial \tau} \chi_k(\tau) \right)] \end{aligned} \quad (B3)$$

Collecting terms proportional to $\delta(t)$ gives an integral equation for ψ_{1k} and the remaining terms yield an equation for χ_k . The final results are:

$$\begin{aligned}
\psi_{1k}(P) + \frac{1}{2\pi} \iint_{S_0} dS \psi_{1k} \frac{\partial}{\partial n_Q} \left(\frac{1}{r} - \frac{1}{r'} \right) \\
= \frac{1}{2\pi} \iint_{S_0} dS \left(\frac{1}{r} - \frac{1}{r'} \right) n_k
\end{aligned} \tag{B4}$$

$$\begin{aligned}
x_k(P, t) + \frac{1}{2\pi} \iint_{S_0} dS x_k(t) \frac{\partial}{\partial n_Q} \left(\frac{1}{r} - \frac{1}{r'} \right) \\
+ \frac{1}{2\pi} \int_0^t d\tau \iint_{S_0} dS x_k(\tau) \frac{\partial \tilde{G}(P, Q, t-\tau)}{\partial n_Q} \\
+ \frac{U_0^2}{2\pi g} \int_0^t d\tau \int_{\Gamma} d\eta \left(x_k(\tau) \frac{\partial \tilde{G}(t-\tau)}{\partial \xi} - \frac{\partial x_k(\tau)}{\partial \xi} \tilde{G}(t-\tau) \right) - \\
- \frac{U_0^2}{2\pi g} \int_0^t d\tau \int_{\Gamma} d\eta \left(x_k(\tau) \frac{\partial \tilde{G}(t-\tau)}{\partial \tau} - \frac{\partial x_k(\tau)}{\partial \tau} \tilde{G}(t-\tau) \right) =
\end{aligned} \tag{B5}$$

$$\begin{aligned}
= \frac{1}{2\pi} \iint_{S_0} dS m_k \left(\frac{1}{r} - \frac{1}{r'} \right) + \frac{1}{2\pi} \int_0^t d\tau \iint_{S_0} dS m_k \tilde{G}(t-\tau) + \\
+ \frac{1}{2\pi} \iint_{S_0} dS n_k \tilde{G}(P, Q, t) - \frac{1}{2\pi} \iint_{S_0} dS \psi_{1k} \frac{\partial \tilde{G}(P, Q, t)}{\partial n_Q}
\end{aligned}$$

It should be noted that in deriving equations (B4) and (B5) use has been made of the relations:

$$\int_0^t d\tau f(\tau) \delta(t-\tau) \delta(\tau) = f(0) \delta(t)$$

$$\int_0^t d\tau f(\tau) \delta(t-\tau) = f(t)$$

where $f(t)$ is an arbitrary function of time. It is implied that the integration limits are from 0^- to t^+ .

Alternatively, in order to avoid expressions involving products of generalized functions, one could obtain equations (B4) and (B5) in two steps. The first step is to substitute G from equation (5) into Green's theorem equation (14) and evaluate the integrations with respect to time. The second step is to use:

$$\phi_k(P, t) = \psi_{1k}(P) \delta(t) + \chi_k(P, t)$$

and separate the terms proportional to $\delta(t)$ from the other terms. The final equations are the same as equations (B4) and (B5).

Because $\frac{\partial \chi_k(\tau)}{\partial \tau}$ is difficult to evaluate numerically the term involving it is reduced by an integration by parts:

$$\begin{aligned} \int_0^t d\tau \int_{\Gamma} d\eta \frac{\partial \chi_k(\tau)}{\partial \tau} \tilde{G}(t-\tau) &= \int_{\Gamma} d\eta \int_0^t d\tau \frac{\partial \chi_k(\tau)}{\partial \tau} \tilde{G}(t-\tau) = \\ &= \int_{\Gamma} d\eta \tilde{G}(t-\tau) \chi_k(\tau) \Big|_{\tau=0}^{\tau=t} - \int_{\Gamma} d\eta \int_0^t d\tau \chi_k(\tau) \frac{\partial \tilde{G}(t-\tau)}{\partial \tau} \quad (B6) \end{aligned}$$

The boundary term vanishes since $\chi_k(0) = 0$ on the free surface, and $\tilde{G}(0) = 0$.

In view of (B6) the integral equation (B5) may be rewritten as:

$$\chi_k(P, t) + \frac{1}{2\pi} \iint_{S_0} dS \chi_k(t) \frac{\partial}{\partial n_Q} \left(\frac{1}{r} - \frac{1}{r'} \right)$$

$$\begin{aligned}
& + \frac{1}{2\pi} \int_0^t d\tau \iint_{S_0} dS \chi_k(\tau) \frac{\partial G(P, Q, t-\tau)}{\partial n_Q} \\
& + \frac{U_0^2}{2\pi g} \int_0^t d\tau \int_{\Gamma} d\eta \left(\chi_k(\tau) \frac{\partial \tilde{G}(t-\tau)}{\partial \xi} - \frac{\partial \chi_k(\tau)}{\partial \xi} \tilde{G}(t-\tau) \right) - \\
& - \frac{U_0}{\pi g} \int_0^t d\tau \int_{\Gamma} d\eta \chi_k(\tau) \frac{\partial \tilde{G}(t-\tau)}{\partial \tau} = \frac{1}{2\pi} \iint_{S_0} dS m_k \left(\frac{1}{r} - \frac{1}{r'} \right) \\
& + \frac{1}{2\pi} \int_0^t d\tau \iint_{S_0} dS m_k \tilde{G}(P, Q, t-\tau) + \frac{1}{2\pi} \iint_{S_0} dS n_k \tilde{G}(P, Q, t) - \\
& - \frac{1}{2\pi} \iint_{S_0} dS \psi_{1k} \frac{\partial \tilde{G}(P, Q, t)}{\partial n_Q} \tag{B7}
\end{aligned}$$

The integral equations (B4) and (B6) are the final equations (22) and (23) for the components of the potential ψ_{1k} and χ_k .

APPENDIX C

Derivation of equation (31) relating the present formulation to that of Ogilvie (1964).

In order to prove this relationship we start with the integral equation for the potential for χ_{2k} as given by Ogilvie (1964):

$$\begin{aligned} \chi_{2k}(P, t') &+ \frac{1}{2\pi} \iint_{S_0} dS \chi_{2k}(Q, t') \frac{\partial}{\partial n_Q} \left(\frac{1}{r} - \frac{1}{r'} \right) + \\ &+ \frac{1}{2\pi} \int_0^{t'} d\tau \iint_{S_0} dS \chi_{2k}(\tau) \frac{\partial}{\partial n_Q} \tilde{G}(P, Q, t-\tau) \\ &= \frac{1}{2\pi} \iint_{S_0} dS \psi_{2k} \frac{\partial \tilde{G}(P, Q, t')}{\partial n_Q} + \frac{1}{2\pi} \iint_{S_0} dS m_k \tilde{G}(P, Q, t') \quad (C1) \end{aligned}$$

Integrating both sides with respect to time from 0 to t we get:

$$\begin{aligned} \int_0^t \chi_{2k}(P, t') dt' &+ \frac{1}{2\pi} \int_0^t dt' \iint_{S_0} dS \chi_{2k}(Q, t') \frac{\partial}{\partial n_Q} \left(\frac{1}{r} - \frac{1}{r'} \right) + \\ &+ \frac{1}{2\pi} \int_0^t dt' \int_0^{t'} d\tau \iint_{S_0} dS \chi_{2k}(\tau) \frac{\partial}{\partial n_Q} \tilde{G}(P, Q, t-\tau) \\ &= - \frac{1}{2\pi} \int_0^t dt' \iint_{S_0} dS \psi_{2k} \frac{\partial \tilde{G}(P, Q, t')}{\partial n_Q} \\ &+ \frac{1}{2\pi} \int_0^t dt' \iint_{S_0} dS m_k \tilde{G}(P, Q, t') \quad (C2) \end{aligned}$$

Interchanging the order of the spatial and the time integration on the left hand side we may write:

$$\begin{aligned}
 & \int_0^t \chi_{2k}(P, t') dt' + \frac{1}{2\pi} \iint_{S_0} dS \left(\int_0^t \chi_{2k}(P, t') dt' \right) \frac{\partial}{\partial n_Q} \left(\frac{1}{r} - \frac{1}{r'} \right) + \\
 & + \frac{1}{2\pi} \iint_{S_0} dS \int_0^t dt' \int_0^t d\tau \chi_{2k}(\tau) \frac{\partial}{\partial n_Q} \tilde{G}(P, Q, t' - \tau) \\
 = & - \frac{1}{2\pi} \int_0^t dt' \iint_{S_0} \psi_{2k} \frac{\partial \tilde{G}(P, Q, t')}{\partial n_Q} + \frac{1}{2\pi} \int_0^t dt' \iint_{S_0} dS m_k \tilde{G}(P, Q, t') \\
 & \hspace{15em} (C3)
 \end{aligned}$$

Look at the term

$$I = \iint_{S_0} dS \int_0^t dt' \int_0^t d\tau \chi_{2k}(\tau) \frac{\partial}{\partial n_Q} \tilde{G}(P, Q, t' - \tau)$$

Setting $\tau' = t' - \tau$ this term may be rewritten as:

$$I = \iint_{S_0} dS \int_0^t dt' \int_0^t d\tau' \chi_{2k}(t' - \tau') \frac{\partial}{\partial n_Q} \tilde{G}(P, Q, \tau')$$

Interchanging the two time integrations yields:

$$\begin{aligned}
 I &= \iint_{S_0} dS \int_0^t d\tau' \int_{\tau'}^t dt' \chi_{2k}(t' - \tau') \frac{\partial}{\partial n_Q} \tilde{G}(P, Q, \tau') = \\
 &= \iint_{S_0} dS \int_0^t d\tau' \frac{\partial \tilde{G}(P, Q, \tau')}{\partial n_Q} \int_{\tau'}^t dt' \chi_{2k}(t' - \tau)
 \end{aligned}$$

Setting $\tau'' = t - \tau'$ and $t'' = t' - \tau'$ we may write:

$$I = \iiint_{S_0} dS \int_0^t d\tau'' \frac{\partial \tilde{G}(P, Q, t - \tau'')}{\partial n_Q} \int_0^{\tau''} dt'' x_{2k}(t'') \quad (C4)$$

Returning to the integral equation (C3) we substitute the integral term I from (C4):

$$\begin{aligned} & \int_0^t x_{2k}(P, t') dt' + \frac{1}{2\pi} \iiint_{S_0} dS \left(\int_0^t x_{2k}(P, t') dt' \right) \frac{\partial}{\partial n_Q} \left(\frac{1}{r} - \frac{1}{r'} \right) + \\ & + \frac{1}{2\pi} \iiint_{S_0} dS \int_0^t d\tau \frac{\partial \tilde{G}(P, Q, t - \tau)}{\partial n_Q} \left(\int_0^{\tau} dt' x_{2k}(t') \right) \\ & + \frac{1}{2\pi} \int_0^t dt' \iiint_{S_0} dS \psi_{2k} \frac{\tilde{G}(P, Q, t')}{\partial n_Q} + \frac{1}{2\pi} \int_0^t dt' \iiint_{S_0} dS m_k \tilde{G}(P, Q, t') \end{aligned} \quad (C5)$$

The integral equation for x_{1k} is:

$$\begin{aligned} x_{1k}(P, t) + \frac{1}{2\pi} \iiint_{S_0} dS x_{1k}(Q, t) \frac{\partial}{\partial n_Q} \left(\frac{1}{r} - \frac{1}{r'} \right) + \\ + \frac{1}{2\pi} \int_0^t d\tau' \iiint_{S_0} dS x_{1k}(\tau) \frac{\partial \tilde{G}(P, Q, t - \tau)}{\partial n_Q} \\ = - \frac{1}{2\pi} \iiint_{S_0} dS \psi_{1k} \frac{\tilde{G}(P, Q, t')}{\partial n_Q} + \frac{1}{2\pi} \iiint_{S_0} dS n_k \tilde{G}(P, Q, t) \end{aligned} \quad (C6)$$

Adding (C6) to (C5) gives:

$$\begin{aligned}
 & \left[\chi_{1k}(P, t) + \int_0^t \chi_{2k}(P, t') dt' \right] \\
 & + \frac{1}{2\pi} \iint_{S_0} dS \left[\chi_{1k}(P, t) + \int_0^t \chi_{2k}(P, t') dt' \right] \frac{\partial}{\partial n_Q} \left(\frac{1}{r} - \frac{1}{r'} \right) \\
 & + \frac{1}{2\pi} \iint_{S_0} dS \int_0^t d\tau \frac{\partial \tilde{G}(P, Q, t-\tau)}{\partial n_Q} \left[\chi_{1k}(P, \tau) + \int_0^\tau \chi_{2k}(P, t') dt' \right] \\
 & = \frac{1}{2\pi} \iint_{S_0} dS n_k \tilde{G}(P, Q, t) - \frac{1}{2\pi} \int_0^t d\tau \iint_{S_0} dS \psi_{2k} \frac{\partial \tilde{G}(P, Q, t-\tau)}{\partial n_Q} \\
 & - \frac{1}{2\pi} \iint_{S_0} dS \psi_{1k} \frac{\partial \tilde{G}(P, Q, t)}{\partial n_Q} + \frac{1}{2\pi} \int_0^t d\tau \iint_{S_0} dS m_k \tilde{G}(P, Q, t-\tau)
 \end{aligned} \tag{C7}$$

If we set $\chi_{1k}(P, t) + \int_0^t \chi_{2k}(P, t') dt' = \bar{\chi}_k(P, t)$ then the above equation (C7) becomes identical to the integral equation (29) which proves the equivalence of the the present formulation to that of Ogilvie (1964).

APPENDIX D

Integration over an Element

To evaluate the elements of the kernel matrix in equations (51) and (56), the influence of a plane quadrilateral panel on a collocation point P must be determined. Following Hess and Smith (1964), to each panel a local coordinate system is assigned such that the quadrilateral lies in the plane $z^* = 0$. As shown in figure D.1, the coordinates of the four corner points of the quadrilateral in this coordinate system are (x_1^*, y_1^*) , (x_2^*, y_2^*) , (x_3^*, y_3^*) and (x_4^*, y_4^*) .

In order to integrate numerically over the quadrilateral element it is convenient to transform it into a standard region. For the numerical work presented in this paper the standard region was chosen as a square defined by $(-1, -1)$, $(-1, 1)$, $(1, 1)$, and $(1, -1)$ (see figure D.1).

The coordinates of a point x^*, y^*, z^* can be expressed as a function of ξ^*, η^*, ζ^* by the following transformation

$$\begin{aligned} x^* &= N_1(\xi^*, \eta^*)x_1^* + N_2(\xi^*, \eta^*)x_2^* \\ &\quad + N_3(\xi^*, \eta^*)x_3^* + N_4(\xi^*, \eta^*)x_4^* \\ y^* &= N_1(\xi^*, \eta^*)y_1^* + N_2(\xi^*, \eta^*)y_2^* \\ &\quad + N_3(\xi^*, \eta^*)y_3^* + N_4(\xi^*, \eta^*)y_4^* \\ z^* &= \zeta^* \end{aligned}$$

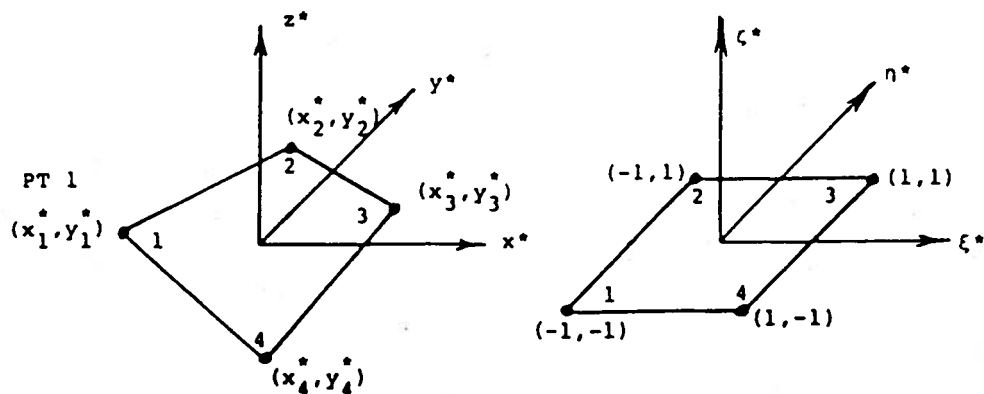


Figure D-1: Coordinate Mapping of Arbitrary Quadrilateral into a Square

$$\text{where } N_1 = \frac{1}{4}(1 - \xi)(1 - \eta)$$

$$N_2 = \frac{1}{4}(1 - \xi)(1 + \eta)$$

$$N_3 = \frac{1}{4}(1 + \xi)(1 + \eta)$$

$$N_4 = \frac{1}{4}(1 + \xi)(1 - \eta)$$

$(x_j^*, y_j^*, 0)$ = coordinate of the j^{th} vertex of the quadrilateral.

The integral over the quadrilateral can then be written as

$$\begin{aligned}
& \iint_{S_m} F(x^*, y^*, z^*) dx^* dy^* \\
&= \iint_{S_m} F(x^*(\xi^*, \eta^*), y^*(\xi^*, \eta^*), z^*) \left| \frac{D(x^*, y^*)}{D(\xi^*, \eta^*)} \right| d\xi^* d\eta^*
\end{aligned} \tag{D2}$$

where $\left| \frac{D(x^*, y^*)}{D(\xi^*, \eta^*)} \right|$ is the Jacobian of the above transformation.

The integral (D2) may be evaluated numerically by applying a product rule:

$$\begin{aligned}
& \iint_{S_m} F(x^*(\xi^*, \eta^*), y^*(\xi^*, \eta^*), z^*) \left| \frac{D(x^*, y^*)}{D(\xi^*, \eta^*)} \right| d\xi^* d\eta^* \\
& \approx \sum_{j=1}^{M_\zeta} \sum_{k=1}^{M_\eta} \left\{ F(x_j^*(\xi^*, \eta^*), y_k^*(\xi^*, \eta^*), z^*) \left| \frac{D(x^*, y^*)}{D(\xi^*, \eta^*)} \right| \right\} w_j w_k
\end{aligned} \tag{D3}$$

where w_j, w_k are the ξ^* and η^* integration weights respectively.

In general, it is more accurate to subdivide the body into a large number of panels with a 2×2 Gauss rule instead of fewer panels with a higher order integration rule.

For the present calculation a 2×2 Gaussian rule is used for most of the panels. Only for certain panels adjacent to the free surface for the Series 60 hull case a 4×4 rule was required.

APPENDIX E

Asymptotic analysis of the integral term in equation (64).

Define by F the complex integral:

$$F = \frac{1}{\sqrt{\pi}i} \int_0^{\pi/2} d\phi \left[(\mu - i\sqrt{1-\mu^2}\cos\phi)^{-3/2} - 2\beta^2(\mu - i\sqrt{1-\mu^2}\cos\phi)^{-5/2} \right] \\ \times \exp\left(-\frac{\beta^2}{4(\mu - i\sqrt{1-\mu^2}\cos\phi)}\right) \quad (E1)$$

The integral term appearing in equation (64) is the real part of the complex function F . Due to the presence of the large parameter β in the exponential, the major contribution to the value of the integral comes from the neighborhood of the point $\phi=0$. At that point the real part of the complex function $(\mu - i\sqrt{1-\mu^2})^{-1}$ that multiplies β^2 in the exponential has a maximum. The asymptotic behavior as $\beta \rightarrow \infty$ of this integral may be obtained by using Laplace's method. Following this method, we first expand the integrand in a series expansion around the point $\phi=0$. First replace $\cos\phi$ by its Taylor expansion around zero:

$$\begin{aligned}
F = & \frac{1}{\sqrt{\pi}i} \int_0^\epsilon d\phi \left[(\mu - i\sqrt{1-\mu^2})^{-3/2} \left(1 + \frac{i\sqrt{1-\mu^2} \phi^2}{2(\mu - i\sqrt{1-\mu^2})} \right. \right. \\
& - \frac{i\sqrt{1-\mu^2} \phi^4}{4!(\mu - i\sqrt{1-\mu^2})} + \frac{i\sqrt{1-\mu^2} \phi^6}{6!(\mu - i\sqrt{1-\mu^2})} - \left. \frac{i\sqrt{1-\mu^2} \phi^8}{8!(\mu - i\sqrt{1-\mu^2})} \right)^{-3/2} \\
& - 2\beta^2 (\mu - i\sqrt{1-\mu^2})^{-5/2} \left(1 + \frac{i\sqrt{1-\mu^2} \phi^2}{2(\mu - i\sqrt{1-\mu^2})} - \frac{i\sqrt{1-\mu^2} \phi^4}{4!(\mu - i\sqrt{1-\mu^2})} \right. \\
& \left. \left. + \frac{i\sqrt{1-\mu^2} \phi^6}{6!(\mu - i\sqrt{1-\mu^2})} - \frac{i\sqrt{1-\mu^2} \phi^8}{8!(\mu - i\sqrt{1-\mu^2})} \right)^{-5/2} \right] \\
& \times \exp \left[-\beta^2 \left[(\mu - i\sqrt{1-\mu^2}) \left(1 + \frac{i\sqrt{1-\mu^2} \phi^2}{2(\mu - i\sqrt{1-\mu^2})} \right. \right. \right. \\
& \left. \left. - \frac{i\sqrt{1-\mu^2} \phi^4}{4!(\mu - i\sqrt{1-\mu^2})} + \frac{i\sqrt{1-\mu^2} \phi^6}{6!(\mu - i\sqrt{1-\mu^2})} - \frac{i\sqrt{1-\mu^2} \phi^8}{8!(\mu - i\sqrt{1-\mu^2})} \right)^{-1} \right] \right] \quad (E2)
\end{aligned}$$

Note that since only the immediate neighborhood of 0 contributes to the integral we can replace the upper limit $\pi/2$ with a small number ϵ . This change of the upper limit introduces only exponentially small errors. It is natural to require that the asymptotic expansion of F does not depend on ϵ . Using the binomial theorem expression (E2) may be written as:

$$\begin{aligned}
F &= \frac{1}{\sqrt{\pi i}} \int_0^\varepsilon d\phi \left[(\mu - i\sqrt{1-\mu^2})^{-3/2} \right. \\
&\quad \left(1 - \frac{3}{2} \left(\frac{i\sqrt{1-\mu^2} \phi^2}{2(\mu - i\sqrt{1-\mu^2})} - \frac{i\sqrt{1-\mu^2} \phi^4}{4!(\mu - i\sqrt{1-\mu^2})} \right. \right. \\
&\quad \left. \left. + \frac{i\sqrt{1-\mu^2} \phi^6}{6!(\mu - i\sqrt{1-\mu^2})} - \frac{i\sqrt{1-\mu^2} \phi^8}{8!(\mu - i\sqrt{1-\mu^2})} \right) \right. \\
&\quad \left. + \frac{15}{8} \left(\frac{i\sqrt{1-\mu^2} \phi^2}{2(\mu - i\sqrt{1-\mu^2})} - \frac{i\sqrt{1-\mu^2} \phi^4}{4!(\mu - i\sqrt{1-\mu^2})} \right. \right. \\
&\quad \left. \left. + \frac{i\sqrt{1-\mu^2} \phi^6}{6!(\mu - i\sqrt{1-\mu^2})} - \frac{i\sqrt{1-\mu^2} \phi^8}{8!(\mu - i\sqrt{1-\mu^2})} \right)^2 \right. \\
&\quad \left. - \frac{105}{48} \left(\frac{i\sqrt{1-\mu^2} \phi^2}{2(\mu - i\sqrt{1-\mu^2})} - \frac{i\sqrt{1-\mu^2} \phi^4}{4!(\mu - i\sqrt{1-\mu^2})} \right. \right. \\
&\quad \left. \left. + \frac{i\sqrt{1-\mu^2} \phi^6}{6!(\mu - i\sqrt{1-\mu^2})} - \frac{i\sqrt{1-\mu^2} \phi^8}{8!(\mu - i\sqrt{1-\mu^2})} \right)^3 + \dots \right) \\
&\quad - 2 \beta^2 (\mu - i\sqrt{1-\mu^2})^{-5/2} \\
&\quad \times \left(1 - \frac{5}{2} \left(\frac{i\sqrt{1-\mu^2} \phi^2}{2(\mu - i\sqrt{1-\mu^2})} - \frac{i\sqrt{1-\mu^2} \phi^4}{4!(\mu - i\sqrt{1-\mu^2})} \right. \right. \\
&\quad \left. \left. + \frac{i\sqrt{1-\mu^2} \phi^6}{6!(\mu - i\sqrt{1-\mu^2})} - \frac{i\sqrt{1-\mu^2} \phi^8}{8!(\mu - i\sqrt{1-\mu^2})} \right) \right)
\end{aligned}$$

$$\begin{aligned}
& + \frac{35}{8} \left(\frac{i\sqrt{1-\mu^2} \phi^2}{2(\mu-i\sqrt{1-\mu^2})} - \frac{i\sqrt{1-\mu^2} \phi^4}{4!(\mu-i\sqrt{1-\mu^2})} \right. \\
& + \left. \frac{i\sqrt{1-\mu^2} \phi^6}{6!(\mu-i\sqrt{1-\mu^2})} - \frac{i\sqrt{1-\mu^2} \phi^8}{8!(\mu-i\sqrt{1-\mu^2})} \right)^2 \\
& - \frac{315}{48} \left(\frac{i\sqrt{1-\mu^2} \phi^2}{2(\mu-i\sqrt{1-\mu^2})} - \frac{i\sqrt{1-\mu^2} \phi^4}{4!(\mu-i\sqrt{1-\mu^2})} \right. \\
& + \left. \frac{i\sqrt{1-\mu^2} \phi^6}{6!(\mu-i\sqrt{1-\mu^2})} - \frac{i\sqrt{1-\mu^2} \phi^8}{8!(\mu-i\sqrt{1-\mu^2})} \right)^3 + \dots \Big]
\end{aligned}$$

$$\exp \left[-\beta^2 [(\mu-i\sqrt{1-\mu^2}) \left(1 + \frac{i\sqrt{1-\mu^2} \phi^2}{2(\mu-i\sqrt{1-\mu^2})} \right) \right.$$

$$\left. - \frac{i\sqrt{1-\mu^2} \phi^4}{4!(\mu-i\sqrt{1-\mu^2})} + \frac{i\sqrt{1-\mu^2} \phi^6}{6!(\mu-i\sqrt{1-\mu^2})} - \frac{i\sqrt{1-\mu^2} \phi^8}{8!(\mu-i\sqrt{1-\mu^2})} \right)^{-1} \Big]$$

(E3)

The exponential term may be also expanded around $\phi=0$ with the result:

$$\begin{aligned}
F &= \frac{1}{\sqrt{\pi}i} \int_0^\epsilon d\phi \left[(\mu-i\sqrt{1-\mu^2})^{-3/2} \right. \\
& \left. \left(1 - \frac{3}{2} \left(\frac{i\sqrt{1-\mu^2} \phi^2}{2(\mu-i\sqrt{1-\mu^2})} - \frac{i\sqrt{1-\mu^2} \phi^4}{4!(\mu-i\sqrt{1-\mu^2})} \right) \right) \right]
\end{aligned}$$

$$\begin{aligned}
& + \frac{i\sqrt{1-\mu^2} \phi^6}{6! (\mu - i\sqrt{1-\mu^2})} - \frac{i\sqrt{1-\mu^2} \phi^8}{8! (\mu - i\sqrt{1-\mu^2})} \\
& + \frac{15}{8} \left(\frac{i\sqrt{1-\mu^2} \phi^2}{2(\mu - i\sqrt{1-\mu^2})} - \frac{i\sqrt{1-\mu^2} \phi^4}{4! (\mu - i\sqrt{1-\mu^2})} \right) \\
& + \frac{i\sqrt{1-\mu^2} \phi^6}{6! (\mu - i\sqrt{1-\mu^2})} - \frac{i\sqrt{1-\mu^2} \phi^8}{8! (\mu - i\sqrt{1-\mu^2})} \\
& - \frac{105}{48} \left(\frac{i\sqrt{1-\mu^2} \phi^2}{2(\mu - i\sqrt{1-\mu^2})} - \frac{i\sqrt{1-\mu^2} \phi^4}{4! (\mu - i\sqrt{1-\mu^2})} \right) \\
& + \frac{i\sqrt{1-\mu^2} \phi^6}{6! (\mu - i\sqrt{1-\mu^2})} - \frac{i\sqrt{1-\mu^2} \phi^8}{8! (\mu - i\sqrt{1-\mu^2})} + \dots \\
& - 2 \beta^2 (\mu - i\sqrt{1-\mu^2})^{-5/2} \\
& \times \left(1 - \frac{5}{2} \left(\frac{i\sqrt{1-\mu^2} \phi^2}{2(\mu - i\sqrt{1-\mu^2})} - \frac{i\sqrt{1-\mu^2} \phi^4}{4! (\mu - i\sqrt{1-\mu^2})} \right) \right. \\
& \left. + \frac{i\sqrt{1-\mu^2} \phi^6}{6! (\mu - i\sqrt{1-\mu^2})} - \frac{i\sqrt{1-\mu^2} \phi^8}{8! (\mu - i\sqrt{1-\mu^2})} \right) \\
& + \frac{35}{8} \left(\frac{i\sqrt{1-\mu^2} \phi^2}{2(\mu - i\sqrt{1-\mu^2})} - \frac{i\sqrt{1-\mu^2} \phi^4}{4! (\mu - i\sqrt{1-\mu^2})} \right)
\end{aligned}$$

$$\begin{aligned}
& + \left(\frac{i\sqrt{1-\mu^2} \phi^6}{6!(\mu-i\sqrt{1-\mu^2})} - \frac{i\sqrt{1-\mu^2} \phi^8}{8!(\mu-i\sqrt{1-\mu^2})} \right)^2 \\
& - \frac{315}{48} \left(\frac{i\sqrt{1-\mu^2} \phi^2}{2(\mu-i\sqrt{1-\mu^2})} - \frac{i\sqrt{1-\mu^2} \phi^4}{4!(\mu-i\sqrt{1-\mu^2})} \right. \\
& \left. + \frac{i\sqrt{1-\mu^2} \phi^6}{6!(\mu-i\sqrt{1-\mu^2})} - \frac{i\sqrt{1-\mu^2} \phi^8}{8!(\mu-i\sqrt{1-\mu^2})} \right)^3 + \dots \Big] \\
& \times \left[1 - \frac{\beta^2}{(\mu-i\sqrt{1-\mu^2})} \left(\frac{i\sqrt{1-\mu^2} \phi^4}{4!(\mu-i\sqrt{1-\mu^2})} - \frac{i\sqrt{1-\mu^2} \phi^6}{6!(\mu-i\sqrt{1-\mu^2})} \right. \right. \\
& \left. \left. - \frac{i\sqrt{1-\mu^2} \phi^4}{4!(\mu-i\sqrt{1-\mu^2})} + \frac{i\sqrt{1-\mu^2} \phi^6}{4!(\mu-i\sqrt{1-\mu^2})} + \frac{i\sqrt{1-\mu^2} \phi^6}{8!(\mu-i\sqrt{1-\mu^2})} \right) \right. \\
& \left. + \frac{\beta^4}{2(\mu-i\sqrt{1-\mu^2})} \left(\frac{i\sqrt{1-\mu^2} \phi^4}{4!(\mu-i\sqrt{1-\mu^2})} - \frac{i\sqrt{1-\mu^2} \phi^6}{6!(\mu-i\sqrt{1-\mu^2})} \right. \right. \\
& \left. \left. - \frac{i\sqrt{1-\mu^2} \phi^4}{4!(\mu-i\sqrt{1-\mu^2})} + \frac{i\sqrt{1-\mu^2} \phi^6}{4!(\mu-i\sqrt{1-\mu^2})} + \frac{i\sqrt{1-\mu^2} \phi^6}{8!(\mu-i\sqrt{1-\mu^2})} \right)^2 + \dots \right] \\
& \times e^{-\frac{\beta^2}{(\mu-i\sqrt{1-\mu^2})} - \frac{i\phi^2\beta^2}{2(\mu-i\sqrt{1-\mu^2})^2}} \tag{E4}
\end{aligned}$$

Let $t^2 = -\frac{i\phi^2}{2(\mu-i\sqrt{1-\mu^2})^2}$. The variable t is real on

the steepest descent path. Expression (E4) for F may be

rewritten as:

$$\begin{aligned}
 F &= \frac{e^{-\frac{\beta^2}{\mu_C}}}{\sqrt{\pi} i} \int_0^\infty dt e^{-\beta^2 t^2} [\mu_C^{-3/2} \\
 &\times (1 - \frac{3i}{2} \sqrt{1-\mu^2} (i\mu_C t^2 + \frac{\mu_C^3 t^4}{3!} - \frac{8i}{6!} \mu_C^5 t^6 - \frac{16}{8!} \mu_C^7 t^8) \\
 &- \frac{15}{8} (1-\mu^2) (i\mu_C t^2 + \frac{\mu_C^3 t^4}{3!} - \frac{8i}{6!} \mu_C^5 t^6 - \frac{16}{8!} \mu_C^7 t^8)^2 \\
 &+ \frac{105}{48} (1-\mu^2)^{3/2} (i\mu_C t^2 + \frac{\mu_C^3 t^4}{3!} - \frac{8i}{6!} \mu_C^5 t^6 - \frac{16}{8!} \mu_C^7 t^8)^3 \\
 &+ \dots) - 2\beta^2 \mu_C^{-5/2} \\
 &\times (1 - \frac{5i}{2} \sqrt{1-\mu^2} (i\mu_C t^2 + \frac{\mu_C^3 t^4}{3!} - \frac{8i}{6!} \mu_C^5 t^6 - \frac{16}{8!} \mu_C^7 t^8) \\
 &- \frac{35}{8} (1-\mu^2) (i\mu_C t^2 + \frac{\mu_C^3 t^4}{3!} - \frac{8i}{6!} \mu_C^5 t^6 - \frac{16}{8!} \mu_C^7 t^8)^2 \\
 &+ \frac{315}{48} i (1-\mu^2)^{3/2} (i\mu_C t^2 + \frac{\mu_C^3 t^4}{3!} - \frac{8i}{6!} \mu_C^5 t^6 - \frac{16}{8!} \mu_C^7 t^8)^3 \\
 &+ \dots)] [1 - i\beta^2 \sqrt{1-\mu^2} (-\frac{\mu_C^2 t^4}{3!} + \frac{8i\mu_C^4 t^6}{6!} \\
 &- i\mu_C^2 t^4 - \frac{8}{4!} \mu_C^4 t^6 - i\mu_C^4 t^6)
 \end{aligned}$$

$$\begin{aligned}
& - \frac{\beta^4(1-\mu^2)}{2} \left(- \frac{\mu_C^2 t^4}{3!} + \frac{8i\mu_C^4 t^6}{6!} - i\mu_C^2 t^4 \right. \\
& \left. - \frac{8}{4!} \mu_C^4 t^6 - i\mu_C^4 t^6 \right)^2 + \dots] \quad (E5)
\end{aligned}$$

where we have set $\mu - i\sqrt{1-\mu^2} = \mu_C$

The most convenient way to evaluate the integral (E5) is to extend the integration region to infinity that is replace ϵ by ∞ . Again the change of upper integration limit introduces only exponentially small errors and does not affect the final asymptotic series. The procedure of first replacing the upper limit by a small number ϵ , then Taylor expanding around the lower integration limit and finally replacing the upper limit ϵ by ∞ is probably the most convenient way to obtain the asymptotic series for F . A complete description of this method may be found in Bender and Orszag (1978).

After replacing ϵ by ∞ in (E5) and collecting terms the resulting integrals may be evaluated analytically using the formula:

$$\int_0^{\infty} e^{-\frac{S^2}{2}} S^{2n} dS = \frac{\sqrt{\pi}}{\sqrt{2}} 1 \cdot 3 \dots (2n-1)$$

The final result after taking the real part of the resulting expression is:

$$\begin{aligned}
\operatorname{Re} \{F\} = & -\frac{e^{-\beta^2 \mu/4}}{\sqrt{2}} \left(\frac{\beta}{(1-\mu^2)^{1/4}} \sin\left(\frac{\beta^2 \sqrt{1-\mu^2}}{4} + \frac{3\theta}{2}\right) \right. \\
& + \frac{1}{2\beta(1-\mu^2)^{3/4}} \cos\left(\frac{\beta^2 \sqrt{1-\mu^2}}{4} - \frac{\theta}{2}\right) \\
& + \frac{1}{\beta^3(1-\mu^2)^{3/4}} \sin\left(\frac{\beta^2 \sqrt{1-\mu^2}}{4} - \frac{3\theta}{2}\right) \\
& - \frac{9}{8\beta^3(1-\mu^2)^{5/4}} \sin\left(\frac{\beta^2 \sqrt{1-\mu^2}}{4} - \frac{5\theta}{2}\right) - \\
& - \frac{9}{\beta^5(1-\mu^2)^{3/4}} \cos\left(\frac{\beta^2 \sqrt{1-\mu^2}}{4} - \frac{7\theta}{2}\right) \\
& \left. + \frac{24}{\beta^5(1-\mu^2)^{3/4}} \cos\left(\frac{\beta^2 \sqrt{1-\mu^2}}{4} - \frac{5\theta}{2}\right) \right] + O(\beta^{-7}) \quad (E6)
\end{aligned}$$

where

$$\theta = \sin^{-1}(\mu)$$

REFERENCES

REFERENCES

- Abramowitz, M., and Stegun, I.A. (1964). Handbook of Mathematical Functions, National Bureau of Standards, Washington, D.C.
- Adachi, H. and Ohmatsu, S. (1979). On the influence of irregular frequencies in the integral equation solutions of the time-dependent free surface problems. Journal of Engineering Mathematics, Vol. 16, No. 2, pp. 97-119.
- Adachi, H. and Ohmatsu, S. (1980). On the time dependent potential and its application to wave problems. Proceedings 13th Symposium on Naval Hydrodynamics, ONR, Washington D.C., pp. 281-302.
- Bailey, D.J., Griffiths, D.J., and Maskell, S.J. (1976). On the Experimental Observations of a Heaving Sphere. Schifftechnik, Bd. 23, pp. 31-48.
- Barakat, R. (1962). Vertical motion of a floating sphere in a sine-wave sea. Journal of Fluid Mechanics, Vol. 13, pp. 540-556. Also corrections in an unpublished report entitled "Forced periodic heaving of a semi-immersed sphere."
- Bender, C.M. and Orszag, S.A. (1978). Advanced Mathematical Methods for Scientists and Engineers, McGraw-Hill Book Co.
- Chang, M.-S. (1977). Computation of three-dimensional ship-motions with forward speed. Proceedings Second International Conference on Numerical Ship Hydrodynamics, University of California, Berkeley, pp. 124-135.
- Cody, W.J., Paciorek, K.A. and Thacher, H.C. (1970). Chebychev Approximations for Dawson's Integral Math. Comp., Vol. 24, pp. 171-178.
- Cummins, W.E. (1962). The impulse response function and ship motions. Schiffstechnik, Vol. 9, pp. 101-109.

- Daoud, N. (1975). Potential flow near to a fine ship's bow. Report No. 177, Department of Naval Architecture and Marine Engineering, The University of Michigan.
- Doctors, L.J. and Beck, R.F. (1985). Numerical aspects of the Neuman-Kelvin Problem. Submitted for publication to the Journal of Ship Research.
- Filon, L.N.G. (1929). On a Quadrature Formula for Trigonometric Integrals. Proceedings of the Royal Society Of Edinbrough, Vol., 49, pp. 38-47.
- Finkelstein, A.B. (1957). The initial value problem for transient water waves. Communications on Pure and Applied Mathematics, Vol. 10, pp. 511-522.
- Gautchi, W. (1970). Efficient Computation of the Complex Error Function. SIAM Journal of Numerical Analysis. Vol. 7, pp. 187-198.
- Gerritsma, J. and Beukelman, W. (1964). The distribution of the hydrodynamic forces on a heaving and pitching shipmodel in still water. Report No. 22, Shipbuilding Laboratory, Technological University of Delft, Delft, Netherlands.
- Gerritsma, J. Distribution of hydrodynamic forces along the length of a ship model in waves. Report No. 144, Shipbuilding Laboratory, Technological University of Delft, Delft, Netherlands.
- Guevel, P. and Bougis, J. (1982). Shipmotions with forward speed in infinite depth. International Shipbuilding Progress, Vol. 29, No. 332, pp. 105-117.
- Hess, J.L., and Smith, A.M.O. (1964). Calculation of nonlifting potential flow about arbitrary three-dimensional bodies. Journal of Ship Research, Vol. 8, No. 2, pp. 22-44.
- Hulme, A. (1982). The Wave Forces Acting on a Floating Hemisphere Undergoing Forced Periodic Oscillations, Journal of Fluid Mechanics, Vol 121, pp. 443-463.
- Hulme, A. (1983). A Ring-Source/Integral Equation Method for the Calculation of Hydrodynamic Forces Executed on Floating Bodies of Revolution, Journal of Fluid Mechanics, Vol. 128, pp. 387-412.

- Ikebuchi, T. (1981). Hydrodynamic forces on a body moving arbitrary in time on a free surface. Journal Kansai Society of Naval Architects, Japan, No. 181, pp. 45-53.
- Inglis, R.B. (1980). A three-dimensional analysis of the motion of a rigid ship in waves. Ph.D. thesis, Department of Mechanical Engineering, University College, London.
- Inglis, R.B. and Price, W.G. (1982). A three-dimensional ship motion theory -- comparison between theoretical prediction and experimental data of the hydrodynamic coefficients with forward speed. Transactions Royal Institution of Naval Architects, Vol. 124, pp. 141-157.
- Kotik, J., and Lurye, J. (1964). Some Topics in the Theory of Coupled Ship Motions, Proceedings 5th Symposium on Naval Hydrodynamics, ONR, Washington, D.C., pp. 407-424.
- Kotik, J., and Lurye, J. (1968). Heave oscillation of a floating cylinder or sphere. Schiffstchnik, Vol. 15, pp. 37-38.
- Lamb, H. (1932). Hydrodynamics, Cambridge University Press.
- Lin, W.C. (1966). An initial-value problem for the motion of a ship moving with constant mean velocity in an arbitrary seaway. Report No. NA-66-9 of College of Engineering, University of California, Berkeley.
- Maskell, S.J., and Ursell, F. (1970). The transient motion of a floating body. Journal of Fluid Mechanics, Vol. 44, part 2, pp. 303-313.
- Newman, J.N., (1985). Transient axisymmetric motion of a floating cylinder. submitted for publication in the Journal of Fluid Mechanics.
- Ogilvie, T.F. (1964). Recent progress toward the understanding and prediction of ship motions. Proceedings 5th Symposium on Naval Hydrodynamics, ONR, Washington, D.C., pp. 3-128.
- Ogilvie, T.F. and Tuck, E.O. (1969). A rational strip theory of ship motion: Part 1. Report No. 13, Department of Naval Architecture and Marine Engineering, The University of Michigan, Ann Arbor.

- Ogilvie, T.F. (1977). Singular perturbation problems in ship hydrodynamics. Advances in Applied Mechanics, Vol. 17, pp. 91-188.
- Salvesen, N., Tuck, E.O., and Faltinsen, O. (1970). Ship motions and sea loads. Transactions Society of Naval Architects and Marine Engineers, Vol. 78, pp. 250-287.
- Stoker, J.J. (1957). Water waves. Interscience Publishers, Inc., New York.
- Ursell, F. (1964). The decay of the free motion of a floating body. Journal of Fluid Mechanics, Vol. 19, pp. 305-314.
- Yeung, R.W. (1982). The transient heaving motion of floating cylinders. Journal of Engineering Mathematics, Vol. 16, pp. 97-119.
- Yeung, R.W., and Kim, S.H. (1984). A new development in the theory of oscillating and translating slender ships. Proceedings 15th Symposium on Naval Hydrodynamics, ONR, Washington, D.C., pp. 195-218.
- Wehausen, J.V. and Laitone, E.V. (1960). Surface waves. Handbuch der Physik, Springer-Verlag, Berlin, pp. 446-778.
- Wehausen, J.V. (1967). Initial-value problem for the motion in an undulating sea of a body with fixed equilibrium position. Journal of Engineering Mathematics, Vol. 1, pp. 1-19.
- Wehausen, J.V. (1971). The motion of floating bodies. Annual Review of Fluid Mechanics, Vol. 3, pp. 237-268.